Resource Management in Dense Wireless Networks

by

Seyed Hamed Mosavat-Jahromi
B.Sc., Iran University of Science and Technology, 2012
M.Sc., University of Tehran, 2015

A Dissertation Submitted in Partial Fulfillment of the
Requirements for the Degree of

DOCTOR OF PHILOSOPHY

in the Department of Electrical and Computer Engineering

Resource Management in Dense Wireless Networks

by

Seyed Hamed Mosavat-Jahromi
B.Sc., Iran University of Science and Technology, 2012
M.Sc., University of Tehran, 2015

Supervisory Committee

Dr. Lin Cai, Supervisor
(Department of Electrical and Computer Engineering)

Dr. Xiaodai Dong, Departmental Member
(Department of Electrical and Computer Engineering)

Dr. Alex Thomo, Outside Member
(Department of Computer Science)

Supervisory Committee

Dr. Lin Cai, Supervisor

(Department of Electrical and Computer Engineering)

Dr. Xiaodai Dong, Departmental Member

(Department of Electrical and Computer Engineering)

Dr. Alex Thomo, Outside Member

(Department of Computer Science)

ABSTRACT

Recently, the wide range of communication applications has greatly increased the number of connected devices, and this trend continues by emerging new technologies such as Internet-of-Things (IoT) and vehicular ad hoc networks (VANETs). The increase in the number of devices may sooner or later cause wireless spectrum shortage. Furthermore, with the limited wireless spectrum, transmission efficiency degrades when the network faces a super-dense situation. In IEEE 802.11ah-based networks whose channel access protocol is basically a contention-based one, the protocol loses its efficiency when the total number of contending users grows. VANETs suffer from the same problem, where broadcasting and receiving safety messages, i.e., beacons, are critical. An inefficient medium access control (MAC) can negatively impact the network's reliability. Effective resource management solutions are needed to improve the network's reliability and scalability considering the features of different types

of networks. In this work, we address the resource management problem in dense wireless networks in vehicle-to-everything (V2X) systems and IoT networks.

For IoT networks, e.g., sensor networks, in which the network topology is quite stable, the grouping technique is exploited to make the stations (STAs) compete in a group to mitigate the contention and improve the channel access quality. While, in VANETs, devices are mobile and the network topology changes over time. In VANETs, beacons should be broadcast periodically by each vehicle reliably to improve road safety. Therefore, how to share the wireless resources to ensure reliability and scalability for these dense static and mobile wireless networks is still a difficult and open problem.

In static IoT networks, we apply the *Max-Min* fairness criterion to the STAs' throughput to group the STAs to ensure network performance and fairness. Formulation of the problem results in a non-convex integer programming optimization problem which avoids hidden terminals opportunistically. As solving the optimization problem has a high time complexity, the Ant Colony Optimization (ACO) method is applied to the problem to find the sub-optimal solution.

To support reliable and efficient broadcasting in VANET, wireless resources are divided into basic resource units in the time and frequency domains, and a distributed and adaptive reservation-based MAC protocol (DARP) is proposed. For decentralized control in VANETs, each vehicle's channel access is coordinated with its neighbors to solve the hidden terminal problem. To ensure the reliability of beacon broadcasting, different kinds of preambles are applied in DARP to support distributed reservation, detect beacon collisions, and resolve the collisions. Once a vehicle reserves a resource unit successfully, it will not release it until a collision occurs due to topology change. Protocol parameters, including transmission power and time slots duration, can be adjusted to reduce collision probability and enhance reliability and scalability. Simulation of urban mobility (SUMO) is used to generated two different city traces to assess the DARP's performance.

Then, a distributed network coding-based MAC protocol (NC–MAC) is proposed

to support reliable single-hop vehicle-to-vehicle (V2V) beacon broadcasting. We combine the preamble-based feedback mechanism, retransmissions, and network coding together to enhance broadcasting reliability. We deploy the preamble mechanism to facilitate the negative acknowledgment (NACK) and retransmission request procedures. Moreover, linear combinations of missed beacons are generated according to the network coding (NC) principles. We also use SUMO to evaluate the NC–MAC's performance in highway and urban scenarios.

Group-casting and applying multi-hop communication can ensure reliability in V2X systems. As an extension of the proposed NC–MAC, a distributed grouping and network coding-assisted MAC protocol (GNC–MAC) is proposed to support reliable group-casting and multi-hop communication, which can address blockchain protocols' requirements. We propose a new grouping protocol by combining preamble-based feedback mechanism, multi-hop communication, and network coding to improve group-casting reliability. The preamble mechanism is responsible for reporting a NACK and requesting retransmission due to beacon missing. The missed beacons are combined according to the NC principles and sent on a resource block.

Contents

List of Tables

List of Figures

List of Abbreviations

AP	Access Point
ACK	Acknowledgment
ACO	Ant Colony Optimization
BLER	Block/Packet Error Rate
BLR	Beacon Loss Ratio
BRD	Beacon Recovery Delay
BS	Base Staion
C–V2X	Cellular Vehicle-to-Everything
CCH	Control Channel
CDF	Cumulative Distribution Function
CSMA/CA	Carrier Sense Multiple Access/Collision Avoidance
DARP	Distributed and Adaptive Reservation-based Protocol
DCC	Distributed Congestion Control
DCF	Distributed Coordination Function
DSRC	Dynamic Short Range Communication
GNC-MAC	Grouping and Network Coding-assisted MAC
GPS	Global Positioning System
HARQ	Hybrid Automatic Repeat Request
IoT	Internet-of-Things
ITS	Intelligent Transportation System
LoD	Level of Deficiency
LoS	Line of Sight
MCS	Modulation and Coding Scheme
MPDU	MAC Layer Protocol Data Unit
NACK	Negative-Acknowledgement
NC	Network Coding

NC–MAC	Network Coding-based MAC Protocol
PDF	Probability Density Function
PDU	Protocol Data Unit
PMF	Probability Mass Function
PPP	Poisson Point Process
RAW	Restricted Access Window
RSS	Received Signal Strength
RSU	Road Side Unit
SCH	Service Channel
SINR	Signal-to-Interference-Plus-Noise Ratio
SNR	Signal-to-Noise Ratio
SUMO	Simulation of Urban Mobility
STA	Station
TDMA	Time Division Multiple Access
TGah	Task Group
TTI	Transmission Time Interval
TTL	Time-to-Live
TXOP	Transmission Opportunity
V2I	Vehicle-to-Infrastructure
V2V	Vehicle-to-Vehicle
VANET	Vehicular Ad Hoc Networks
VE	Vehicle

ACKNOWLEDGEMENTS

There are many, without whom this work would not have been possible and whom I would like to express my gratitude.

First, I would like to express my greatest gratitude to Dr. Lin Cai, for mentoring, support, inspiration, and patience. I can never thank her enough for the exceptional support and encouragement that I received during my study. I was extremely lucky and I could not have asked for a better supervisor. It was truly a privilege to be a member of her team.

In addition, I am very grateful to Dr. Xiaodai Dong and Dr. Alex Thomo as the members of my supervisory committee, and Dr. Ping Wang from York University as my external examiner, for spending their precious time to review my thesis and attend my oral exam. I also would like to thank Dr. Jianping Pan for his constructive comments.

I am also very thankful to all of the CNLAB's members, for all the moments we shared and all the lessons we learned together. Specially, Dr. Yue Li and Dr. Wen Cui, for their kindness and supports in the low moments. They helped me to broaden my knowledge and develop my research skills.

I sincerely appreciate Dr. Adam Zielinski (RIP, 1944–2020), for his kindness, generosity, and support he gave me in the short period of time I knew him.

I would like to thank my mother, father, and brother, for their endless support and love. It was indeed their encouragement and patience that inspired me to come this far and be where I am now.

Last but not least, I would like to thank Leila, who has always been there for me, for her positive attitude, encouragements, and her great soul.

Seyed Hamed Mosavat-Jahromi, Victoria, BC, Canada

DEDICATION

To Vida, my beautiful mother, for her endless love and devotion,

To Abolfazl, my lovely father, for his patience and compassion.

Chapter 1

Introduction

1.1 Background

Advanced wireless technologies have provided ubiquitous network connectivity and accessibility for users. The users can be personal cell phones, laptops, or even vehicles and smart home devices. Since 2010, the number of connected devices had exceeded the human population, and it is predicted that this number will increase to 21.2 and 34.3 Billion in 2020 and 2025, respectively [1, 2]. Recently, the emerging Internet-of-Things (IoT) applications have attracted attention from both academia and industry. These applications require connectivity among a massive number of heterogeneous devices [3].

There are two emerging dense wireless networks with and without user mobility, vehicular ad hoc networks (VANET) and IoT networks. These two types of networks have their own features, requirements, and challenges. How to manage the available resources can highly improve communication efficiency and its quality of service.

An IEEE 802.11ah-based network is aimed to support a massive number of users in its coverage by contention. Obviously, the more contending users, the more collisions in the accessing procedure. Consequently, contention-based schemes are not efficient when the number of contending users is large. The basic idea in the IEEE 802.11ah standard is to limit the total number of contending users by assigning them

into different groups to mitigate contention and collision. However, how to group the users has not been specified in the standard.

Vehicular communication networks have emerged as a promising solution to improve road safety and efficiency. As an important component of Intelligent Transportation Systems (ITS) [4, 5]. The key component of ITS evolution as well as the automotive revolution is connected vehicles. Vehicles connectivity can potentially enhance the safety and efficiency of roads transportation system through intelligent traffic management, and empower the vehicles to communicate with their surrounding vehicles. It will support many applications such as intelligent navigation, emergency message dissemination, in-car entertainment, and autonomous driving assistance. Driving will become easier, more comfortable, and safer than ever before, accompanied by higher fuel efficiency, a lower amount of CO_2, and less traffic jam. To achieve the above benefits, efficient and reliable information exchange among neighbor vehicles is critical [6, 7, 8, 9]. In VANETs, packet losses and network performance degradation are severe in dense scenarios. In this regard, how to utilize the available resources to ensure broadcast beacon messages reliably is critically important. The above challenges motivate us to study how to provide better resource support and reliable communication in super-dense static and mobile scenarios.

Chapter 2 is dedicated to effective grouping solutions in dense scenarios of IoT systems. By using grouping strategies, hidden terminal problem and users contention in accessing the communication channel will be mitigated dramatically which can improve system throughput. In Chapter 3, a new adaptive and distributed MAC protocol is proposed for dense vehicular networks. After accessing a resource block, a reliable communication for beacon broadcasting is a key issue. Therefore, in Chapter 4, a new single-hop communication network coding-based MAC protocol is proposed in which users can request for retransmission. We extend the proposed protocol in Chapter 4 to support multi-hop communication and group-casting in vehicle-to-everything (V2X) systems. A novel yet simple grouping-based network coding-assisted protocol is proposed in Chapter 5. The structure of the thesis is illustrated in Fig. 1.1.

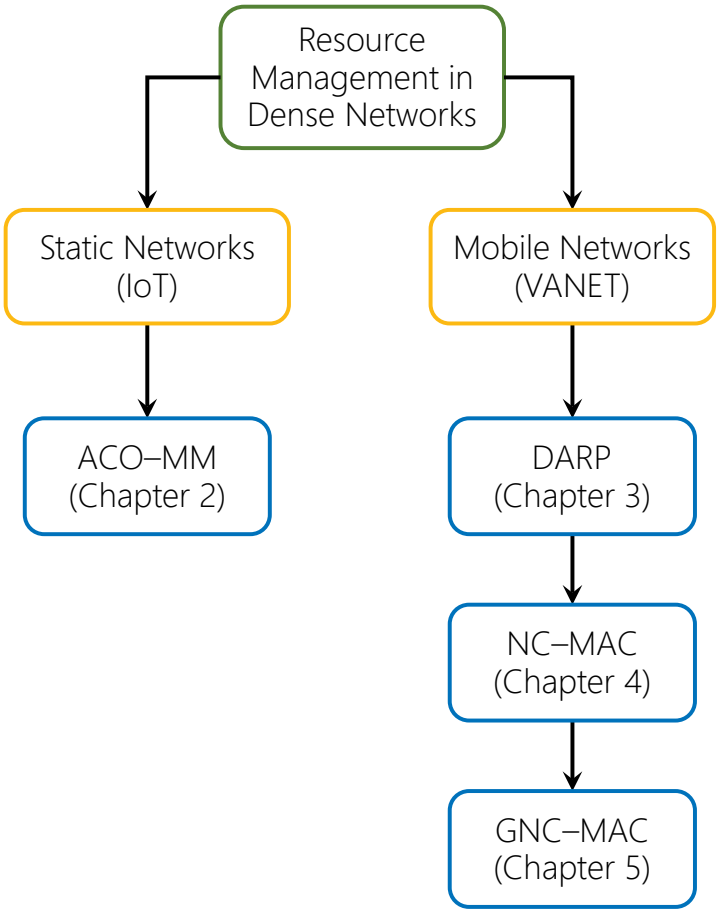

Figure 1.1: Structure of the thesis.

1.2 Research Objectives and Contributions

1.2.1 Fairness-based Grouping Strategy for Dense IEEE 802.11ah Networks

In Chapter 2, we propose a new grouping scheme for dense IoT systems by considering the *Max-Min* fairness and mitigating the hidden terminal problem. The way the STAs are assigned to different groups and the size of groups may influence the network's performance. In this regard, the trade-off between performance and fairness in grouping is investigated. The method utilizes a meta-heuristic algorithm to find the sub-optimal solution to the grouping problem. The contributions of this chapter

are as follows:

1. An analytical model for grouping in a saturated network is studied and the maximum saturated throughput of the network is considered.

2. A new grouping strategy based on the STA's throughput fairness in association with hidden terminal avoidance is proposed.

3. The Ant Colony Optimization (ACO) is applied to the problem to find the fair grouping. Extensive simulations have been conducted to validate the proposed approach and the simulation results demonstrate 40% gain in the total throughput, 37% gain in the minimum per-STA throughput, and 11% reduction in the number of hidden terminals.

1.2.2 DARP: Distributed and Adaptive Reservation-based MAC Protocol

In Chapter 3, the target is on vehicle-to-vehicle (V2V) communications, and we introduce an adaptive distributed beaconing method for dense vehicular networks. We address the broadcasting problem by carefully leveraging the distributed reservation mechanism, the coded preambles, and the adaptation of power and resource unit parameters for effectively sharing the resources in the time/frequency/space and code domains. The contributions of this chapter are as follows:

1. We propose a novel Distributed and Adaptive Reservation-based beacon broadcasting MAC Protocol (DARP), in which vehicles coordinate the channel access in the time and frequency domain. We employ a preamble mechanism in the frame structure to detect and resolve beacon collisions.

2. We analyze the protocol performance in terms of access collision probability and access delay. Based on the analysis, how to fine-tune the protocol parameters to ensure reliability and scalability is proposed.

3. Finally, using NS-3 [10] with vehicle traces generated by simulation of urban mobility (SUMO) [11], extensive simulations have been conducted to validate the analysis and evaluate the performance of DARP.

1.2.3 NC–MAC: Network Coding-based Distributed MAC Protocol

Given the DARP in Chapter 3, we further propose a novel distributed protocol in Chapter 4 to improve the beacon transmission reliability in VANETs. We combine the preamble-based mechanism, beacon retransmission, and the network coding together to enhance the communication reliability. The missed beacons are included in the linear combinations, and in order to recover the missed beacon, a full-rank matrix should be generated upon reception of the linear combinations. The contributions of this chapter are as follows:

1. We propose a novel distributed MAC protocol (NC–MAC) for V2X systems. We employ a preamble mechanism in the frame structure to report a negative acknowledgment (NACK) and request a retransmission.

2. The NC mechanism is deployed to generate independent linear combinations of messages. Furthermore, a complete protocol design, including forwarding operation and feedback, is shown.

3. The SUMO simulator [11] is used to generate two typical traffic scenarios, highway and urban, using different vehicles with different attributes. Extensive simulations have been conducted to validate the NC–MAC's performance in different scenarios.

1.2.4 GNC–MAC: Grouping and Network Coding-assisted MAC for Reliable Group-casting

In Chapter 5, a novel grouping and network coding-assisted MAC (GNC–MAC) is proposed to support a reliable communication in group-casting of V2X systems. This protocol is an extension of the NC–MAC protocol, which is able to deal with multi-hop communication. Therefore, more vehicles in a group within several hops can receive beacons. Moreover, it can help to recover missed beacons and increase in-group communication reliability. The main contributions of this chapter are as follows:

1. A novel protocol is proposed to support group-casting in VANETs.
2. Multi-hop relaying along with the preamble and NC mechanisms are deployed to enlarge group size.
3. Different controlling messages are designed for group management.

Chapter 2

Fairness-based Grouping Strategy for Dense IEEE 802.11ah Networks

2.1 Introduction

The emerging IoT has been recognized as one of the key technologies in the future which can change a wide range of industries dramatically. Communication of different devices as well as integration of multiple systems through the IoT technology provide a higher level of reliability, efficiency, and safety. By the increasing trend in the deployment of different sensors and proliferation of connected devices in IoT networks, keeping the network efficient and providing the devices a fair quality of service are challenging. In static IoT networks, the stations (STAs) communicate with the base station (BS) with random and bursty traffic. Therefore, a reservation-based scheme cannot utilize the resources and accommodate all of the devices well. This chapter focuses on the MAC layer design, and the grouping strategy in dense IoT networks in order to facilitate the accessing procedure.

The classic IEEE 802.11 standard is suitable for small scale networks such as wireless local area networks, since, intrinsically, it has been developed to support high data rate communications for a small number of STAs in a small area [12]. In addition, it operates at 2.4 GHz and 5 GHz frequency bands. Even though these

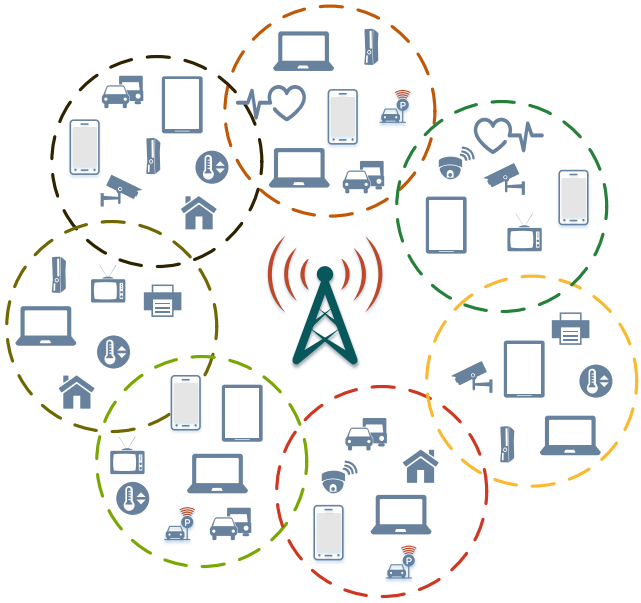

Figure 2.1: Example of an IEEE 802.11ah network with a grouping strategy for different applications.

bands are license-free and provide high data rate communications, the transmission range of the systems working on these ranges are limited due to high frequency. Therefore, the current standard is not able to satisfy the new requirements for future massive IoT connections including managing a large number of users along with the communication range and data rate issues.

To meet the IoT challenges, the IEEE 802.11ah Task Group (TGah) under the IEEE 802 LAN/MAN Standards Committee has been established to design a large-scale energy-efficient protocol [12]. An IEEE 802.11ah network operates at the sub-1 GHz spectrum, specifically at $900 - 928$ MHz, and can support up to 6000 STAs in a network [13]. It supports different modulation and coding schemes (MCS) to maintain a trade-off between energy-efficiency, data rate, and throughput [14]. Different MCSs can support transmission ranges between 100 m and 1 Km with data rates from 0.15 Mbps to 346.67 Mbps. To resolve the problem of the highly dense STAs with power constraints, several mechanisms have been proposed including short MAC header, restricted access window (RAW), and hierarchical organization. As a large number of STAs in the network result in more contentions in channel acquisition, the overall

network performance and efficiency may be degraded considerably by the increase in contention [14], [15]. The idea of limiting the number of STAs involved in the channel contention process, i.e., network grouping, has been proposed by the TGah to alleviate this problem. In the centralized grouping strategy, an 802.11ah access point (AP) divides the STAs in the network into multiple groups in which the STAs contend for channel access in a RAW. Therefore, there will be no collisions between different groups' STAs. However, the grouping strategy has not been specified in the standard. The number and the duration of RAW slots, each group size, and how to assign different STAs to different groups by the AP are some parameters which can be tuned.

Grouping strategies can be divided into centralized and decentralized categories. While the former category offers a fast grouping, it requires more control signaling and pre-established network infrastructure. However, the latter one is more cost-effective and has a good performance in dynamic networks [16]. Fig. 2.1 shows an example of grouping in an IEEE 802.11ah network.

In this chapter, a new grouping strategy in a dense IEEE 802.11ah network is studied. The way the STAs are assigned to different groups and the size of groups may influence network's performance. To the best of our knowledge, the trade-off between performance and fairness in grouping has not been thoroughly investigated so far. Therefore, first, an analytical model for grouping in a saturated network is studied and the maximum saturated throughput of the network will be considered. Then a grouping strategy based on the STA's throughput fairness in association with hidden terminal avoidance is proposed. The ACO is applied to the problem to find the fair grouping. Extensive simulations have been conducted to validate the proposed approach. The results show that it can achieve approximately up to 40% gain in the total throughput and 11% reduction in the total number of hidden terminals compared to the K–means.

2.2 Related Works

In [17], the performance degradation in the IEEE 802.11ah networks resulting from hidden terminals has been analyzed first, and then the hidden matrix-based regrouping scheme has been proposed to resolve this problem. The idea behind this approach is to detect hidden terminals at the AP. Thereafter, the hidden node matrix is generated, and the nodes experiencing hidden terminal are moved to another group. The results show that the proposed algorithm outperforms the IEEE 802.11ah standard grouping algorithm. Meanwhile, another solution to resolve the hidden terminal problem in large-scale IEEE 802.11ah networks has been proposed in [18]. The solution is composed of the collision chain mitigation and hidden-device-aware algorithm. An ongoing collision chain is detected by monitoring energy blocks in a wireless channel and measuring its length in the collision chain mitigation process. In spite of utilizing collision chain mitigation scheme, collision chains still occur in the proposed solution. In order to reduce the number of hidden terminals significantly, they proposed a grouping algorithm.

[16] has studied the modeling of the media access performance using group-synchronized distributed coordination function (GS-DCF). The GS-DCF's throughput has been analyzed using two grouping categories, centralized and decentralized, provided that the number of groups is specified already. The STA's are assigned to the groups uniformly in the centralized case, while in the decentralized one, groups are chosen randomly.

The RAW parameters such as the number of groups, RAW duration, and STAs division have been investigated in [15]. The optimality has been considered not only throughput-wise, but also from latency and energy-efficiency points of view. Simulations in this work have been run in the NS-3 event-based network simulator. [19] proposed a new algorithm based on the number of devices which might increase the system's performance by finding the optimal size of RAW.

A novel real-time grouping algorithm has been proposed in [14] based on the

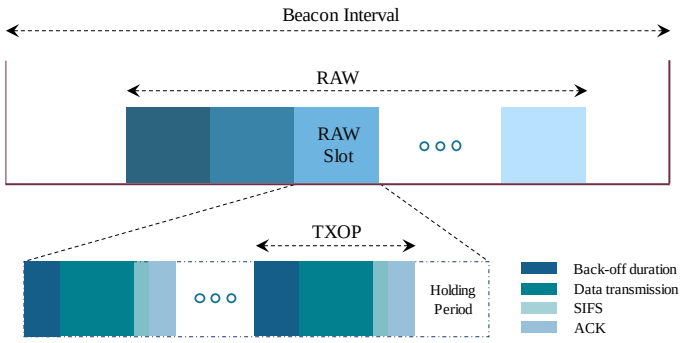

Figure 2.2: Beacon interval, RAW and RAW slot structure in the IEEE 802.11ah.

current traffic situation. The proposed algorithm considers both dynamic and heterogeneous traffic conditions. The parameter estimation takes place in the AP and it uses the available information. This algorithm is run at the beginning of each beacon interval, and this feature makes the algorithm real-time.

Some preliminary simulations have been run by Chang *et al.* in [20] to show that different groups in random grouping strategy will experience different channel utilization based on the groups size and imbalance traffic load. The proposed protocol chooses groups based on the STAs traffic demand to balance the group's traffic load and improve channel utilization.

Ghassemi *et al.* in [21] introduce a new scheme which uses the received signal strength (RSS) in the grouping scheme. In this scheme, the AP chooses the group heads and transmits beacon frames at each grouping update period. Then each group head transmits a pilot. The receiving STAs choose the group corresponding to the largest RSS. Through the simulations, it has been shown that the RSS-based protocol outperforms random and k-mean grouping strategies.

None of the existing works have studied the fairness in terms of the minimum per-STA throughput in association with hidden terminal avoidance has been studied. Therefore, we focus on the fairness problem in this chapter.

2.3 System Model

In this work, we consider an IEEE 802.11ah network in which there are N stationary STAs, and they can communicate directly to the AP. These N STAs will be partitioned into M groups each with group size of S_m, in a way that $\sum_{m=1}^{M} S_m = N$. Throughout this chapter, it is assumed that M and N have been predetermined. The set of these M group heads is denoted as $\mathcal{H}$, and these heads will be chosen by the AP at the beginning of the grouping process uniformly on polygon vertices. The heads are just responsible for groups construction. After constructing a group and assigning new STAs to the groups, the STAs communicate directly with the AP. The beacon period in the MAC protocol consists of several RAWs, which contains some equal RAW slots and each slot is assigned to a group. In each RAW slot, there is an access period in which STAs can contend to obtain a transmission opportunity (TXOP). T_R and T_{Rs} represent the duration of a RAW and a RAW slot time. The end of RAW slot is the holding period in which STAs are idle to avoid RAW slot crossing. Fig. 2.2 depicts a beacon interval TXOP in the IEEE 802.11ah protocol.

2.3.1 Channel Model

We consider the path-loss channel model which is determined by the distance between the transmitter and the receiver as in [22]. The path-loss formula in dB is

$$PL = 8 + 37.6 \log_{10}(d), \tag{2.1}$$

where d is the distance between the transmitter and the receiver, and the carrier frequency has been assumed to be 900 MHz. The channel between the STA and the AP experiences block fading where the channel state remains unchanged during each RAW slot. The channel coefficient of the i-th slot in the m-th RAW, $h_{i,m}$, follows a complex normal distribution. Without loss of generality, we can assume that the channel coefficient, $h_{i,m}$, is related to the i-th STA in the m-th group. Hence, assuming

$\lambda_{i,m}$ is the transmitted signal, the received signal at the AP from the i-th STA is

$$y_{i,m} = h_{i,m}\sqrt{\phi\, d^{\nu}\, P^{t}_{i,m}}\lambda_{i,m} + n_{i,m}, \tag{2.2}$$

in which ϕ and ν are path-loss model coefficients, and $n_{i,m}$ is the white Gaussian noise with zero-mean and variance of N_0. The achievable transmission rate of the i-th STA is [23]

$$R^{m}_{i} = B\log_2\left(1 + \frac{\phi\, d^{\nu}\,|h_{i,m}|^2\, P^{t}_{i,m}}{N_0}\right). \tag{2.3}$$

In (2.3), B is the allocated bandwidth to the user. The IEEE 802.11ah supports 1, 2, 4, 8, and 16 MHz bandwidths [17]. The 2 MHz bandwidth is the basic one and it contains 64 sub-carriers. In this model, we assume that all STAs transmit with a fixed power, i.e., $P^{t}_{i,m} = P$.

2.3.2 Contention Model

The contention process works based on the Enhanced Distributed Channel Access (EDCA) [22] but slightly different from the IEEE 802.11 standard. In the IEEE 802.11ah, each STA has two back-off states where the first one is dedicated to the outside RAW slots, and the other one is used as inside. The first back-off state will be suspended at the beginning of each RAW and later, at the end of the RAW, the back-off function will be restored and the operation is resumed. However, the second back-off state starts with the initial back-off state inside the STA's corresponding to the RAW slot, and it will be discarded at the end of the RAW slot [22]. Whenever a STA in a group has a packet to transmit, a new back-off procedure is invoked. The STA resets the inside back-off window to $CW_{\min}$ at the beginning of the RAW slot. Then, it uniformly chooses a random back-off number in $[0, CW_k - 1]$ where CW and $k = 1, 2, \ldots, K$ are the contention window and back-off stage, respectively. K is the maximum back-off stage such that $CW_{max} = 2^K CW_{\min}$. If any collisions happen in the accessing process, the contention window will be doubled until it reaches the

maximum value.

Our model is based on Bianchi's throughput analysis in [24]. p_m and τ_m denote the conditional collision and packet transmission probabilities in the m-th group, respectively. The latter is the probability that a STA in the m-th group tries to transmit a packet in a chosen RAW slot, and the former represents the probability that a collision happens in a packet transmission. These probabilities are considered in a saturated network where each STA always has a packet to transmit and incoming packets are backlogged in the STA's buffer. In the Markov chain presented in [24], $b^m_{k,j}$ is the stationary probability of the m-th group's chain in which k and j are the back-off stage and contention window counter values, respectively. Based on the equilibrium equations of the Markov chain, the transmission probability is

$$\begin{aligned}\tau_m &= \sum_{k=0}^{K} b^m_{k,0} = \frac{b^m_{0,0}}{1-p_m} \\ &= \frac{2(1-2p_m)}{(1-2p_m)(CW_{\min}+1)+p_m CW_{\min}(1-(2p_m)^K)}.\end{aligned} \tag{2.4}$$

On the other hand, each STA transmits a packet with probability of τ_m. Therefore, the collision probability is

$$p_m = 1-(1-\tau_m)^{S_m-1}. \tag{2.5}$$

Based on (2.4) and (2.5), the transmission probability, i.e., the probability that at least one STA in the m-th group starts transmitting, can be calculated as $P^m_{tr} = 1-(1-\tau_m)^{S_m}$. Accordingly, the success probability which is the probability that only one STA transmits conditioned on at least one STA transmits is

$$P^m_{suc} = \frac{S_m \tau_m (1-\tau_m)^{S_m-1}}{1-(1-\tau_m)^{S_m}}. \tag{2.6}$$

Now, we can focus on *Saturation Throughput* which is defined as the maximum load the system can tolerate and it is the throughput upper bound [24]. According to the transmission and success probabilities, the average throughput corresponding to each

user in the m-th group is achieved as

$$\begin{aligned}\eta_i^m &= \frac{\mathbb{E}\left[i\text{-th user's payload bits successfully transmitted}\right]}{\mathbb{E}\left[\text{Interval between successive transmissions}\right]} \\ &= \frac{1}{S_m}\frac{P_{tr}^m P_{suc}^m T_x R_i^m}{\left(1-P_{tr}^m\right)\sigma + P_{tr}^m P_{suc}^m T_s + P_{tr}^m\left(1-P_{suc}^m\right)T_c},\end{aligned} \tag{2.7}$$

where σ, T_s, T_c, and T_x are empty slot duration, average time the channel is busy with a successful transmission, average time the channel is busy with a collision, and average packet transmission time, respectively. In (2.7), R_i is the i-th user's data rate and it can be found in (2.3). It is worth mentioning that the $\frac{1}{S_m}$ coefficient in (2.7) is to normalize the group's throughput to the group size in order to have each STA's throughput.

2.4 Problem Formulation

We consider a grouping scenario based on the *Max-Min fairness* criterion. In this scenario, the STAs' channel conditions are considered in the objective function, and the STAs are assigned to different groups in a way to maximize the minimum per-STA throughput. There are M groups and N STAs in total, and x_{im} is the decision making binary variable corresponding to the i-th STA in the m-th group. Therefore, there will be $M \times N$ decision making variables. The objective function of the integer programming problem comes from (2.7) in which the equations in (2.3), (2.6), and P_{tr}^m should be plugged. Based on the assignment nature of the problem, each STA should be assigned to just one group. S_m, the m-th group size, can be calculated as the summation of the decision making variables in the m-th group. These constraints can be formulated as

$$\sum_{m=1}^{M} x_{im} = 1, \quad \forall i = 1, \ldots, N, \tag{2.8}$$

$$\sum_{i=1}^{N} x_{im} = S_m, \quad \forall m = 1, \ldots, M. \tag{2.9}$$

The RTS/CTS mechanism is not applicable in the IEEE 802.11ah due to small packet size and dense network. In order to confine the STAs spatially and group the STAs close to each other in general, and avoid hidden terminal problem specifically, a location constraint is considered in the optimization problem. This constraint is to check whether the new STA is in the sensing range of the other STAs in the group. This constraint is satisfied opportunistically, meaning that the constraint satisfaction is a priority as long as there is at least a group in its range which remains hidden terminal-free even if a new STA is assigned to. Furthermore, collision and packet transmission probabilities corresponding to each group, p_m and τ_m, are the controllable parameters which can be adjusted by contention window parameters, K and $CW_{\min}$. Based on the controllability feature of the model, τ_m and p_m can be found in a way that maximizes each group's average throughput. Therefore, the constraint on finding the optimum transmission probability to maximize the throughput can be written as

$$\begin{aligned} \frac{S_m}{T_x R_i^m} \frac{d\eta_i^m}{d\tau_m} = & \frac{\frac{dP_{suc}^m}{d\tau_m} P_{tr}^m}{\left(1 - P_{tr}^m\right)\sigma + P_{tr}^m P_{suc}^m T_s + P_{tr}^m \left(1 - P_{suc}^m\right) T_c} \\ & + \frac{P_{suc}^m \left[\sigma \frac{dP_{tr}^m}{d\tau_m} - \frac{dP_{suc}^m}{d\tau_m} (P_{tr}^m)^2 (T_s - T_c)\right]}{\left[\left(1 - P_{tr}^m\right)\sigma + P_{tr}^m P_{suc}^m T_s + P_{tr}^m \left(1 - P_{suc}^m\right) T_c\right]^2}, \end{aligned} \tag{2.10}$$

where calculating $\frac{dP_{suc}^m}{d\tau_m}$ and $\frac{dP_{tr}^m}{d\tau_m}$ are straightforward and the corresponding final equation of $\frac{d\eta_i^m}{d\tau_m} = 0$ is

$$\left(T_c - \sigma\right)\left(1 - \tau_m\right)^{S_m} + S_m T_c \tau_m - T_c = 0. \tag{2.11}$$

Given S_m, T_c, and σ, the optimum transmission probability can be achieved. The optimal transmission probability is maintained based on $CW_{\min}$ and K as well. In order to group the STAs close to each other in general, and avoid hidden terminal problem, we need to make sure that a new STA which is going to be assigned to a group, does not make any hidden terminals with the existing members of that group.

In other words, the new STA should be in the sensing range of the group members, $\|l_{New} - l_k\| \leq R_s, \ \ \forall k \in \mathcal{K}_m$. Therefore, the *Max-Min* optimization problem is formulated as

$$
\begin{aligned}
\max_{x_{im}} \quad & \min_{i \in \mathcal{N}} \ \eta_i^m \\
\text{s.t.} \quad & \sum_{m=1}^{M} x_{im} = 1, \quad \forall i \in \mathcal{N}, \\
& \sum_{i=1}^{N} x_{im} = S_m, \quad \forall m \in \mathcal{M}, \\
& (T_c - \sigma)\,(1 - \tau_m)^{S_m} + S_m T_c \tau_m - T_c = 0, \forall m \in \mathcal{M}, \\
& \left.\begin{aligned} -\|l_i - l_k\| + R_s \ &\leq \ Q\, x_{im} \\ -R_s + \|l_i - l_k\| \ &\leq \ Q\,(1 - x_{im}) \end{aligned}\right\} \forall k \in \mathcal{K}_m, \\
& x_{im} \in \{0, 1\}\,.
\end{aligned} \tag{2.12}
$$

The optimization problem in (2.12) can be written as the one in (2.13) by defining an auxiliary variable, δ, and introducing a new constraint. This would be as

$$
\begin{aligned}
\max_{x_{im}, \delta} \quad & \delta \\
\text{s.t.} \quad & \eta_i^m \geq \delta, \quad \forall i \in \mathcal{N} \\
& \sum_{m=1}^{M} x_{im} = 1, \quad \forall i \in \mathcal{N}, \\
& \sum_{i=1}^{N} x_{im} = S_m, \quad \forall m \in \mathcal{M}, \\
& (T_c - \sigma)\,(1 - \tau_m)^{S_m} + S_m T_c \tau_m - T_c = 0, \forall m \in \mathcal{M}, \\
& \left.\begin{aligned} -\|l_i - l_k\| + R_s \ &\leq \ Q\, x_{im} \\ -R_s + \|l_i - l_k\| \ &\leq \ Q\,(1 - x_{im}) \end{aligned}\right\} \forall k \in \mathcal{K}_m, \\
& x_{im} \in \{0, 1\}\,, \ \delta \in \mathbb{R}^+.
\end{aligned} \tag{2.13}
$$

where $\mathcal{M} \triangleq \{1, 2, \ldots, M\}$, $\mathcal{N} \triangleq \{1, 2, \ldots, N\}$, and $\mathcal{K}_m$ is the set of all STAs in the m-th group with cardinality of $|\mathcal{K}_m| = S_m$. The functionality of the auxiliary variable, δ, is to bound the STAs' throughput from bottom and guarantee the maximization of the minimum throughput. The first constraint represents the i-th STA's throughput in the m-th group described in (2.7). Also, l and R_s are the location vector and the sensing range, respectively. Q is an arbitrary fixed large number to make sure that the hidden terminal constraints are satisfied concurrently.

Since δ and x_{im} are real- and integer-valued variables, respectively, the optimization problem in (2.13) is a non-convex and non-linear mixed-integer programming problem. If the optimization variables of each group are rearranged in the vector form, $X_m = [x_{1m}, x_{2m}, \ldots, x_{im}]^T$, the third set of constraints can be written as $|\text{supp}(X_m)| = S_m$, where $\text{supp}(x) = \{i \mid x_i \neq 0\}$ denotes the support of a given vector x. Therefore, problem in (2.13) is similar to cardinality-constrained optimization problems which have wide range of applications in the subset selection problem in regression [25] and portfolio optimization problems with constraints on the number of assets [26, 27]. In [28], it has been proved that these problems are NP-hard and it is difficult to find the corresponding optimal solution. Since finding the optimal solution of this problem is complicated and time consuming, we apply a meta-heuristic algorithm named ACO to find the sub-optimal solution faster and with less complexity. This approach will be explained in detail in Section 2.5.

2.5 Ant Colony Optimization

2.5.1 ACO Background

As it was mentioned, the final optimization problem is NP-hard, and we will use a meta-heuristic approach to accelerate the solution finding process. Inherently, meta-heuristic algorithms have some basic heuristics, either a constructive one which is improved from a null solution to a complete one, or a local search starting from a

good solution and modifies it iteratively to achieve a better result. In this regard, ACO can solve the combinatorial optimization problems [29]. Combining a priori information about the solution with a posteriori information of the structure is one of the features which separates the ACO from other meta-heuristic algorithms.

Indeed, the ACO exploits some ants in order to inspect different routes which may have different costs, and chooses the route with the minimum cost. This technique originates from the food hunting behavior of ants species. In this process, ants secrete *pheromone* on the path in order to help other ants in the colony distinguish different paths. This mechanism is the main idea behind the ACO [30]. Actually, the pheromone contains a priori exploration information of a path which facilitates finding the best solution. In addition to *pheromone deposition*, there is *pheromone evaporation* process, in which a portion of the deposited pheromone will evaporate with the passage of time. Based on these two processes, other ants in the colony walking to or from a food source can recognize the pheromone and follow the path with a higher density of the pheromone. Afterwards, the route with the lower cost will be chosen more and becomes the favorite route. In other words, if ants find a route with a better cost, the deposited pheromone of the route will increase over time which eventually leads the ants to the best solution. The ACO is a positive feedback scheme and the system evolves after some time to find the best solution [31, 30].

2.5.2 ACO–MM

The ACO is applied to the optimization problem in (2.13) to find the best grouping scheme. Hereafter, we call the grouping ACO algorithm *ACO–MM*, ACO for the *Max-Min* problem. Before applying the ACO–MM algorithm, the STAs-groups possibilities matrix denoted by C, should be generated based on $\mathcal{H}$ and $\mathcal{A}$ which are group heads and STA's coordinates sets. C is a $|\mathcal{N}| \times |\mathcal{M}|$ matrix containing each STA's candidate groups of which the STAs are in the sensing range. This matrix can be achieved after transmitting a pilot signal by the group heads, measuring the RSS by the STAs, and feeding it back to the AP. Furthermore, the channel coefficients

Algorithm 1 The ACO–MM Algorithm

Input: $\mathcal{M}$, $\mathcal{N}$, $\mathcal{H}$, C, and H
Output: Groups assigned to each STA
Initialize the ACO–MM parameters, α, β, and ρ
Initialize γ, ξ
for $i = 1 : Iter$ **do** ▷ $Iter$: total number of iterations
    Distribute ants and select a candidate
    group randomly
    for $j = 1 : |\mathcal{J}|$ **do** ▷ $\mathcal{J}$ is set of ants
        $[\delta, Tour] = TourCons(\mathcal{M}, \mathcal{N}, H, C, \gamma, \xi)$
        if $\delta > \delta_{Best}$ **then**
            $\delta_{Best} \leftarrow \delta$
            $Tour_{Best} \leftarrow Tour$
        end if
    end for
    Update the pheromone matrix (ξ)
end for
Find STA's throughput for the achieved grouping

vector, H, representing all of the coefficients related to the communication channels from the STAs to the AP, is available beforehand. This vector can be estimated based on the block fading and path-loss models explained in Section 2.3.1. Moreover, the ACO–MM control factors, (α, β) and also, *evaporation rate*, ρ, have to be set. These parameters control the importance of *pheromone* and the heuristic information.

The algorithm is run for a specific number of ants and iterations. The ants are distributed among the STAs and choose a group randomly. Each ant starts the exploring process from the chosen STA and group, constructs a *Tour*, and finds the cost of the explored tour. A non-explored STA, *Next*, is chosen until the ant visits all of the STAs. The group with the maximum transition probability, is chosen for *Next*. p_{im}^{j} is the transition probability regarding to the j-th ant by which STA i is assigned to group m. It is defined as

$$p_{im}^{j} = \frac{\xi_{im}^{\alpha} \gamma_{im}^{\beta}}{\sum_{k \in C_i} \xi_{ik}^{\alpha} \gamma_{ik}^{\beta}}, \tag{2.14}$$

which is a function of the heuristic information, γ, pheromone trail, ξ, and the ACO–MM control factors. p_{nonH} is calculated in the same way as p in (2.14). However, the

Algorithm 2 Tour Construction Function

Input: $\mathcal{M}$, $\mathcal{N}$, H, C, γ, and ξ
Output: Grouping and its cost, $[\delta, Tour]$
$Tour \leftarrow \emptyset$
for $n = 1 : |\mathcal{N}|$ **do**
    $Next \leftarrow$ Choose a non-visited STA randomly
    $Cost \leftarrow$ Find the minimum throughput based on *Next*, its candidate groups, and constraints in (2.13)
    $\gamma \leftarrow 1/Cost$
    $p \leftarrow$ Transition probability based on (2.14)
    $p_{nonH} \leftarrow$ Transition probability of the possible groups w/o hidden terminal problem
    if $p_{nonH} \neq \emptyset$ **then**
        $G \leftarrow$ Group with the maximum p_{nonH}
    else
        $G \leftarrow$ Group with the maximum p
    end if
    $Tour := Tour + (n, G)$
end for
$\delta \leftarrow$ Maximum STA's throughput based on $Tour$
return δ and $Tour$

difference is that p_{nonH} contains the transition probabilities of the groups to which stay hidden-terminal-free after assigning *Next*. In order to make sure whether the group may be hidden-terminal-free or not, the forth constraint in (2.12) should be checked.

It can be learned from (2.14) that the transition probability is a function of heuristic information and the pheromone trails concurrently. ACO parameters, $\alpha > 0$ and $\beta > 0$ are the influence factors of the pheromone trails and the heuristic information, respectively and play important roles in finding better *Tour*s. If $\alpha = 0$, the group with the maximum attractiveness is chosen which corresponds to a classical stochastic greedy approach. In contrast, if $\beta = 0$, just the pheromone amplification is considered and leads to emergence of a *stagnation*, i.e. a situation that all of the ants choose the same tour [32].

Afterwards, the maximum throughput, δ, is found according to (2.7) and *Tour*. Then, the function returns the *Tour* and δ. The returned cost by each ant is compared

to the best achieved cost, and the best cost is replaced with the new one. At the end of each iteration, the deposited pheromones of all of the tours are updated. Algorithm 1 and 2 show the details of the ACO–MM algorithm.

2.6 Simulation Results

The effectiveness of the proposed grouping scheme is investigated by carrying out extensive simulations. The STAs are distributed in a circle centered at the AP with a radius of 600 m, and the STAs' sensing range is $R_s = 300$ m. In the simulations, the empty slot's duration, the average time channel is busy with a successful transmission, and the average time channel is busy with a collision are set to be $\sigma = 50\,\mu$s, $T_s = 8.668$ ms, and $T_R = 8.528$ ms, respectively. Average packet transmission time is set to $T_x = 8$ ms. The minimum contention window size and the maximum back-off stage are $CW_{\min} = 32$ and $K = 5$. A TXOP and RAW duration are 1.1 ms and 500 ms, respectively. The payload size is 64 bytes. From the channel point of view, STAs' power transmission, bandwidth, and noise power are set to be $P = 1$ mW, $B = 1$ MHz, and $N_0 = -100$ dB, respectively. $(\alpha, \beta) = (0.1, 2)$ in the ACO–MM algorithm. ρ is set to be 0.05. There are 50 ants in total and the algorithm has been run for 100 iterations of ants exploration. We compare the ACO–MM algorithm with the K–means and random grouping strategies. The former is a sub-optimal distance-based approach, while the latter is a simple method with a low overhead. K-means is one of the most popular clustering algorithms and stores k centroids it uses to define clusters. A new point is considered to be in a particular cluster if it is closer to that cluster's centroid than any other centroid [33].

Fig. 2.3 depicts the accumulative throughput for different number of STAs and groups, using the ACO–MM, K–means, and random grouping schemes. In all of the cases, the ACO–MM achieves approximately 35–40% gain compared to the other two approaches. By increasing the number of STAs while the number of groups is fixed, the accumulative throughput decreases, which is reasonable due to more contention.

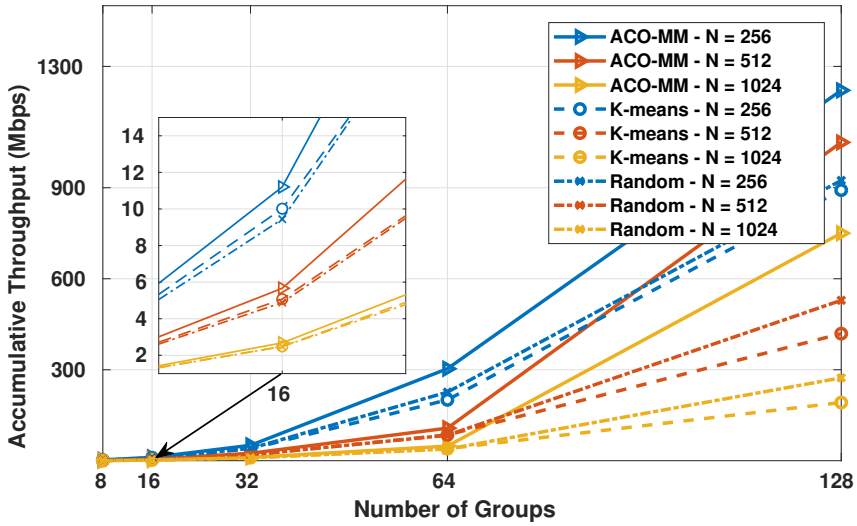

Figure 2.3: Accumulative throughput of the ACO–MM, K–means, and random grouping.

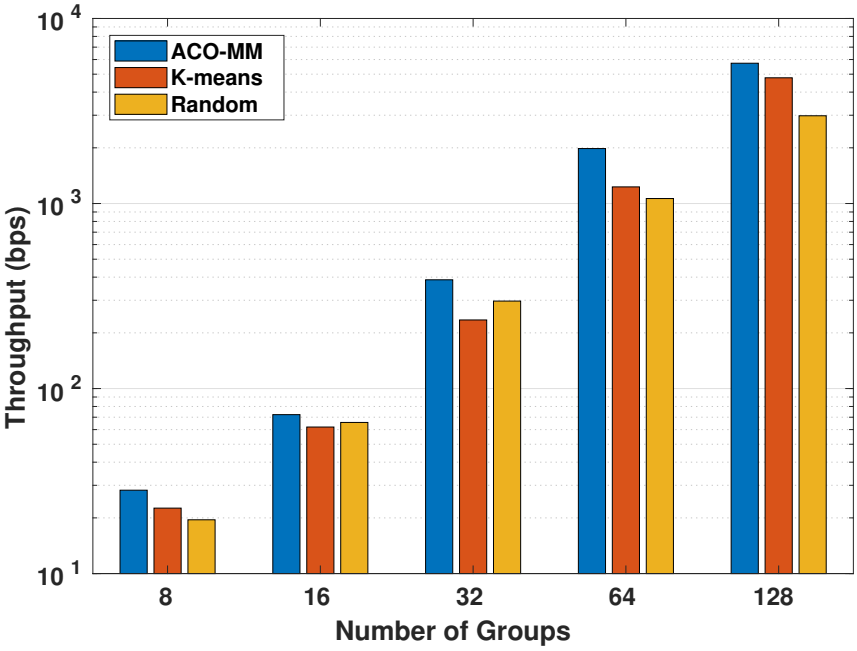

Figure 2.4: Minimum achieved throughput for $N = 2048$ and different number of groups.

Fig. 2.4 represents the minimum per-STA throughput in the network for $N = 2048$ STAs. As our objective in the optimization problem is to maximize the minimum

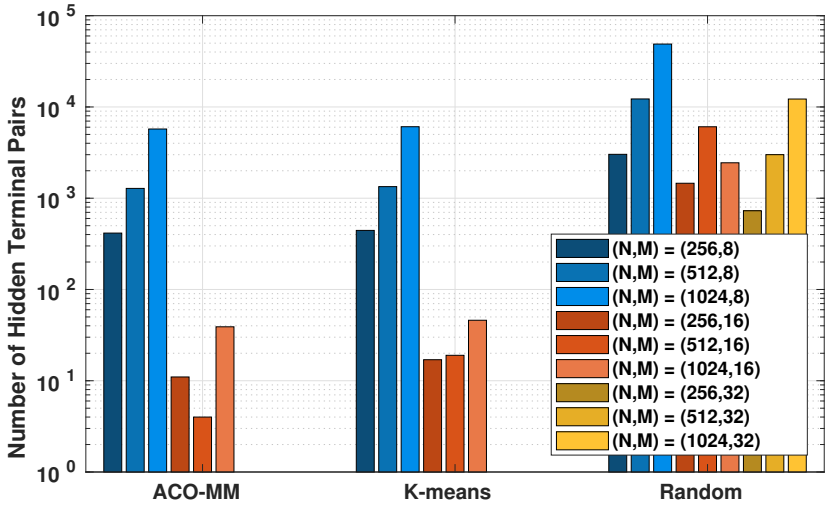

Figure 2.5: Number of hidden terminal pairs for $N = 256, 512, 1024$.

per-STA throughput, we expect that the ACO–MM has a higher minimum STA's throughput, which is confirmed in Fig. 2.4. The ACO–MM reaches up to 37% increase in the minimum per-STA throughput compared to the K–means.

The numbers of hidden terminal pairs in different schemes are presented in Fig. 2.5. There is no hidden terminal in the ACO–MM and K–means when $M = 32$. While the ACO–MM has lower numbers of hidden terminal pairs, 415 and 1281, compared to 444 and 1340 with K–means for $M = 8$ and 16, respectively. Typically, there is a fairness and total throughput trade-off for resource sharing. The 40% and 37% gains in the total throughput and minimum per-STA one are significant, and they largely attribute to the fewer hidden terminals in the ACO–MM.

2.7 Summary

A new grouping scheme for dense and large scale static networks was introduced based on the IEEE 802.11ah in this chapter to provide a fair grouping strategy from throughput point of view. The *Max-Min* throughput fairness was exploited as the criterion of the network performance. Along with assignment constraints of the problem,

an opportunistic hidden terminal avoidance constraint was applied to the problem. The problem was formulated as integer programming optimization problem. Since the problem is NP-hard, the ACO–MM was applied to the problem to accelerate finding the grouping strategy. Simulation results show that since the ACO–MM can avoid hidden terminals, it achieves a higher performance in terms of accumulative throughput, minimum throughput, and number of hidden terminals compared to the other methods.

Chapter 3

DARP: Distributed and Adaptive Reservation-based MAC Protocol

3.1 Introduction

In Chapter 2, we focused on the grouping strategy in dense IoT networks where the network is quite static. In this chapter, we study resource management in dense VANETs which is more complicated network compared to the IoT network from mobility and reliability points of view. Generating and sending beacons and safety messages constitute a key part of V2X networks. Besides the possible accidents avoidance by knowing the status of the surrounding vehicles, when a collision or accident occurs, beacons can carry important safety messages to avoid chain reaction and catastrophe. Therefore, a reliable communication protocol which works properly even in dense scenarios with resource scarcity problem is of high importance. Since there are large territories that have not been covered by network infrastructures like cellular systems, in this chapter, we focus on beacon broadcasting in VANETs using V2V communications. Therefore, vehicles' status information and safety-related messages can be disseminated timely and independently to the neighbor vehicles, no matter whether or not infrastructure is available and accessible. We explore and investigate to design an adaptive and distributed MAC protocol for vehicular networks to avoid

hidden terminal and congestion problems.

Different technologies and architectures have been proposed and developed for vehicular communication networks, including V2V communications, vehicle-to-infrastructure (V2I) communications, or a hybrid of them [34, 8]. For V2V, vehicles within each others communication range communicate directly. Thanks to the low control overhead and delay, V2V is suitable for vehicles exchanging data, including position, speed, and event-related information timely and periodically. V2I allows vehicles communicate with roadside infrastructure to coordinate and exchange data. When possible, a hybrid V2V/V2I network can allow a vehicle to communicate with the roadside infrastructures either directly (single-hop) or indirectly through a multi-hop V2V relay path [35]. To support V2V/V2I communications, U.S. Federal Communication Commission (FCC) has approved Dynamic Short Range Communication (DSRC) with seven non-overlapping channels, six service channels (SCH) and one control channel (CCH), each with 10 MHz bandwidth [36, 37].

The MAC protocol in DSRC is specified in the IEEE 802.11p standard. Similar to the IEEE 802.11 Distributed Coordination Function (DCF), it uses the carrier sense multiple access/collision avoidance (CSMA/CA) mechanism to access the shared medium [38]. However, since data collisions occur quickly when the density of vehicles increases, reliable beacon broadcasting cannot be ensured in a congested vehicular network by employing the IEEE 802.11p MAC protocol. Although we have seen various distributed congestion control (DCC) solutions, no existing solutions can fully address the reliable and scalable beacon broadcasting problem yet, given the challenges of high mobility, dynamic network topology, hidden terminal, varying density in both time and location domains, and the inherent difficulties in supporting reliable broadcast services in ad hoc networks [39].

In addition to the DSRC, the 3rd Generation Partnership Project (3GPP) has developed the cellular vehicle-to-everything (C–V2X) which is a Long Term Evolution (LTE)-based radio access technology. It enables vehicles to communicate distributedly over a sufficiently large communication range. It has also been designed to keep the

network operating both in and out of network coverage scenarios [40, 41]. The recent C–V2X standard has some shortages for dense networks too, including difficulty in collisions detection and reliability guarantee.

In this chapter, we address the broadcasting problem by carefully leveraging distributed reservation mechanism, coded preambles, and adaptation of power and resource unit parameters for effectively sharing the resources in the time/frequency/space and code domains. First, we propose a novel distributed and adaptive reservation-based beacon broadcasting MAC protocol, DARP, in which vehicles coordinate the channel access in the time and frequency domain. We employ a preamble mechanism in the frame structure to detect and resolve beacon collisions. Second, we analyze the protocol performance in terms of access collision probability and access delay. Based on the analysis, how to fine tune the protocol parameters to ensure reliability and scalability is proposed. Finally, using NS-3 [10] with vehicle traces generated by SUMO [11], extensive simulations have been conducted to validate the analysis and evaluate the performance of DARP.

3.2 Related Works

IEEE 802.11p has been proposed for wireless access in vehicular communication networks [13]. This standard does not have an efficient and acceptable performance in beacon broadcasting scenario for high density networks. Employing CSMA/CA protocol can lower the collisions, but the performance degrades dramatically when the density is very high [42]. For the broadcasting scenario, ACK and request-to-send/clear-to-send are removed due to the ACK explosion and frequent collisions, respectively. Consequently, the collisions are no longer detectable, the contention window size has to remain unchanged, and the hidden terminal problem remains unsolved [43, 44]. Furthermore, due to the small size of each beacon message and advanced techniques such as high-order modulations and multi-input-multi-output combining with a large bandwidth, e.g. 10 MHz in IEEE 802.11p, the transmission

time interval (TTI) is shorter than typical WiFi applications. When the TTI becomes closer to the propagation delay, the channel utilization performance of CSMA/CA degrades to the Aloha protocol [45]. Therefore, although time division multiple access (TDMA) protocol needs time synchronization to access different time slots, it is still one of the main choices in collision-free MAC protocols.

The existing TDMA-based protocols can be classified into two categories, centralized resource allocation and distributed medium access.

3.2.1 Centralized Protocols

Centralized control methods can effectively reduce collisions. Normally, additional control nodes or infrastructure are needed which may not be practical in remote areas. In [46], Sahoo *et al.* proposed the Congestion Controlled Coordinator based MAC (CCC MAC) where no extra control nodes are needed, and a vehicle will be selected as a coordinator for each road segment. In order to perform centralized scheduling, the global information and scheduling messages need to be collected and delivered, respectively, which increases the control overhead.

3.2.2 Distributed Protocols

The time slot-sharing MAC (SS-MAC) approach proposed in [47] supports distributed periodical message broadcasting with different beacon broadcasting rates. In this method, time slots are shared among different users after collecting occupancy states of time slots. In the state-of-the-art time slot-sharing work for vehicular communication networks, two algorithms were proposed for slot sharing and vehicle-slot sharing. SS-MAC relies on the broadcast frame information from neighbor nodes to select time slot to use, and to detect collisions. In dense networks where multiple new users within each other's communication range access the channel simultaneously, and the broadcast frames may be unreliable due to channel impairments, how to avoid and detect collisions remain an open issue. As shown in Section 3.5, such collisions be-

tween new arrivals may occur in dense network scenarios. This motivated our work, and in the proposed protocol, DARP, preambles are responsible for the avoidance and resolution of hidden terminals and collisions, and sending the preambles by different users in the communication range can reduce the negative impact of channel impairments.

In [48], a new distributed and adaptive congestion control algorithm, LInear Message Rate Integrated Control (LIMERIC), is proposed. This algorithm takes advantage of full-precision control inputs available on the wireless channel aiming to converge to a fair and efficient channel utilization. The purpose of this algorithm is to achieve fairness such that all the nodes converge to the same rate. In this algorithm, there is a trade-off between the convergence speed and the distance to the optimal value. However, the only case in which convergence can be guaranteed is when all vehicles are in range.

Javier Ros *et al.* in [49] have studied the problem of broadcasting without any infrastructure support. The aim is to enhance the reliability by minimizing the total number of retransmissions under different traffic scenarios. They focused on non-safety and delay-tolerant applications and proposed the Acknowledged Broadcast from Static to highly Mobile (ABSM) protocol which is a distributed adaptive one. Using ABSM, a vehicle in the network receiving a broadcast beacon will not retransmit it instantly. It will wait to detect whether retransmissions from other vehicles in the network cover the whole area or not. In this protocol, the vehicles which received the beacon will feedback the reception through sending an ACK. It results in a high volume of overhead in high mobility scenarios. In highly dense environments, increased beacon collisions may raise the redundant retransmissions and degrade the protocol performance [50].

In [51] and [52] a multichannel TDMA protocol has been developed based on ADHOC MAC [53]. The protocol provides a single- or multi-hop broadcasting on the CCH. Disjoint sets of time slots are assigned to the RSUs and vehicles moving in the opposite directions. This scheme can alleviate the hidden terminal problem, while the

overhead of frame transmission may lower the network throughput. Space-division-TDMA (SD-TDMA) utilizes different channels adaptively in a dynamic topology to broadcast the vehicles beacons. Since the protocol provides the vehicles geographic locations, most users can access the SCH and acquire time slots based on the provided information. A distributed protocol has been proposed in [54] which assigns a SCH to each segment of the road. Even though some feedback overhead is introduced in this protocol, time slots utilization and contention increases and alleviates, respectively.

Another TDMA-based approach is introduced in [55] as mobility-aware TDMA MAC (MoMAC). In this protocol, each frame is divided into different sections corresponding to different lanes, directions, and intersections. Two common mobility scenarios have been considered in this work which may potentially lead to an excessive level of collisions. The one-hope nodes' information is stored in the header of each packet which may increase the signalling overhead. Also, the protocol may face resource underutilization when the traffic densities in both directions are highly different. SCMAC is another MAC protocol introduced in [56] focusing on cooperative medium access control. This protocol exploits the CCH in different time slots, and the future state of the channel is broadcast through the cooperative beacon broadcasting process. The beacon broadcasting period is adaptive and determined based on the current node density. Although the protocol performance is reasonable in terms of collision probability and reliability, the hidden terminal is not considered in this work, which may cause unexpected packet losses.

Another category of existing works focuses on distributed multi-hop broadcasting. The authors in [57] proposed the DRIVE protocol in order to broadcast data in an area of interest. The problem of broadcast storm is mitigated, and the delay and control overhead can also be reduced. Bharati *et al.* proposed the Cooperative Relay Broadcasting (CRB) method in [58]. The transmission efficiency is improved in this protocol by utilizing unused slots and finding the best helper nodes.

In practice, a vehicle can analyze the received beacons, and piggyback the abstract of critical information in its own beacon broadcasting to disseminate it to a

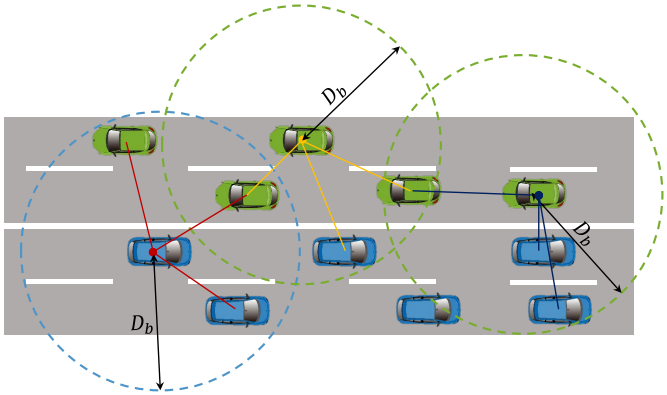

Figure 3.1: Vehicles in a VANET with beacon broadcasting range of D_b.

larger area. Most of the information included in the beacon message is just useful for the nearby vehicles and should not occupy too much wireless resources. Therefore, in this chapter, we only focus on the single-hop beacon broadcasting. In DARP, we stick to distributed control methods, in order to reduce the overhead and make the protocol usable in remote areas. Different from the majority of the distributed control methods, we apply the request-to-reserve scheme, allow dynamic transmission power adjustment, and introduce a new preamble mechanism by which the problem of hidden terminal is solved and the collision probability is significantly reduced.

3.3 System Model

Consider a VANET in which the vehicles have been distributed randomly in a multi-lane road as shown in Fig. 3.1. Short status messages, i.e. beacons, are transmitted by each user[1] periodically to notify the neighbors its presence. T and W denote the beacon broadcasting period for each vehicle and the total channel bandwidth, respectively. As shown in Fig. 3.2, in each period, channel time is divided into some slots, and channel bandwidth is divided into sub-channels. Time synchronization is achieved assuming that each vehicle can use the global positioning system (GPS) for global synchronization. Within a beacon broadcasting period, a time slot in one

[1]The words "user" and "vehicle" are used interchangeably throughout this chapter.

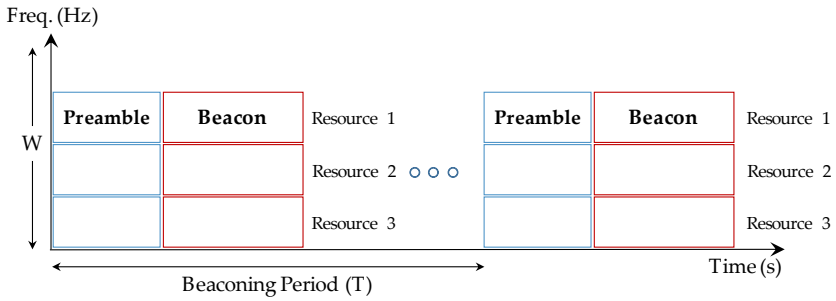

Figure 3.2: Available resources in one beacon broadcasting period and bandwidth of W, in DARP.

sub-channel is defined as a resource unit.

Each resource unit consists of two parts, one for the preambles (short control messages) and the other for the beacons (which carry the data). The preambles are used to detect reservation and beacon collisions. It is assumed that once a resource unit is reserved successfully by a vehicle for beacon broadcasting, it will not be released until the vehicle leaves the system or collision happens due to topology change. Also, it is assumed that each user has a packet or beacon ready for transmission at the beginning of the reserved time slot.

For the wireless channel model, we consider the path-loss determined by the transmission distance between the vehicles. The path-loss model in device-to-device communications can be applied here [59]. The relationship between the reception and the transmission power as a function of the distance between the transmitter and receiver, d, is given by $P_r = P_t K_0 d^{-\alpha}$, where K_0 is a constant depending on the channel and antenna characteristics, and α is the path-loss exponent. The Signal-to-Interference-plus-Noise Ratio (SINR) between two vehicles, v_i and v_j, is given by

$$\text{SINR}_{ij} = \frac{P_{t,i} K_0 d^{-\alpha}}{I_j^x + N_0}, \tag{3.1}$$

where $P_{t,i}$ is the transmission power of v_i and N_0 represents the noise power. Assuming v_i is using the resource x, I_j^x is the interference power received by v_j on the same resource. In this chapter, v_j, a neighbor of v_i, can successfully receive a beacon from v_i if the received SINR is greater than the threshold Γ, i.e. $\text{SINR}_{ij} \geq \Gamma$, and we name

v_j as an effective neighbor of v_i. Γ should be set based on the MCS that is used for the beacon broadcasting, and may be fixed in a zone.

3.4 Protocol Design

DARP design objectives and its accessing procedure are explained in the following subsections, respectively.

3.4.1 Design Objectives

To ensure reliable and scalable beacon broadcasting, the design objectives of DARP are summarized as follows. (I) The probability of beacon collision should be maintained low, and collisions should be detectable and be stopped timely. (II) When new vehicles try to access (or re-access) the network, the vehicles which have already occupied resources should not be affected. (III) The wireless spectrum resource is precious, so it should be efficiently utilized in order to support as many users as possible, especially in high density scenarios. (IV) As the focus of this paper is on the beacon broadcasting scheme, a stable and periodic transmission should be guaranteed if a vehicle has successfully occupied a resource. (V) Overshooting the beacon broadcasting range is undesirable, so beacons should be received by a target number of neighbors regardless of the topology. (VI) The protocol should work in any places, including the remote areas without any infrastructure, and it should be scalable for high density networks.

As mentioned in Section 3.2, CSMA/CA-based protocols alone cannot satisfy the above design objectives for beacon broadcasting. Since the beacon broadcasting procedure has a predictable transmission pattern (the users have beacons to broadcast at the beginning of each frame) and fixed data size[2], reservation solutions are more suitable. Hence, we propose a distributed reservation scheme to ensure relia-

[2]The assumption of *fixed data size* means a fixed MAC layer protocol data unit (MPDU), which is the unit of maximum data size exchanged between MAC entities.

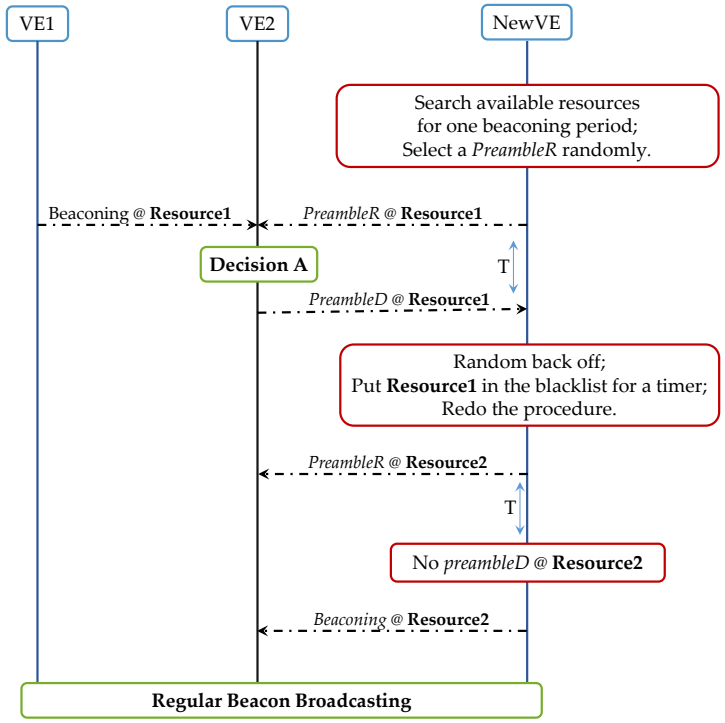

(a) Case I

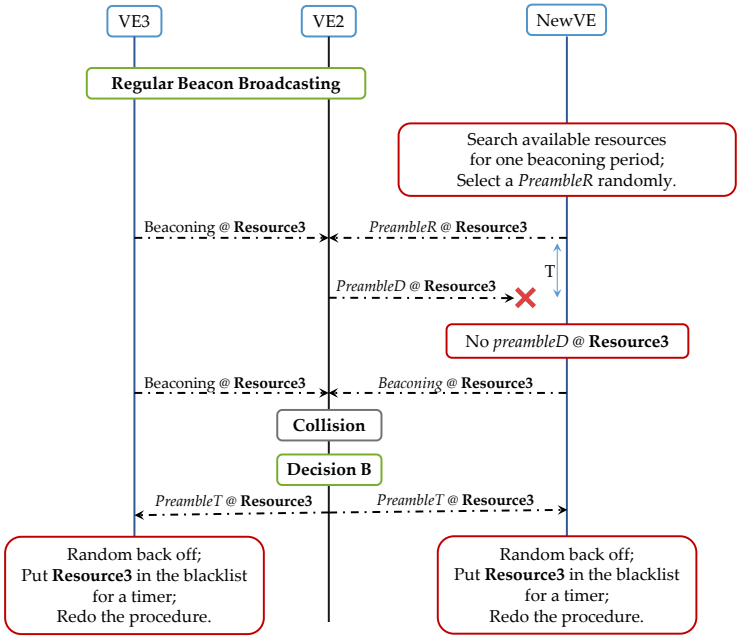

(b) Case II

Figure 3.3: Diagram of DARP in accessing and beacon broadcasting process.

bility and scalability. Once a resource is reserved successfully, the vehicle can use it periodically. Therefore, if the topology is given and fixed over a certain period of time, the number of users successfully reserving the resource for beacon broadcasting can be monotonically increased.

The preamble mechanism has been used in cellular systems as an effective way even in superdense scenarios [60]. Preambles are responsible for collision detection, and by employing orthogonal preambles, the code dimension diversity is obtained, which can help to detect and avoid access collisions without affecting the existing beacon broadcasting users. Although preambles introduce more signaling overhead, the overhead is negligible compared to the achieving gain and collision-free communication. The preamble combined with distributed reservation can address the first four design objectives mentioned above.

In order to ensure the applicability of DARP in remote areas, the distributed reservation solution is adopted. Although a centralized control may further enhance the performance based on the global information, significant control overhead will be introduced by collecting requests and sending scheduling decisions, which may sacrifice the performance gain. To guarantee a certain number of neighbors can effectively receive the beacons, a distributed dynamic power control method is introduced as well. These two methods can ensure that the last two objectives can be satisfied.

3.4.2 Accessing and Beacon Broadcasting Procedure

Preambles are sequences which are responsible for collision detection and facilitation of accessing the channel. These sequences are generated from cyclic shifts of root Zadoff–Chu sequences. The amplitude of the sequences is constant which provides low peak-to-average-ratio from the implementation point of view. Moreover, the cross-correlation between any two preambles of the same Zadoff–Chu root sequemce is zero based on which there is no interference from reception of different preambles [61].

In DARP, four types of preambles are defined, regular ($preambleR$), data trans-

mission (*preambleDT*), decline (*preambleD*), and terminate (*preambleT*), which are used for channel access, data transmission, access request rejection, and transmission stop, respectively. Since the preambles are coded in a way that are orthogonal to each other, a receiver can detect all the preambles transmitted simultaneously in the same resource unit. *PreambleR* is used to make reservation, and *preambleD* is deployed to solve the hidden terminal problem. Detecting and resolving beacon collisions caused by topology changes can be done by *preambleDT* and *preambleT*, respectively. In this chapter, we assume that there are 64 available preambles.

Among these 64 preambles, 50, 12, 1, and 1 preambles are allocated to *preambleR*, *preambleDT*, *preambleD*, and *preambleT*, respectively [60].

Considering Fig. 3.3 as an example, we explain how DARP works. In Case I, a new vehicle (*NewVE*) tries to enter the network with two existing vehicles, *VE1* and *VE2*. *VE1* and *NewVE* cannot sense each other, while *VE2* can sense both of them. First, in order to make a reservation, *NewVE* needs to listen to the channel for one beacon broadcasting period to identify which resource units have not been occupied. Then, it selects one of the resource units randomly and sends a reservation message which is a *preambleR* on the chosen resource unit.

Decision A is made if a vehicle receives either a *preambleR* for the resource unit currently occupied by its neighbors, or multiple *preambleR*s for the same resource unit are received simultaneously. Since the preambles are orthogonal to each other, vehicles are capable of detecting multiple preambles at the same time. In the case that some vehicles choose the same *preambleR* in order to occupy a resource, the selection process will be successful. However, in the next period, beacon collision will be detected by colliding or other existing vehicles.

Upon receiving a *preambleR*, the existing vehicles check whether a *Decision A* should be made. In Case I, Fig. 3.3(a), when *VE2* receives *NewVE*'s *preambleR* for Resource1 while Resource1 has been occupied by *VE1*, it makes a *Decision A* and sends a *preambleD* in the next period to *NewVE* at the preamble part of Resource1. If *NewVE* cannot use the chosen resource due to the reception of *preambleD*, it will

put the resource in a blacklist for a random period of time and select another resource unit right after reception of *preambleD* to make a reservation. On the other hand, if *NewVE* picks an unoccupied resource, sends a *preambleR*, and does not receive any *preambleD*s in the next period at the chosen resource, the reservation is successful and it can occupy the resource unit. Right after elapsing the preamble part of the chosen resource, the vehicle can start the beacon broadcasting process.

However, if two vehicles select the same resource and the same *preambleR* for reservation, both of them will find their reservations successful. To address this issue, for each beacon transmission, each vehicle always randomly selects a *preambleDT* and sends it in the preamble part, by which the beacon collisions can be quickly detected and resolved.

A *Decision B* is made when a vehicle receives non-decodable beacons in succession, or receives different *preambleDT* at the same resource. Consequently, a *preambleT* will be sent out at the chosen resource. Upon receiving a *preambleT*, the vehicle should put the resource in the blacklist for a timer and access the network again. In Case II, Fig. 3.3(b), the case with an error in receiving *preambleD* on *Resource3* has been shown. Failure in reception of *preambleD* which may be due to transmission error or interference, causes channel access for NewVE. In this case, two users, VE3 and NewVE, send beacon on a signle resource. If they use two different *preambleDT*, VE2 will detect a collision and make Decision B. By making this decision, it will send a *preambleT* on *Resource3* and both of the users will release the resource. In the rare case that NewVE choose the same *preambleDT* as VE3 is using, VE2 receives non-decodable beacons in succession and similarly, it detects a collision and sends a *preambleT* to terminate the beacon broadcasting.

3.5 Performance Analysis and Parameter Optimization

In this section, we first investigate *Access Collision Probability* and *Access Delay* as the performance metrics to evaluate the protocol performance. Then, we study how to optimize protocol parameters to enhance the performance.

3.5.1 Access Collision Probability

Access collision probability is defined as the probability that at least two vehicles access the same resource. In this subsection, we derive the probability mass function (PMF) of the access collision. Since the dynamic change of available resources and chain collisions are not considered here, the analysis is an approximation.

We assume a fixed topology which has N_v vehicles and N_a available resources. Obviously, the number of resources should be greater than or equal to the number of vehicles, i.e. $N_a \geq N_v$. Otherwise, some vehicles may never access the channel and access collision is unavoidable. In order to find the number of collisions, the resources occupied by at least two vehicles should be counted. To give a better insight, we can model the problem as a problem of distributing N_v distinguishable balls among N_a distinguishable baskets. For the case of zero collision, it is simple and straightforward. The total number of ways assigning N_a baskets to N_v balls in a way that each basket has at most one ball equals to

$$\frac{N_a!}{(N_a - N_v)!}. \tag{3.2}$$

Before we move to the next part, the number of ways which m balls can be distributed in k baskets in such a way that all these k baskets have at least p balls should be found. This problem is called p-associated Stirling number of the second kind, $S_p(m, k)$. The triangular recurrence relation for these numbers is [62]

$$S_p(m+1,k) = k\,S_p(m,k) + \binom{m}{p-1} S_p(m-p+1,k-1). \tag{3.3}$$

For the case of $p = 2$, it is simplified as

$$S_2(m+1,k) = k\,S_2(m,k) + m\,S_2(m-1,k-1). \tag{3.4}$$

The problem can be divided into different cases. Here, C_{mi} represents the total number of combinations where m is the number of baskets with more than one ball, while i indicates the number of baskets with exactly one ball. For the case that $i = 0$, we select N_v balls and m baskets in $\binom{N_v}{N_v}$ and $\binom{N_a}{m}$ ways, respectively. The baskets have $m!$ permutation among each other. Also, there are $S_2(N_v, m)$ ways that these N_v balls can be distributed among m baskets with the condition that each basket has at least two balls. Therefore, the total number of combinations will be

$$C_{m0} = \binom{N_v}{N_v} \binom{N_a}{m} m! S_2(N_v, m). \tag{3.5}$$

In the next step, we can generalize this distribution for an arbitrary i. $(N_v - i)$ balls are chosen to be distributed in m baskets in $\binom{N_v}{N_v - i} S_2(N_v - i, m)$ ways. Also, there are $\binom{N_a}{i+m} (i+m)!$ ways to choose $(i+m)$ baskets among N_a baskets. Therefore, the total number of combinations in this case is

$$C_{mi} = \binom{N_v}{N_v - i} \binom{N_a}{i+m} (i+m)! S_2(N_v - i, m). \tag{3.6}$$

It is obvious that the variable i starts from zero and its maximum value is $(N_v - 2m)$. The extreme case happens if $2m$ balls are chosen for m baskets, and the remaining $(N_v - 2m)$ balls are assigned to i different baskets. The total number of choices in

which m baskets have more than one ball is the summation of C_{mi} over i. The total number of possible choices in distributing N_v balls among N_a baskets and collision states are $N_a^{N_v}$ and $\left\lfloor \frac{N_v}{2} \right\rfloor$, respectively. If A_m is defined as the event in which m resources are in collision, $P(A_m|N_v, N_a)$ will be the corresponding probability. This probability is

$$P(A_m|N_v, N_a) = \sum_{i=0}^{N_v-2m} \binom{N_v}{N_v-i} \binom{N_a}{i+m} \frac{(i+m)! S_2(N_v-i, m)}{N_a^{N_v}}. \tag{3.7}$$

It is worth mentioning that if the N_v's PMF is known, a more precise access collision probability will be achieved.

3.5.2 Access Delay

The access delay is defined as the time duration needed by a new vehicle to access a resource successfully for beacon broadcasting. It is assumed that the number of vehicles contending for the resources is stable. Once a vehicle tries to access a resource, if it is not allowed to use it, it will receive a *preambleD* from the neighbors and if there are not any, the vehicle itself will detect the occupied resource. Afterward, it attempts again to choose another resource. Reception of a *preambleD* is due to two different cases, (a) access collision, (b) collision with a hidden terminal.

In order to find the probability of failure in accessing a resource, we define D_b as the beacon broadcasting range in which the vehicles can receive the broadcast beacon. This range can be determined based on the SINR threshold. We consider two regions around a tagged vehicle, namely S_1 and S_2 corresponding to $0 \leq r \leq D_b$ and $D_b \leq r \leq 2D_b$, respectively. S_1 contains N_v vehicles contending for the available resources, and the vehicles in S_2 are treated as hidden terminals. We define S_1 and S_2 regions only for the preamble transmission, since they are responsible for collision detection and hidden terminal avoidance. Preamble and beacon may have different transmission ranges, but we intentionally make the preamble range the same

as the beacon one by setting an appropriate preamble SINR target. In this way, preamble and beacon can have the same range in the analysis. This assumption leads to conservative analytical results.

The access failure probability is as follows.

$$P_f = \sum_{m=0}^{\lfloor \frac{N_v}{2} \rfloor} \left[1 - \frac{N_a - m}{N_a} \frac{N_a - 2D_b\lambda}{N_a} \right] P(A_m | N_v, N_a), \tag{3.8}$$

where λ is the vehicle density, and the terms $\frac{N_a - m}{N_a}$ and $\frac{N_a - 2D_b\lambda}{N_a}$ are corresponding to successful channel access in S_1 and S_2 regions, respectively. The probability of having a successful channel access after X failed trials follows a Geometric distribution which for $k = 1, 2, 3, \ldots$ is

$$Pr\{X = k\} = {P_f}^{k-1} (1 - P_f). \tag{3.9}$$

Therefore, the expected value of k is $\frac{1}{1-P_f}$. Once a vehicle is going to access a resource, first, it will search available resources for one period. When a resource is selected and *preambleR* is transmitted, the vehicle will be notified whether it can use the resource after a period of time, T. If not, it will attempt to access another resource. The duration between reception of the notification and the next try (including the very first resource selection after scanning the available resources) is a random variable, z, following a Uniform distribution, $z \sim U(0, T)$, and obviously, its mean is $T/2$. Now, based on this analysis, the access delay can be calculated as follows.

$$\mathbb{E}[Access\ Delay] = T + \left(T + \frac{T}{2} \right) \frac{1}{1 - P_f}. \tag{3.10}$$

Here, we assumed that the users in S_2 are occupying different resources from the users in S_1 which is an extreme case. Based on the assumptions, the obtained access delay will be an upper-bound of the delay in the real scenario.

In order to make DARP scalable, two parameters can be optimized. The first one is the total number of available resources per period, N_a. It is obvious that a larger number of resource units can reduce the access collision probability. This

parameter can be increased by either reducing the time duration of each resource, L_b, or increasing T. However, the maximum period of beacon broadcasting should be determined by the quality of service requirements. Therefore, we only focus on the former case. We cannot blindly choose the shortest resource length because assuming a fixed packet size, a shorter length results in a higher beacon transmission rate, and a higher receiving SINR is required. In the following analysis, we optimize the length of each resource based on the number of effective neighbors, MCS selections, and the target SINR.

The second optimization parameter is the transmission power. In DARP, rather than using a fixed power, each vehicle is allowed to adjust its transmission power in a distributed way. A larger power may not necessarily increase the received SINR and the number of effective neighbors. The reason is that it also increases the interference which consequently decreases the SINR, and results in less number of effective neighbors. Different from existing works on the power control issue in VANET [63, 64, 65], we set beacon transmission power not only based on the density of the vehicles, but also on the selected MCS, the target SINR, and the number of effective neighbors.

These two parameters can be optimized according to different objective functions, such as minimizing the average access delay, maximizing the average number of effective neighbors, etc. In this chapter, we assume that a target average number of effective neighbors, N, can be guaranteed, then collision probability, P_C, will be minimized by adjusting vehicle's transmission power P_t and L_b. P_t will not exceed the vehicle's maximum transmission power, $P_{\max}$, and we also assume a minimum transmission power, $P_{\min}$, to ensure the minimum range of the beacon broadcasting. Therefore, $P_t \in [P_{\min}, P_{\max}]$. On average, the total available resources, $\frac{T\,N_{ch}}{(L_p+L_b)}$, will be occupied by all of the vehicles on a length of D_r when it is free to be occupied. The average number of vehicles on a length of D_r is $D_r\lambda$. Therefore, the average reuse distance for a resource is given by

$$D_r = \frac{T\,N_{ch}}{(L_p + L_b)\,\lambda}, \tag{3.11}$$

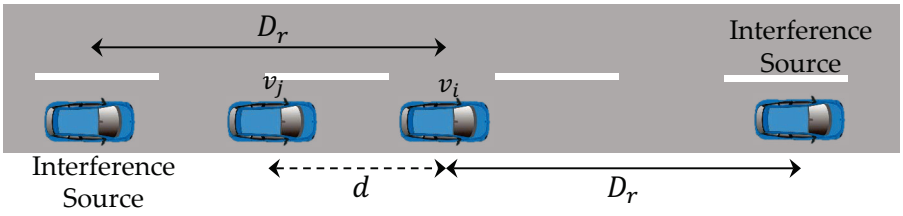

Figure 3.4: The reuse distance from two interference sources.

where N_{ch} and L_p are the number of available sub-channels and duration of a preamble, respectively. The reuse distance is shown in Fig. 3.4. We consider the closest interfering vehicles on each side (in front and behind) as the dominant interference sources. Therefore, the SINR as a function of distance is

$$\text{SINR} = \frac{P_t\, K_0\, d^{-\alpha}}{N_0 + P_t\, K_0\, (D_r - d)^{-\alpha} + P_t\, K_0\, (D_r + d)^{-\alpha}}. \tag{3.12}$$

In order to bound the SINR to Γ at $d = D_b$, equation $f(D_b) = \Gamma$ should be solved.

Given a fixed block error rate, the relationship between Γ and MCS can be found in [60]. For a fixed size of the beacon, if L_b is reduced, the transmission rate needs to be increased, and thus a higher SINR threshold should be applied. Therefore, Γ is a function of L_b, i.e. $\Gamma = g(L_b)$. Based on [60], $g(.)$ is a monotonically decreasing function.

Based on the total vehicle density, the average number of effective neighbors in the beacon broadcasting range is estimated by $N = 2\lambda D_b$. By substituting equation (3.11) and simplifying the equation $\Gamma = f(D_b)$, the following equation will be obtained.

$$\frac{1}{\Gamma} = \frac{N_0}{P_t K_0}(\frac{2\lambda}{N})^{-\alpha} + (\frac{2\lambda D_r}{N} - 1)^{-\alpha} + (\frac{2\lambda D_r}{N} + 1)^{-\alpha}. \tag{3.13}$$

Between two adjustable parameters in the above equation, L_b should be coarsely set according to different areas such as downtown, uptown, highway, and etc. L_b can be known for the vehicles based on the predefined information associating with the GPS location. Therefore, when a vehicle enters a district with different setting of L_b, it will release the previous occupied resource and re-access the network using the new

setting of L_b.

Each vehicle can adjust its transmission power based on the vehicle density in a smaller region around it. However, we roughly assume a homogeneous distribution for all vehicles in a large region, so the average density is used to facilitate the selection of L_b. If N_v is given, the objective function of the optimization problem is the access collision probability, P_C. By minimizing the access collision probability, the access delay will be minimized as well. The PMF of access collisions was obtained in Section 3.5.1.

Minimizing the access collision probability is equivalent to maximizing the number of available resources. In other words, the more resources are available, the lower the access collision probability is. Thus, we can consider the total number of available resources as the objective function with the same constraints. The total number of available resources equals to

$$\begin{aligned} N_a &\approx (D_r\lambda - N)^+ \\ &= \left(\frac{TN_{ch}}{L_p + L_b} - N\right)^+, \end{aligned} \tag{3.14}$$

where $t^+ = \max(0, t)$. Considering the existing MCS table and fixed-size beacon message, L_b should be chosen within several choices.

To maximize N_a in (3.14), a search on the possible L_b choices should be run in the ascending order. Based on the achieved L_b and (3.13), P_t will be calculated and the search will end once the power constraint is satisfied. Since N_a decreases monotonically with L_b, the search procedure can give the optimal result. If all the possible options of L_b cannot satisfy the power constraint, the L_b corresponding to the largest non-negative P_t, $P_t < P_{\min}$, should be selected. It guarantees the average number of effective neighbors, while does not overshoot it too much. On the other hand, if all the possible values of P_t are negative when $P_t < P_{\min}$, the one corresponding to the smallest non-negative P_t is the solution.

Different average densities result in different optimal L_b. The performance of the

above procedure can be examined by $\lambda_{\max}$ and $\lambda_{\min}$ for the peak and off-peak hours, respectively. Once the optimal L_b is obtained, by estimating the real-time vehicle density, $\hat{\lambda}$, and substituting it in (3.13), the corresponding power is calculated.

Remark: The total number of available resources in the protocol is a function of each resource duration, L_b, and the total number of channels. For the case that the protocol is confronted an ultra-dense environment where the power control scheme is not deployed and L_b is fixed, there may be some users which cannot acquire any resource and lead to starvation. To solve this issue, power control or other congestion control mechanisms should be devised, which could be important further research topics.

3.6 Simulation Results

This section presents the performance assessment of DARP simulated by NS-3 driven by SUMO traces. SUMO is a microscopic traffic flow simulator which can generate real vehicle routes and simulate how traffic changes in a large road network. To generate a traffic trace, SUMO needs a road map which can be defined directly or be imported. NS-3 uses the SUMO's output trace file to define the vehicles' position and change their driving route dynamically [66]. Using this platform, extensive simulations have been conducted to evaluate DARP in two different scenarios: (I) a linear network, and (II) a map-based network. For each of these scenarios, four different MAC approaches have been used and compared, including DARP, DARP without power control (W/O PC), IEEE 802.11p, and IEEE 802.11p with power control (W/ PC). In the simulation, DARP is implemented as follows. Each vehicle keeps a list recording the status of all resource blocks. The operation of each vehicle is based on the knowledge from the list. Multi-channel devices are installed such that the vehicles can listen to all channels and broadcast their beacons on the selected resources. IEEE 802.11p is implemented based on the existing NS-3 modules with data rate of 3 Mbps and beacon broadcasting range of 250 m. The physical layer platform used for DARP

Table 3.1: Transmission Power for Different Vehicle Densities

Beacon duration	$N = 10$		$N = 15$	
	λ (Vehicle/km)	Power (dBm)	λ (Vehicle/km)	Power (dBm)
$L_b = 1\,\text{ms}$	[0.054, 0.4]	$[-7, 25]$	[0.081, 0.4]	$[-0.45, 25]$
$L_b = 2\,\text{ms}$	[0.036, 0.054]	[18.7, 25]	[0.055, 0.081]	[18.76, 25]
$L_b = 3\,\text{ms}$	[0.0295, 0.036]	[21.94, 25]	[0.044, 0.055]	[21.65, 25]
$L_b = 6\,\text{ms}$	[0.02, 0.0295]	[19.6, 25]	[0.031, 0.044]	[19.7, 25]
	< 0.02	25	< 0.031	25

Table 3.2: MCS and Beacon Duration

Order	MCS	SINR range (Γ)	Beacon duration
0	Transmission failed	$(0, 0.6]$	—
1	QPSK, Rate 1/3	$(0.6, 2.135]$	$L_b = 6\,\text{ms}$
2	QPSK, Rate 2/3	$(2.135, 4.565]$	$L_b = 3\,\text{ms}$
3	16-QAM, Rate 1/2	$(4.565, 19.498]$	$L_b = 2\,\text{ms}$
4	64-QAM, Rate 2/3	$(19.498, \infty)$	$L_b = 1\,\text{ms}$

is the same as IEEE 802.11p in which the total number of subcarriers and symbol interval are 52 and 8 μs, respectively. The bandwidth of the IEEE 802.11p system and DARP are 10 MHz and 50 MHz, respectively. The packets are successfully received by a vehicle if the received SINR is more than the determined threshold, and failed when there are more than one transmitters using the same resource block within the receiver's beacon broadcasting range i.e., the received SINR is not high enough.

The transmission power for different vehicle densities can be calculated using (3.11) and (3.12) based on the target SINRs 0.6, 2.135, 4.565, and 19.498 which corresponds to the beacon duration of 6 ms, 3 ms, 2 ms, and 1 ms, respectively. The results for $N = 10$, 15 can be found in Table 3.1. In DARP simulation, we applied four different MCS options which the target SINR range given 10% block error rate and the corresponding beacon duration are summarized in Table 3.2 [60, 67]. The simulation

Table 3.3: Simulation Parameters

Parameter	Value
Simulation time	19 s
Average vehicle speed	70 km/h
Beacon broadcasting period	84 ms
Beacon size	375 Byte
Number of channels DARP	5
IEEE 802.11p	1
Channel bandwidth	10 MHz
Noise spectral density	-174 dBm/Hz
Maximum transmission power	25 dBm
Maximum beacon broadcasting range	250 m
Modulation DARP	QPSK, 16-QAM, 64-QAM
IEEE 802.11p	QPSK
Number of preambles	64
Preamble duration	1 ms
Path-loss coefficients (α, K_0)	(3.68, $10^{-4.38}$)

parameters are summarized in Table 3.3. The channel model used in the simulation is the path-loss model described in Section 3.3. Ordinarily, the beacon broadcasting period is 100 ms [68]. However, in the simulations, the beacon broadcasting period is set to 84 ms which is the least common multiple of resource duration for different MCSs. We used the beacon loss ratio (BLR) as a performance metric for the protocols comparison. This metric is defined as

$$\text{BLR} = 1 - \frac{\#\text{ of received beacons}}{\#\text{ of expected beacons to be received}}. \tag{3.15}$$

For the linear networks simulation, we consider a road with effective length of 2 km, meaning that the road length is more than 2 km to avoid the users on the edge with less neighbours. The results from DARP and DARP W/O PC are compared to the results from IEEE 802.11p and IEEE 802.11p W/ PC.

Fig. 3.5 compares the access delay simulation results with the analytical ones for different vehicle densities. The beacon broadcasting range of the vehicles is set to

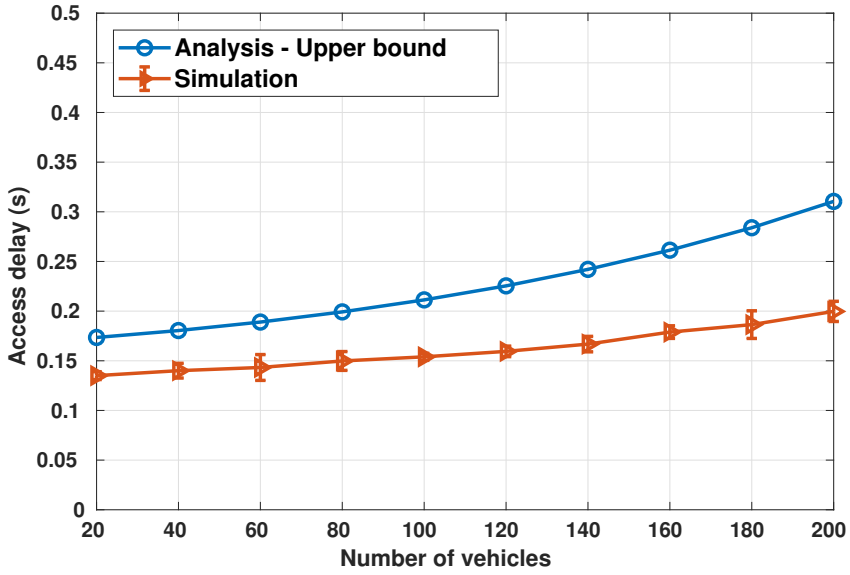

Figure 3.5: Comparison of access delay for different number of vehicles.

250 m and the power control mechanism is not deployed to have a fair comparison with the theoretical results. The beacon duration is set to 1 ms and there are totally 210 available resources. The simulations have been run ten times, and the average values along with the standard deviations have been graphed. As it was mentioned in Section 3.5.1, the derived access collision probability and access delay are approximations. Thus, the analytical results give an upper bound of the access delay. There is a small gap between the bound and the access delay in the simulation, and the gap tends to be higher when the density is very high and the chain collisions occur more frequently. Nevertheless, from Fig. 3.5, even when the density of the vehicles increases by a fold of ten, the access delay merely increases to around 0.25 seconds. Thus, the proposed DARP is scalable, and can guarantee an almost stable access delay up to a certain number of users.

Fig. 3.6(a) and Fig. 3.6(b) present the BLR and the number of received beacons for different vehicle densities, respectively. The simulations have been run for two different numbers of effective neighbors. It can be seen from the results that DARP protocol has a one- to two-order lower BLR in comparison to that using the

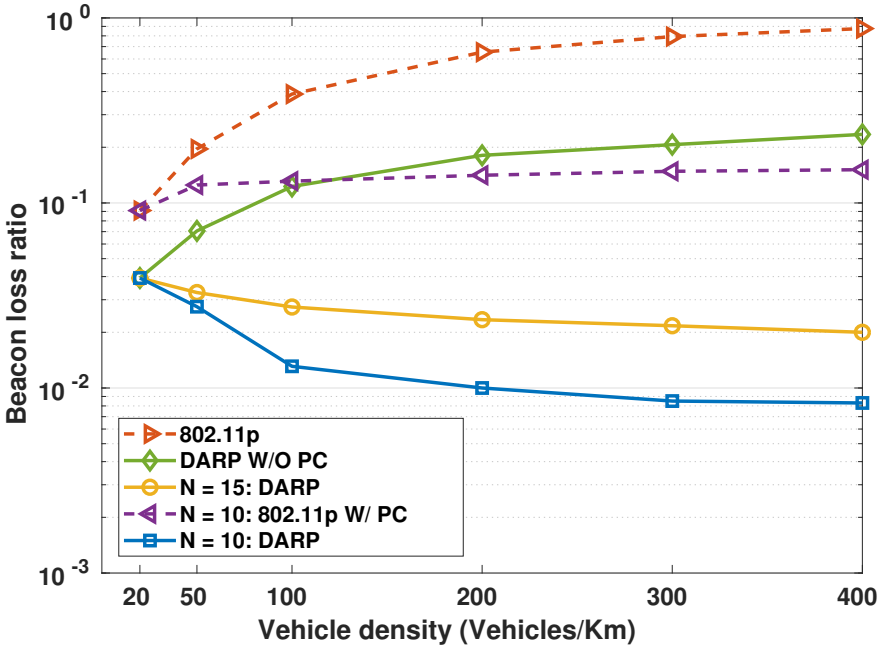

(a) Beacon loss ratio

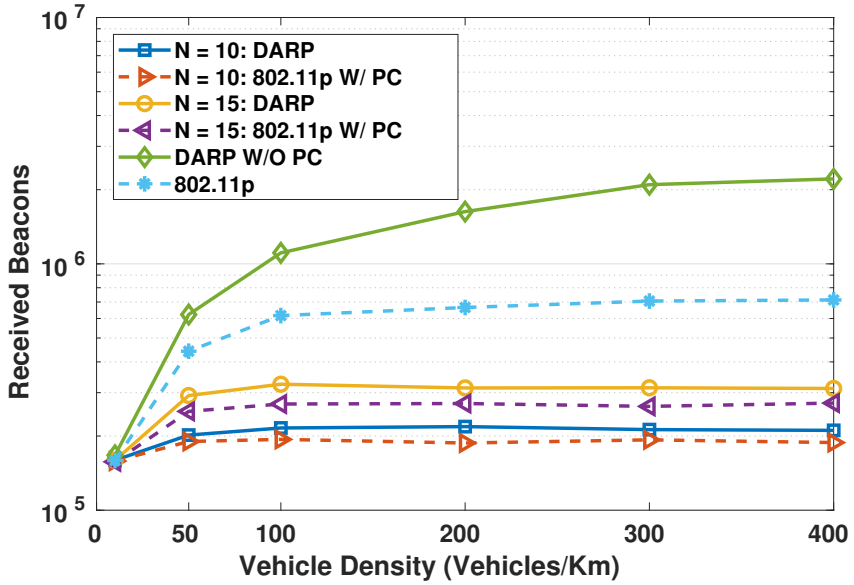

(b) Received beacons

Figure 3.6: Linear network.

IEEE 802.11p protocol. For IEEE 802.11p W/ or W/O PC, and DARP W/O PC, the loss ratio increases when the vehicle density increases, due to heavier collisions. The BLR using DARP remains around 0.01 when the vehicle density is above 100

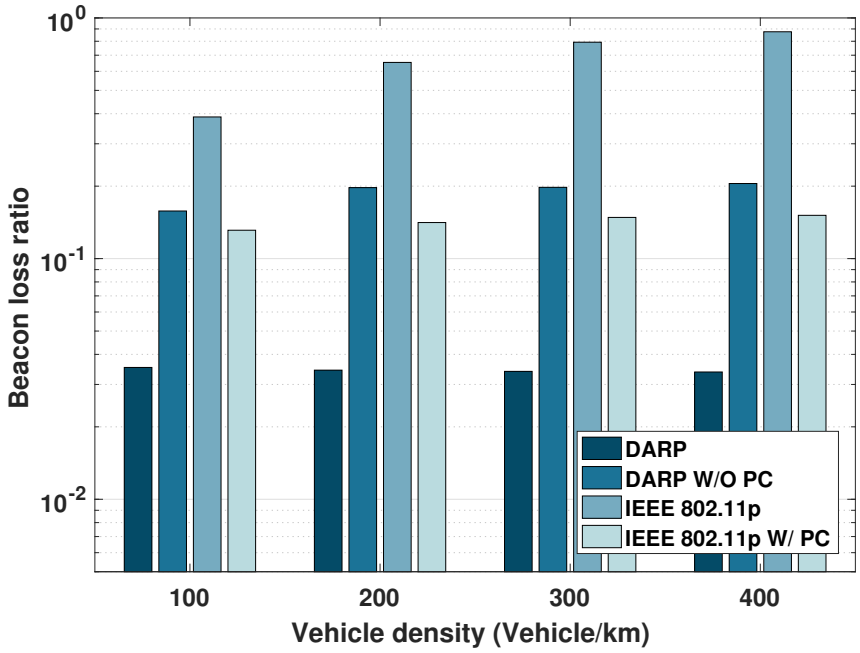

Figure 3.7: Comparison of beacon loss ratio for different protocols for $N = 10$, with the same bandwidth, $W = 10$ MHz.

vehicles/km. When the density is low, due to a larger distance between vehicles and higher transmission errors, the loss rate is higher. Hence, we note that the loss ratio for DARP is slightly higher when the density is much lower than 100 vehicles/km. As it is expected, the performance of IEEE 802.11p in terms of BLR is degrading by increasing the density, while DARP achieves 96% and 75% gains in W/ PC and W/O PC scenarios, respectively. Due to occupying all of the available resources, the BLR will reach the saturated state by increasing the vehicle density.

By increasing the vehicle density, it is expected to have more received beacons in all of the schemes which is verified by the results in Fig. 3.6(b). The figures in Fig. 3.6 can be considered jointly. From Fig. 3.6(b), more beacons can be received in DARP compared to the IEEE 802.11p (for both W/ and W/O PC). From Fig. 3.6(a), it is observed that due to less collision probability and less hidden terminals, the proposed protocol when bundling five 10 MHz channels can achieve lower BLR compared to IEEE 802.11p that uses only one default channel. According to these figures, DARP

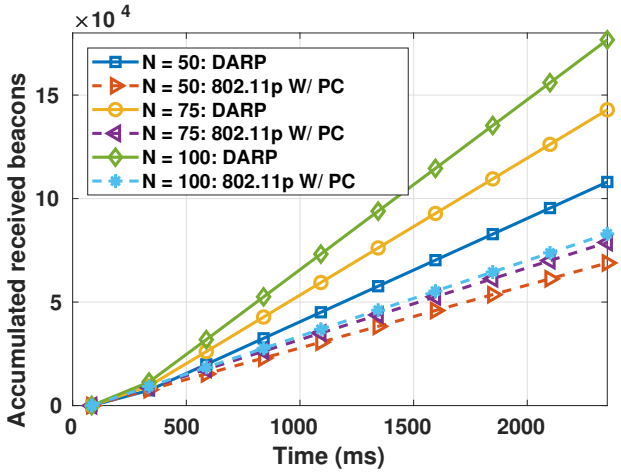

(a)

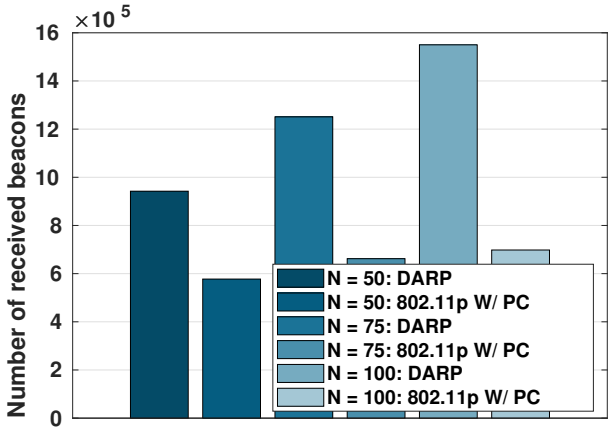

(b)

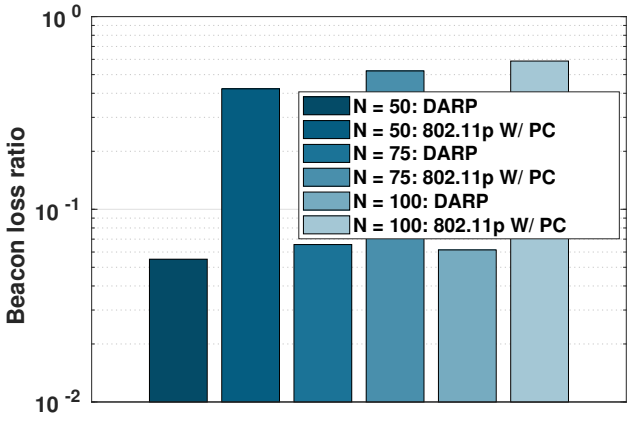

(c)

Figure 3.8: Accumulated received beacons, number of received beacons, and beacons loss ratio for the ultra-dense scenario

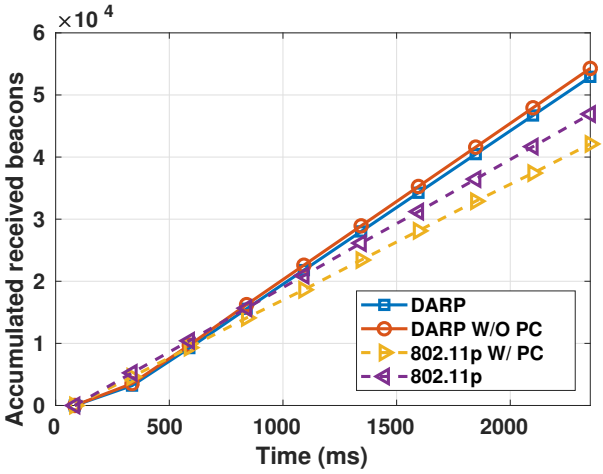

(a)

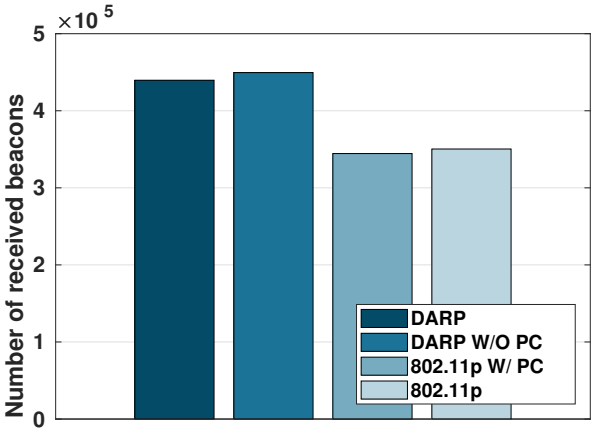

(b)

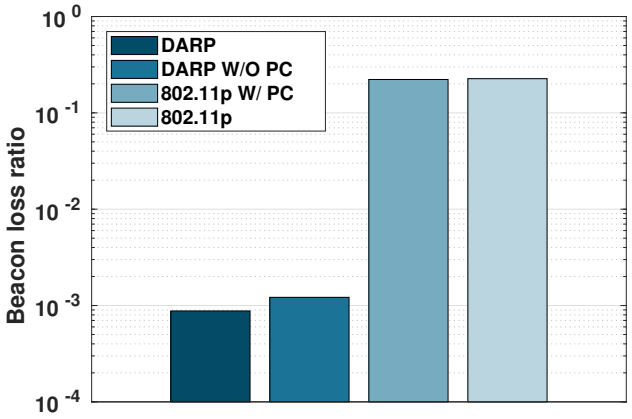

(c)

Figure 3.9: Accumulated received beacons, number of received beacons, and beacons loss ratio for the City1 scenario

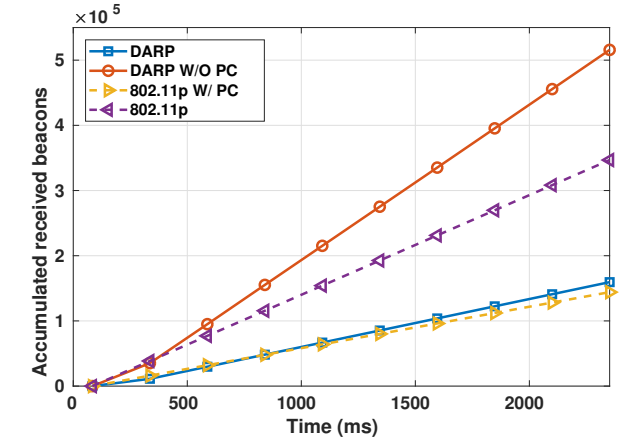

(a)

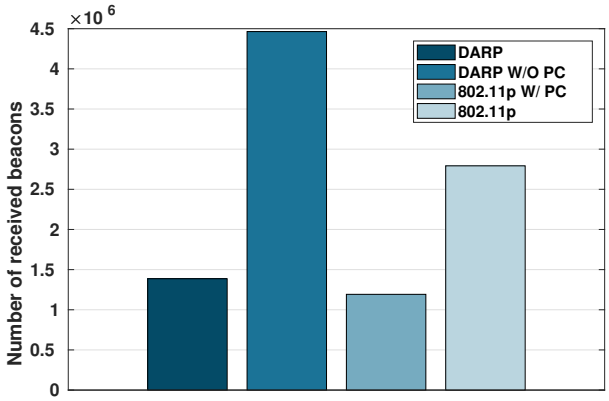

(b)

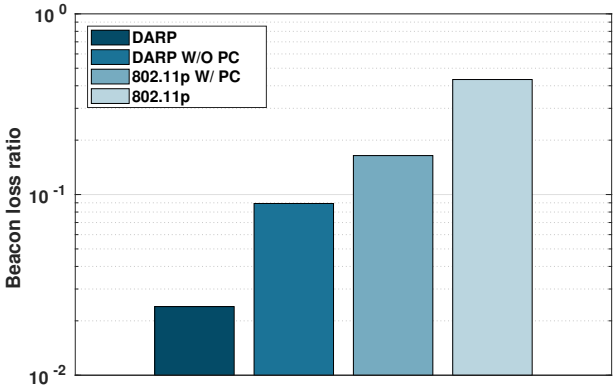

(c)

Figure 3.10: Accumulated received beacons, number of received beacons, and beacons loss ratio for the City2 scenario

is more reliable and scalable. In DARP W/O PC, the beacons are transmitted with a fixed beacon duration and the maximum power. Accordingly, the beacon broadcasting range of the users are maximum which includes more users compared to the case with power control capability. Therefore, more number of beacons are received in DARP W/O PC, Fig. 3.6(b). On the other hand, higher transmission power results in more mutual interference and losses. As the result, the loss ratio increases for DARP W/O PC in Fig. 3.6(a). Fig. 3.7 depicts the BLR of different protocols for $N = 10$ with the same bandwidth ($W = 10$ MHz). Contrary to the results in Fig. 3.6, in Fig. 3.7, DARP and IEEE 802.11p protocols are using two 5 MHz and one 10 MHz channels, respectively. The results verify the DARP's outperformance in terms of BLR compared to the IEEE 802.11p when both of the protocols occupy the same bandwidth.

Fig. 3.8–3.10 shows the accumulated received beacons, number of received beacons, and beacons loss ratio of DARP and IEEE 802.11p for map-based networks and different scenarios of ultra-dense linear network where the vehicle density and number of effective neighbours are $\lambda = 0.4$, $N = 50$, 75, 100, respectively. For the map-based scenarios, we compare DARP with IEEE 802.11p for two different cities, based on real maps. City1 is a low density city block whose size is 3000×3000 m^2 with 99 moving vehicles, while City2 is a high density 4300×2200 m^2 city block in which 500 vehicles are moving. The mobility model is created with the help of SUMO, and the simulation is run by NS-3. In the simulations, just the mobility models were used and the radio channel models, i.e., shadowing and fading effects were not taken into account.

Fig. 3.8 shows the results corresponding to an ultra-dense linear topology. Fig. 3.8(a) depicts the accumulated received beacons for DARP and IEEE 802.11p W/ PC for different number of effective neighbors. It shows that by the time passage and accommodating more vehicles, DARP can exchange 50% to 100% more beacons. The total number of received beacons illustrated in Fig. 3.8(b) showing it changes slightly by increasing the number of effective neighbors in IEEE 802.11p W/ PC,

while these numbers are doubled in DARP. In terms of BLR depicted in Fig. 3.8(c), DARP maintains a reduction of 80%. Based on Fig. 3.8, it can be concluded that DARP is scalable and reliable in ultra-dense scenarios.

Fig. 3.9 illustrates the results corresponding to City1 which is a low density city block. As it is observable in these figures, in this scenario, DARP and DARP W/O PC have approximately the same performance due to sparsity. As shown in Fig. 3.9(a), the accumulated received beacons in DARP and DARP W/O PC are roughly 25% and 15% higher compared to IEEE 802.11p W/ PC and IEEE 802.11p, respectively. DARP and DARP W/O PC achieve 28% gains in total number of received beacons which is shown in Fig. 3.9(b). In addition to the higher number of received beacons, the proposed protocol maintains a lower BLR which is half of the results from IEEE 802.11p as shown in Fig. 3.9(c). According to the results, in low-density scenarios, power control mechanism does not help improving the performance of the protocols. Moreover, DARP is quite reliable even in sparse regimes.

The results corresponding to City2 which is a busy city with dense roads and a high vehicle density are shown in Fig. 3.10. Based on Figs. 3.10(a, b), since the beacon broadcasting range is fixed and maximum in the scheme W/O PC, both of the protocols perform better in terms of number of received beacons and accumulated ones. When the power control mechanism is applied to the protocols, the beacon broadcasting range is reduced due to the high density of the city causing the lower number of received beacons. From beacons loss ratio point of view, DARP W/ and W/O PC have a smaller loss ratio showing in busy and high density scenarios, the performance of the proposed protocol is acceptable.

Figs. 3.8–3.10 show that in all scenarios, a reservation-based protocol will outperform a contention-based one in terms of the BLR. It can be concluded that the BLR of DARP in both cases, W/ or W/O PC, are significantly lower than IEEE 802.11p W/ or W/O PC. It can also be concluded that DARP has a higher number of received beacons. Consequently, the proposed protocol is scalable and reliable in dense scenarios.

3.7 Summary

In this chapter, the beacon broadcasting problem was studied. The CSMA/CA-based MAC protocols performance degrades when the density becomes high, and DARP, the novel distributed and adaptive reservation-based broadcasting MAC layer protocol was proposed to address broadcasting and delivery of beacons. In order to detect and mitigate the beacon collision probability, four different kinds of preambles were used in the proposed protocol under the assumption of periodic beaconing and a fixed MPDU. In DARP, as a decentralized and reservation-based protocol, the channel access chance of a vehicle is controlled by its neighbors and the occupied resources will not be released until collision occurs due to topology change or the vehicle leaves the system. Transmission power and the resource duration were optimized in the protocol to minimize the access collision probability. The 50 MHz DARP with variable data rate was simulated by NS-3 and SUMO traces for two different scenarios, linear network and map-based network, and compared to the 10 MHz IEEE 802.11p fixed data rate protocol. The results showed a substantial improvement in DARP in comparison to the existing standard performance. Although the access delay of the proposed protocol is at least two beaconing periods, it can secure stable and reliable communication in different scenarios. The simulation results demonstrate that the proposed DARP with power control is highly scalable and efficient in realistic vehicular network scenarios.

Chapter 4

NC–MAC: Network Coding-based Distributed MAC Protocol

4.1 Introduction

In Chapter 3, a reservation-based MAC layer protocol was proposed to provide a collision-free channel access scheme for beacon broadcasting. However, the reliability of the beacon transmission is a key issue in V2X. Reception of unreliable safety-related messages would defeat the purpose of beaconing, which leads to public safety concerns. In this chapter and Chapter 5, the focus will be on improvement of the reliability of the beacon broadcasting.

In 5G C–V2X [69], a more compact resource allocation scheme has been introduced for the physical sidelink control and shared channels compared to the LTE sidelink mechanism. According to the new scheme, the latency and collisions can be reduced by deployment of the semi-persistent scheduling and sensing-oriented access scheme [70, 71]. In Release–15, the resource sharing method between mode–3 and mode–4 users has been investigated. However, an additional control overhead is introduced to avoid any collisions, and the collisions problem remains unsolved when users are out of coverage of cellular network.

Although a larger broadcasting range and higher transmission power may help

vehicles to collect more beacons and ensure a higher signal-to-noise-ratio (SNR), respectively, they naturally intensify the collisions on the air-interface. In the current C–V2X system, not only are collisions inevitable, but also there is no hybrid automatic repeat request (HARQ) feedback for broadcasting [72]. Without the HARQ feedback, collisions are undetectable and cannot be stopped timely. Therefore, the reliability of beaconing cannot be guaranteed. Blind HARQ retransmissions have been proposed to improve the reliability the V2X systems, which, however, are not efficient from the resource usage point of view. Overall, the existing C–V2X system is not ready to fully support a reliable and scalable beaconing process.

NC has been extensively studied in recent years [73, 74, 75]. In this scheme, a sender combines successfully received original packets and generates a new packet using their linear combination. The coefficients and operations are done in a Galois field [76]. When the received linear combinations construct a full-rank matrix, the receiver can recover the original packets included in the linear combination by solving a system of linear equations. As NC is used widely for local data exchange and cellular communications [77], it is also capable of enhancing transmission efficiency and reliability in V2X networks.

Considering NC's advantages in packet exchange and broadcast/multicast scenarios, it is applicable to the VANETs in order to improve the reliability of the beaconing process. Reference [78] exploits NC for data exchange between vehicles and roadside base stations. A random coefficient generation method is proposed in [79] for the linear combinations to enhance both security and reliability. NC is applied in a multi-hop broadcasting protocol in [80]. It reduces the total number of transmissions and improves the packet dissemination ratio. Although it has been assumed that the vehicles in a network are aware of the global information, the detailed signaling design and corresponding control overhead as well as resource allocation and collision avoidance were not addressed yet.

Though the existing works applying NC to the vehicular network demonstrate a promising direction, the protocol design issues including collision, reliability, and

communication range have not yet been considered. A practical protocol is needed to be designed in detail to support the required functions and performance. The main challenge is how to ensure reliability of beacon broadcasting in a mobile ad hoc network with time-varying, error-prone wireless channels, and hidden terminals.

In this chapter, first, we propose a novel network coding-based distributed MAC protocol (NC–MAC) which can substantially increase the reliability of the beacon transmission. We employ a preamble mechanism similar to the mechanism used in DARP in Chapter 3 in the frame structure to report NACK and request a re-transmission. Then, the NC mechanism is deployed to generate independent linear combinations of messages. Therefore, more neighbors in a larger broadcasting range can receive beacons. Moreover, it can help recover missed beacons. By combining the HARQ and NC schemes together, the BLR is reduced substantially. Third, we use the SUMO [11] to generate two typical traffic scenarios, highway and urban, using different vehicles with different attributes.

4.2 NC–MAC Design

4.2.1 Protocol in a Nut-shell

In the V2X systems, it is assumed that time in a beaconing period is divided into time slots, and the available bandwidth is divided into several sub-channels. The medium access protocol is a TDMA-based one. Time synchronization is achieved assuming that each vehicle (VE) can use the GPS. The same as the assumption in Chapter 3, if the GPS signal is lost, it is assumed that the GPS local oscillator is stable enough to keep the users synchronized. Each VE in the V2X system can acquire an available resource block successfully through a resource request and allocation process described in Chapter 3 [81]. Therefore, VEs always broadcast beacon messages to their neighbors on their dedicated resource blocks. The basic principles of transmissions in an allocated resource block are summarized as follows:

Figure 4.1: Structure of a resource block in the NC–MAC protocol.

- Each resource block consists of three parts, including a preamble part and two data transmission opportunities. Fig. 4.1 depicts this structure.
- Preambles are orthogonal sequences responsible for resolution of collisions and assisting NACKs during the accessing and beaconing processes, respectively. Different types of preambles use orthogonal codes. Therefore, they are detectable even when collisions happen.
- For the two transmission opportunities, each VE sends its own original message and an independent linear combination of its own original beacon message and the previously received beacons from others that need to be retransmitted on the first and the second transmission opportunities, respectively. If there is no other beacon to send, its own original beacon message will be transmitted twice using the two transmission opportunities.
- When a vehicle fails to receive an original message, a *preambleN* is sent on the preamble part.

A beacon message may be sent directly or included in a linear combination according to the NC principles. If a user fails to receive an original message due to poor channel condition or failure in the recovering process, a NACK is reported on a common feedback channel which is monitored by all of the VEs in the system. According to the above feedback mechanism, transmission failures are detectable and the NACKs coming from multiple users can be considered as diversity reception. By reception of a NACK, it implies that at least a user has failed to receive the corresponding message within a certain beacon range.

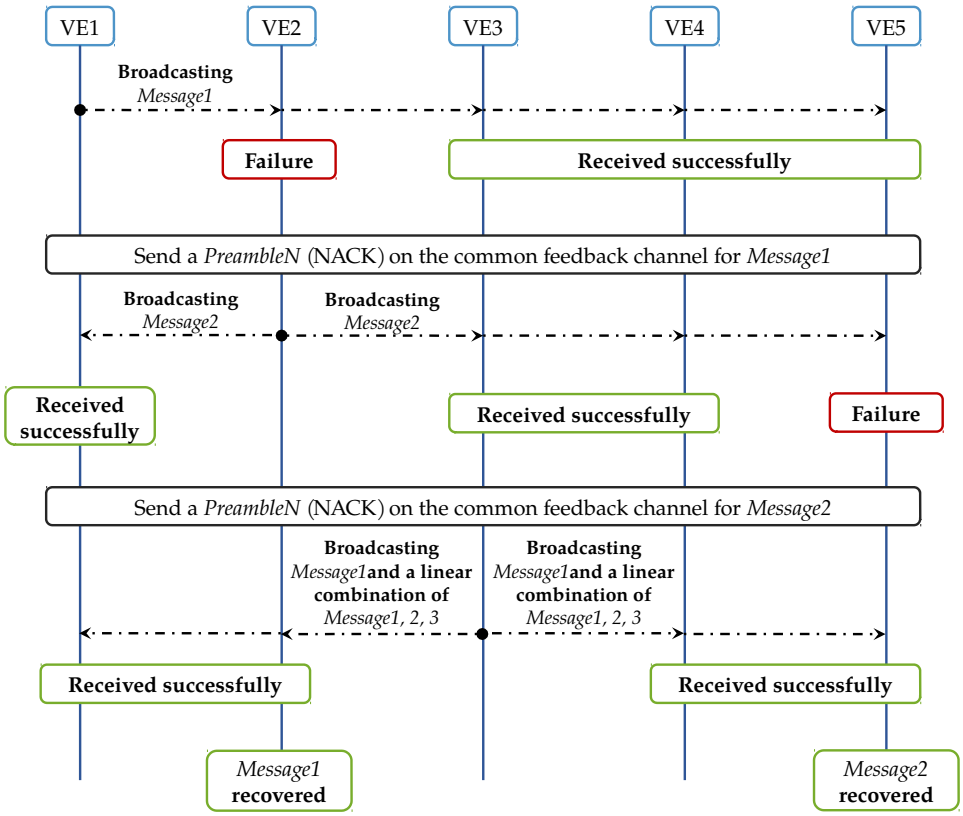

Figure 4.2: An example of the NC–MAC protocol.

4.2.2 Diversity Transmissions with Linear Combinations

A user may broadcast linear combinations of the previously received messages based on the received NACKs. These linear combinations can be used to recover transmission failures and/or multi-hop forwarding. Fig. 4.2 shows how the NC–MAC works in an example.

At the beginning of the beaconing process, *VE*1 sends its original message, *Message*1. It is successfully received by *VE*3–5, while *VE*2 fails to receive it. It sends a *preambleN* on the common feedback channel to notify the failure. *VE*2 starts sending *Message*2 in the next time slot which is successfully received by other VEs except by *VE*5. *VE*3 broadcasts a *preambleN* to notify the failed reception. After reception of the NACKs corresponding to *Message*1 and *Message*2, *VE*3 is notified that the messages have not been successfully received by some users. Thus, it sends

its own beacon on the first transmission opportunity, and generates and sends a linear combination using the successfully received messages and its own beacon in the second transmission opportunity as follows,

$$\begin{aligned} C_1 &= \alpha_{13} m_3, \\ C_2 &= \alpha_{21} m_1 + \alpha_{22} m_2 + \alpha_{23} m_3, \end{aligned} \tag{4.1}$$

where C_1, C_2 are the two linear combinations, and m_1, m_2, m_3 are the original beacon messages sent by *VE*1, *VE*2, and *VE*3, respectively. Each linear combination consists of a coefficient vector and three original packets, $\alpha_{ij} \in GF(2^k); i = 1, 2, j = 1, 2, 3$. Note that each *VE* also includes its own original message in the linear combination. It this case, *VE*3 needs to decode m_1 and m_2 first. After decoding m_1 and m_2, *VE*3 can generate the above linear combinations to send. Since *VE*2 has its own message, m_2, if it successfully receives C_1, C_2, it can build a coefficient matrix A as follows,

$$A = \begin{bmatrix} 0 & 1 & 0 \\ 0 & 0 & \alpha_{13} \\ \alpha_{21} & \alpha_{22} & \alpha_{23} \end{bmatrix}. \tag{4.2}$$

If A is a full-rank matrix, *VE*2 can recover m_1 by solving the system of equations. The independent coefficients of the linear combination can be achieved from the well-known Vandermonde matrix which is a full-rank matrix if its entries are distinct.

$$\begin{bmatrix} m_1 \\ m_3 \end{bmatrix} = \begin{bmatrix} 0 & 1 \\ \alpha_{21} & \alpha_{23} \end{bmatrix}^{-1} \begin{bmatrix} C_1 \\ C_2 - \alpha_{22} m_2 \end{bmatrix}. \tag{4.3}$$

The same procedure may be carried out by *VE*5 in order to recover the missed *Message*2.

4.2.3 Forwarding Principles

If a VE successfully receives an original message and at the same time, it detects a NACK in the feedback channel, the received message is considered as a forwarding message and added to a forwarding queue. Each VE maintains two independent queues, one queue stores the VE's own beacon messages and the forwarding queue stores other VEs' messages that need to be forwarded.

If the forwarding queue is not empty at the time of transmission, a linear combination is generated using the VE's own message and the K oldest forwarding messages in the forwarding queue. $K = \min[F_s, F_l]$, where F_s and F_l are the size of the forwarding queue according to the protocol's setting and the length of the queue, i.e., number of the existing forwarding messages in the forwarding queue, respectively.

Once the beacons in the forwarding queue are sent in a linear combination, they are removed from the queue. In other words, each message can be forwarded once per VE. We assume that the beacon messages have a limited lifetime and they expire after a period since a new beacon will be generated periodically and make the old one useless.

The coefficients vector, the total number of messages included in a linear combination, and owners of the messages are all included in the header of protocol data unit (PDU).

4.2.4 Feedback

In order to reflect the transmission needs, the forwarding/retransmission procedure should be well-designed. The NACK mechanism plays a pivotal role in this regard. To have an active NACK mechanism, a VE should report a NACK on the pre-configured feedback channel if

- a message is expected to be received on a certain resource block, but the receiver fails to decode or detect the signal; or

- a linear combination is successfully received, but the receiver fails to recover the sender's own message from it.

In Fig. 4.2, for example, if *VE*1 transmits *Message*1 twice and *VE*2 receives none of them, *VE*2 broadcasts a NACK. Also, if *VE*2 receives one linear combination but cannot recover the sender's message, *Message*1, it broadcasts a NACK.

Whether a user should expect beacon messages on a specific resource block depends on the user's neighbor list. Each user maintains and updates its neighbor list according to the SINR of the received messages on all of the resource blocks. The updating procedure is based on the long-term averaged results to avoid any ping-pong effects. Temporary poor channels will be compensated by NACK reporting and other's forwarding as proposed in the NC–MAC.

Reception of a NACK is also dependent on the averaged SINR threshold. A VE can forward a missing beacon only if it receives the corresponding NACK. Evidently, the received power of the NACK should be above a certain threshold. By adjusting this threshold, the forwarding scale can be controlled. A lower threshold results in more VEs to forward the beacon.

4.3 Theoretical Analysis

In order to evaluate the performance of the NC–MAC in terms of delay and reliability, the very first step is to find the PMF of the needed number of transmissions to enable a receiver to recover a certain beacon message. Either a beacon message is sent originally or forwarded by a user's linear combination, it is considered as one transmission.

4.3.1 PMF of the Number of Transmissions

In order to find the PMF of the number of transmissions, we assume that by each resource block, an original beacon and an independent linear combination of the

original beacon and previous successfully received beacons are transmitted, which help a receiver to recover the missing beacons. Here, we introduce a variable named level of deficiency (LoD) which is equal or less than zero and indicates how many more linear combinations a user needs to have a full-rank coefficient matrix and be able to recover the missing beacons. Upon reception of a linear combination, the receiver expects a new beacon associated with the transmitter. If the receiver receives both the original message and the linear combination successfully, the LoD is increased by one since the linear combination may be used in the recovery of the missing beacons. In the case that either the original message or the linear combination is missed, the LoD will not change, due to the fact that the received packet may not change the rank of matrix A in (4.2). In other words, by considering the coefficient matrix A, there is a new variable and a new equation corresponding to the received packet on the transmission opportunity. In the last case, if no packet is received, the LoD will decrease by one. Here, the aim is to find the probability that the LoD of a user which is zero initially, reaches zero after n transmissions.

We model the transmissions as a sequence, i.e., $\mathbb{X}_n^r = \{X_1, \ldots, X_n\}$ where $X_i \in \{-1, 0, +1\}$, n is the number of transmissions, and r stands for the initial state of LoD. $X_i = 0$, $+1$ represent successful reception of one and two linear combinations, respectively. Failure reception of the linear combinations is modeled by $X_i = -1$. The probabilities of different possibilities of X_i are given by

$$\Pr(X_i) = \begin{cases} p_1, & X_i = 1, \\ p_0, & X_i = 0, \\ p_{-1}, & X_i = -1, \end{cases}$$

which are dependent on channel fluctuations and redundancy of the received linear combinations.

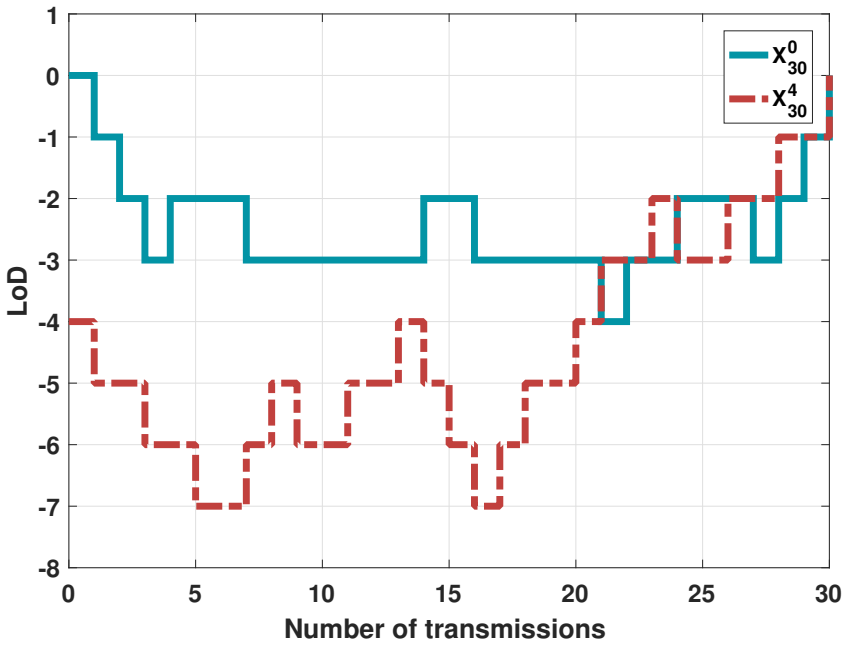

Figure 4.3: Examples of possible sequences for $\mathbb{X}^0_{30}$ and $\mathbb{X}^4_{30}$.

Zero Initial LoD

The initial state of the LoD is zero in this case, i.e., $r = 0$, meaning that the receiver has all of the transmitted beacons. Fig. 4.3 shows an example of this sequence. If the elements of $\mathbb{X}^0_n$ satisfy the following constraints, $\mathbb{X}^0_n$ is considered as a possible sequence.

$$
\begin{aligned}
&X_1 = -1, \\
&X_1 + X_2 < 0, \\
&X_1 + X_2 + X_3 < 0, \\
&X_1 + X_2 + X_3 + X_4 < 0, \\
&\qquad \vdots \\
&X_1 + X_2 + X_3 + \cdots + X_{n-1} < 0, \\
&X_1 + X_2 + \cdots + X_n = 0,\ X_n = +1,
\end{aligned}
\tag{4.4}
$$

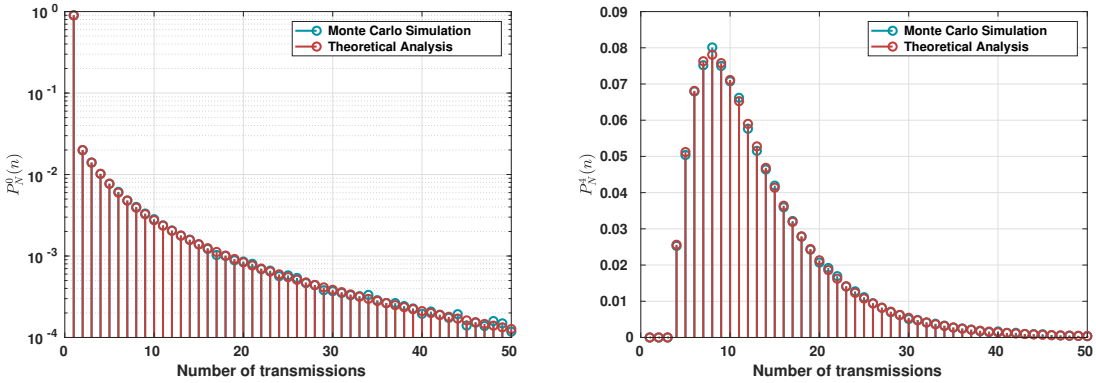

(a) $P_N^0(n)$ with $p_1 = 0.2$, $p_0 = 0.7$, $p_{-1} = 0.1$ (b) $P_N^4(n)$ with $p_1 = 0.4$, $p_0 = 0.5$, $p_{-1} = 0.1$, $r = 4$.

Figure 4.4: Monte Carlo validation of $P_N^0(n)$ and $P_N^4(n)$.

which the inequalities in the matrix form are

$$\begin{bmatrix} 1 & 0 & 0 & 0 & \dots & 0 \\ 1 & 1 & 0 & 0 & \dots & 0 \\ 1 & 1 & 1 & 0 & \dots & 0 \\ \vdots & \vdots & \vdots & \vdots & \ddots & \vdots \\ 1 & 1 & 1 & 1 & \dots & 1 \end{bmatrix} \begin{bmatrix} X_2 \\ X_3 \\ X_4 \\ \vdots \\ X_{n-1} \end{bmatrix} < \begin{bmatrix} 1 \\ 1 \\ 1 \\ \vdots \\ 1 \end{bmatrix} \tag{4.5}$$

Therefore, the PMF of the needed number of transmissions is defined as

$$P_N^0(n) = \Pr\left[\sum_{i=1}^{n} X_i = 0,\ X_1 = -1,\ X_n = 1,\ (4.5)\right]. \tag{4.6}$$

Since the zeros do not change any of the constraints in (4.4), we focus on finding the total number of ways we can distribute Q number of $+1$ and Q number of -1 within $\mathbb{X}_n^0$ such that it satisfies the constraints in (4.4). Afterwards, $n - 2Q$ zeros can be distributed among the already distributed $+1$s and -1s. For example, the possible $\mathbb{X}_{30}^0$ in Fig. 4.3 consists of the following sequence of $+1$ and -1 which have

$\mathbb{Z}_t$, $t = 1, \ldots, 2Q-1$, all-zero sequences in between.

$$\mathbb{X}_{30}^0 = \Big\{ -1, \mathbb{Z}_1, -1, \mathbb{Z}_2, -1, \mathbb{Z}_3, \ldots, +1, \mathbb{Z}_{2Q-1}, +1 \Big\}, \tag{4.7}$$

The problem of finding the total number of non-zero sequences satisfying the constraints in (4.4) has been studied in [82] as a random walk problem which starts from and returns to the origin after $2Q$ steps. The total number of possible non-zero sequences is [82]

$$\frac{1}{2\,(2Q-1)} \binom{2Q}{Q}. \tag{4.8}$$

Now, we can find the total number of ways which zeros can be distributed in different $\mathbb{Z}_t$, $t = 1, 2, \ldots, 2Q-1$ in (4.7). The total number of possible all-zero sequences which overall have $n - 2Q$ zeros can be obtained by enumerating possible choices, and it is obtained by solving the following equation

$$|\mathbb{Z}_1| + |\mathbb{Z}_2| + |\mathbb{Z}_3| + \cdots + |\mathbb{Z}_{2Q-1}| = n - 2Q, \quad |\mathbb{Z}_t| \geq 0. \tag{4.9}$$

where $|\,.\,|$ represents cardinality of Z_t. The equation in (4.9) has $\binom{n-2}{2Q-2}$ solutions. Since $\mathbb{X}_n^0$ may have at most $\left\lfloor \frac{n}{2} \right\rfloor$ number of $+1$ and -1, the total number of $\mathbb{X}_n^0$ satisfying the constraints in (4.5) is

$$\left|\mathbb{X}_n^0\right| = \sum_{Q=1}^{\left\lfloor \frac{n}{2} \right\rfloor} \frac{1}{2\,(2Q-1)} \binom{n-2}{2Q-2} \binom{2Q}{Q}. \tag{4.10}$$

Now, finding the probability of occurrence of $\mathbb{X}_n^0$ according to the constraints in (4.4) is straightforward based on this analysis. This PMF is as follows

$$P_N^0(n) = \begin{cases} 1 - p_{-1}, & n = 1, \\ P_n^0, & n \geq 2, \end{cases}$$

where P_n^0 is

$$P_n^0 = \sum_{Q=1}^{\lfloor \frac{n}{2} \rfloor} \frac{1}{2\,(2Q-1)} \binom{n-2}{2Q-2} \binom{2Q}{Q} (p_1\, p_{-1})^Q\, p_0^{n-2Q}. \tag{4.11}$$

The results from the theoretical analysis and Monte Carlo simulation are shown in Fig. 4.4 (a) for $p_1 = 0.2$, $p_0 = 0.7$, and $p_{-1} = 0.1$.

Non-zero Initial LoD

Next, we can extend what was achieved in (4.11) to a general case, i.e., $P_N^r(n)$ given the initial LoD of r, $r = 1, 2, 3, ...$ For the $\mathbb{X}_n^r$ whose starting point is r and ends at zero, obviously $n \geq r$ and the set of inequalities which were presented in (4.4) are modified as

$$\begin{aligned}
&X_1 < r, \\
&X_1 + X_2 < r, \\
&X_1 + X_2 + X_3 < r, \\
&X_1 + X_2 + X_3 + X_4 < r, \\
&\qquad \vdots \\
&X_1 + X_2 + X_3 + \cdots + X_{n-1} < r, \\
&X_1 + X_2 + \cdots + X_n = r,\ X_n = +1.
\end{aligned} \tag{4.12}$$

The matrix form of these inequalities is

$$\begin{bmatrix} 1 & 0 & 0 & 0 & \dots & 0 \\ 1 & 1 & 0 & 0 & \dots & 0 \\ 1 & 1 & 1 & 0 & \dots & 0 \\ \vdots & \vdots & \vdots & \vdots & \ddots & \vdots \\ 1 & 1 & 1 & 1 & \dots & 1 \end{bmatrix} \begin{bmatrix} X_1 \\ X_2 \\ X_3 \\ \vdots \\ X_{n-1} \end{bmatrix} < \begin{bmatrix} r \\ r \\ r \\ \vdots \\ r \end{bmatrix} \tag{4.13}$$

The same as the previous proof, Q, S, and Z represent the total number of $+1$, -1, and 0 in $\mathbb{X}_n^r$, respectively. A set of equations can be written on Q, S, and Z as

$$\begin{aligned} Q - S = r, \quad &\Longrightarrow \quad Q = \frac{n - Z + r}{2}, \\ Q + S = n - Z, \quad &\Longrightarrow \quad S = \frac{n - Z - r}{2}. \end{aligned} \tag{4.14}$$

According to the famous ballot theorem in [82] the total number of possible $\mathbb{X}_n^r$ which only consists of $+1$ and -1 is

$$\frac{r}{Q+S}\binom{Q+S}{\frac{Q+S+r}{2}}. \tag{4.15}$$

The next step is to distribute Z number of zeros by inserting sets of zeros, $\mathbb{Z}_t$, $t = 1, 2, \ldots, Q+S$ among $+1$ and -1 of the $\mathbb{X}_r^n$. With the same argument in (4.7), there are totally $Q+S$ spots to distribute zeros. Therefore, the total number of ways to distribute Z zeros among these $Q+S$ spots can be enumerated by solving the following equation.

$$|\mathbb{Z}_1| + |\mathbb{Z}_2| + |\mathbb{Z}_3| + \cdots + |\mathbb{Z}_{Q+S}| = Z, \quad |\mathbb{Z}_t| \geq 0, \tag{4.16}$$

where $|.|$ represents cardinality of $\mathbb{Z}_t$. This equation has $\binom{Z+Q+S-1}{Q+S-1} = \binom{n-1}{n-Z-1}$ number of solutions. By multiplying the results in (4.16) and $\frac{r}{Q+S}\binom{Q+S}{\frac{Q+S+r}{2}}$, and summing over Z, the total number of $\mathbb{X}_n^r$ is

$$|\mathbb{X}_n^r| = \sum_{Z=0}^{n-r} \frac{r}{n-Z}\binom{n-Z}{\frac{n-Z+r}{2}}\binom{n-1}{n-Z-1}\mathcal{I}(Z), \tag{4.17}$$

where $\mathcal{I}(Z)$ is defined as

$$\mathcal{I}(Z) = \begin{cases} \frac{1+(-1)^Z}{2}, & \mathrm{mod}(n-r, 2) = 0, \\ \frac{1-(-1)^Z}{2}, & \mathrm{mod}(n-r, 2) = 1. \end{cases} \tag{4.18}$$

According to the total number of sequences starting form LoD of r and ending at zero in (4.17), the corresponding PMF is

$$P_N^r(n) = \sum_{Z=0}^{n-r} \frac{r}{n-Z} \binom{n-Z}{\frac{n-Z+r}{2}} \binom{n-1}{n-Z-1} \mathcal{I}(Z) p_{-1}^S p_0^Z p_1^Q, \quad n \geq r, \tag{4.19}$$

where Q and S are found as functions of n, r, and Z from (4.14). The results from the theoretical analysis and Monte Carlo simulation are shown in Fig. 4.4 (b) for $p_1 = 0.4$, $p_0 = 0.5$, and $p_{-1} = 0.1$.

4.3.2 Modeling p_{-1}, p_0, and p_1

Assuming that the neighbor list and the NACK receiving range are based on the averaged SINR, and applying the same large-scale fading channel model to every VE, the neighbor list and the NACK receiving range can be approximately modeled by the distance between the transmitter and the receiver. The variables $D^{(rx)}$ and $D^{(nack)}$ are defined as the receiving range and feedback range, respectively. Any two VEs with a distance less than $D^{(rx)}$ are considered as each other's neighbors, and VEs within the distance of $D^{(nack)}$, can successfully receive the transmitted NACKs. Reporting a NACK to a VE farther than $D^{(rx)}$ is not necessary. Moreover, by increasing $D^{(nack)}$ to $D^{(rx)}$, more unwanted messages from other VEs may be included in the linear combinations which can make them useless. Therefore, $D^{(nack)}$ is assumed to be less than $D^{(rx)}$ to avoid any possible waste of resources. The probabilities of p_{-1}, p_0, and p_1 are all dependent of the previous received or non-received beacons. In their modeling, we use some approximations to simplify the problem.

a) p_{-1}

It is defined as the probability that a receiver receives neither the original beacon on the first transmission opportunity nor the linear combination on the second one

corresponding to a neighboring VE. This probability is modeled as

$$p_{-1} = \Pr[A_1, F_1, F_2] + \Pr[A_1, F_1, \overline{F_2}, U], \tag{4.20}$$

where A_1 is the event that the transmitter is in the receiver's neighbor list, i.e., $d \leq D^{(rx)}$, F_1 and F_2 denote the events that the receiver fails to receive the first and the second transmission opportunities, respectively. Evidently, their complementary sets represent successful receiving. Moreover, U denotes the event where the received linear combination includes unwanted beacon messages, i.e., the messages which originally were sent by non-neighbor VEs. Receiving a linear combination containing a message from a non-neighbor VE makes the whole linear combination useless due to recovery impossibility.

The probabilities of above events are modeled as follows.

$$\begin{aligned}
\Pr[A_1] &= \int_0^{+\infty} \Pr[A_1 | D_s = x] f_{D_s}(x) \mathrm{d}x \\
&= \int_0^{+\infty} \min\left[\frac{2D^{(rx)}}{x}, 1\right] f_{D_s}(x) \mathrm{d}x \\
&\approx \min\left[\frac{2D^{(rx)}}{\mathbb{E}[D_s]}, 1\right],
\end{aligned} \tag{4.21}$$

where D_s is reuse distance, the distance between two VEs using the same resource as defined in (3.11), and $f_{D_s}(x)$ is the corresponding probability distribution function (PDF). The PDF of D_s depends on sensing sensitivity in the accessing procedure and vehicles density. In order to approximate $\Pr[A_1]$, the expectation of D_s, $\mathbb{E}[D_s]$ was used in (4.21) according to the Taylor expansion for the first moment of function of a random variable [83]. In the simulation, we assumed that there are sufficient resources for the VEs. Therefore, in order to have a fair comparison with the theoretical analysis, the reuse distance is set to the length of the road.

We assume that two transmission opportunities experiencing the same error distribution on the channel, and $F_1|A_1$ and $F_2|A_1$ are two correlated Bernoulli

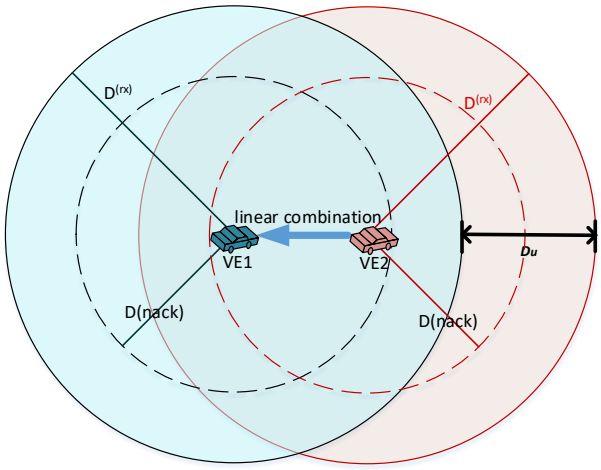

Figure 4.5: Illustration of the event $U|A_1$.

events where $\Pr[F_1|A_1] = \Pr[F_2|A_1] = p_e$ and p_e denotes block/packet error rate (BLER). Covariance of these two events which represents temporal correlation of the communication channel over two successive transmission opportunities in the same resource unit is $Cov[F_1, F_2|A_1] = \mathbb{E}[F_1, F_2|A_1] - \mathbb{E}[F_1|A_1]\mathbb{E}[F_2|A_1]$, and also, $\Pr[F_1, F_2|A_1] = \mathbb{E}[F_1, F_2|A_1]$. The Pearson correlation coefficient, ρ in terms of $Cov[F_1, F_2|A_1]$ and p_e is

$$\rho = \frac{Cov[F_1, F_2|A_1]}{\sigma_{F_1|A_1}\sigma_{F_2|A_1}} = \frac{\mathbb{E}[F_1, F_2|A_1] - \mathbb{E}[F_1|A_1]\mathbb{E}[F_2|A_1]}{p_e(1-p_e)}. \tag{4.22}$$

Therefore, the first term in (4.20) is modeled as

$$\begin{aligned}\Pr[A_1, F_1, F_2] &= \Pr[A_1]\Pr[F_1, F_2|A_1] = \Pr[A_1]\mathbb{E}[F_1, F_2|A_1] \\ &= \Pr[A_1]\left(\mathbb{E}[F_1|A_1]\mathbb{E}[F_2|A_1] + Cov[\epsilon_1, \epsilon_2]\right) \\ &\approx \min\left[\frac{2D^{(rx)}}{\mathbb{E}[D_s]}, 1\right]\left(p_e^2 + \rho p_e(1-p_e)\right). \end{aligned} \tag{4.23}$$

It is assumed that each VE's channel is a stationary random process and the probability density function (PDF) of the received SNR given the transmission distance, d, is denoted by $f_{\mathrm{SNR}|d}(x)$. In order to decode the received message successfully,

the SNR needs to be above a certain threshold, SNR_T. The BLER is obtained as follows

$$p_e = \int_0^{D^{(rx)}} \int_0^{\mathrm{SNR}_T} f_{\mathrm{SNR}|d}(x) f_d(y) \mathrm{d}x\mathrm{d}y. \tag{4.24}$$

Considering a Rayleigh fading channel and a device-to-device communication path loss model, p_e is achieved as

$$\begin{aligned} p_e &= \int_0^{D^{(rx)}} \int_0^{\mathrm{SNR}_T} \frac{1}{\overline{\mathrm{SNR}(y)}} e^{-\frac{1}{\overline{\mathrm{SNR}(y)}}x} \frac{1}{D^{(rx)}} \mathrm{d}x\mathrm{d}y \\ &= \int_0^{D^{(rx)}} \int_0^{\mathrm{SNR}_T} \frac{y^\alpha N_0}{P_t K_0} e^{-\frac{y^\alpha N_0}{P_t K_0}x} \frac{1}{D^{(rx)}} \mathrm{d}x\mathrm{d}y \\ &= \frac{1}{D^{(rx)}} \int_0^{D^{(rx)}} 1 - e^{-\frac{y^\alpha N_0}{P_t K_0}\mathrm{SNR}_T} \mathrm{d}y, \end{aligned} \tag{4.25}$$

where P_t is the transmission power, $\overline{\mathrm{SNR}(y)}$ is the average SNR as a function of distance, N_0 is the noise power. K_0 and α are a constant and an exponent corresponding to the path loss model, respectively. The PDF of the transmission distance, $f_d(y)$, is assumed to follow a uniform distribution, $d \sim \mathcal{U}\left(0, D^{(rx)}\right)$.

The event U is independent of the events F_1 and $\overline{F_2}$. Therefore, the second term in (4.20) is modeled as

$$\Pr[A_1, F_1, \overline{F_2}, U] = \Pr[A_1] \Pr[F_1, \overline{F_2}|A_1] \Pr[U|A_1]. \tag{4.26}$$

Using the argument in the calculation of (4.23),

$$\begin{aligned} \Pr[F_1, \overline{F_2}|A_1] &= \Pr[F_1|A_1] - \Pr[F_1, F_2|A_1] \\ &= p_e - p_e^2 - \rho p_e(1 - p_e) \\ &= (1 - \rho) p_e (1 - p_e). \end{aligned} \tag{4.27}$$

The event $U|A_1$ is illustrated in Fig. 4.5 where VE2 transmits a linear combination to VE1. In this figure, if the transmitted linear combination includes any beacons from the VEs located outside of the VE1's receiving range $D^{(rx)}$, the linear combination is

useless for VE1 and should be discarded due to lack of possibility of recovery. Given that VE2 only forwards the beacons in its forwarding queue to the VEs inside the feedback range, $D^{(nack)}$, the event $U|A_1$ happens if any VEs inside the VE2's feedback range fails to receive a beacon generated outside the VE1's receiving range, i.e., the crescent area in Fig. 4.5. Assuming a linear road model and a PPP for the topology of the VEs [84], the crescent area is simplified to the segment of $D_u = d$ in the figure, and $\Pr[U|A_1]$ is obtained as follows,

$$\Pr[U|A_1] = 1 - \sum_{k=0}^{\infty} \int_0^{D^{(rx)}} \Bigg(\left[\hat{p}_e + (1-\hat{p}_e)B(x)\right]^k f_{D_u}(x) \times \frac{(\lambda x)^k}{k!} e^{-\lambda x} \Bigg) \mathrm{d}x, \tag{4.28}$$

where $B(x)$ is the probability that a beacon generated by a VE on a segment with length of x is successfully received by all VEs inside the VE2's feedback range. In other words, there will be no corresponding NACK for this beacon. $\hat{p}_e$ denotes the probability that VE2 fails to receive and recover the beacon sent from a VE on the segment of D_u, and thus it cannot further forward it to VE1. Since $\hat{p}_e$ is dependent on the VE2's current LoD, its derivation is not straightforward. However, it obviously is less than p_e since in the best case where the VE2's LoD is zero, $\hat{p}_e$ is equal to p_e, $\hat{p}_e = p_e$. Hence, we apply the approximation of $\hat{p}_e \approx p_e$. Underestimating $\hat{p}_e$ results in overestimation of $\Pr[U|A_1]$ and p_{-1}. A larger p_{-1} makes our theoretical analysis conservative. $f_{D_u}(x)$ represents the PDF of D_u. Assuming location of each VE is uniformly distributed and independent to other VEs' location, $f_{D_u}(x) = 1/D^{(rx)}$.

Given a random point on segment D_u, d_u denotes the distance from this point

to the right boundary of the receiving range of VE2 in Fig. 4.5.

$$B(D_u) = \sum_{k=0}^{\infty} \int_0^{D_u} \Bigg(\frac{\left(\lambda \min\left[D^{(nack)} + d_u, 2D^{(nack)}\right]\right)^k}{k!} \times e^{-\lambda \min\left[D^{(nack)}+d_u, 2D^{(nack)}\right]} \times \left(1 - \tilde{p}_e(d_u, D_u)\right)^k \frac{1}{D_u} \Bigg) \mathrm{d}d_u, \tag{4.29}$$

where $\tilde{p}_e(d_u, D_u)$ is the probability that a single VE within the feedback range of VE2 reports a NACK to the transmitted beacon from the segment of D_u as described in $B(D_u)$. Closed-form derivation of $\tilde{p}_e(d_u, D_u)$ is not straightforward due to its dependency on the VE's current LoD. $\tilde{p}_e(d_u, D_u)$ is function of the distance between a targeted communication pair which varies from 0 to $D^{(rx)}$. With the same argument on $\hat{p}_e \approx p_e$, we approximate $\tilde{p}_e(d_u, D_u)$ as $\tilde{p}_e(d_u, D_u) \approx p_e$. This approximation underestimates $\tilde{p}_e(d_u, D_u)$ and p_{-1}, and thus overestimates the performance.

For the case that the segment's length is less than the feedback range, i.e., $0 \leq d_u \leq D_u \leq D^{(nack)}$, (4.29) is derived as

$$\begin{aligned} B(D_u) &= \sum_{k=0}^{\infty} \int_0^{D_u} \Bigg(\frac{\lambda^k \left(D^{(nack)} + d_u\right)^k}{k!} e^{-\lambda\left(D^{(nack)}+d_u\right)} \times \left(1 - p_e\right)^k \frac{1}{D_u} \Bigg) \mathrm{d}d_u \\ &= \sum_{k=0}^{\infty} \frac{\left(1-p_e\right)^k}{D_u} \int_{D^{(nack)}}^{D_u + D^{(nack)}} \frac{(\lambda x)^k}{k!} e^{-\lambda x} \mathrm{d}x \\ &= \sum_{k=0}^{\infty} \frac{\left(1-p_e\right)^k}{D_u} \frac{1}{\lambda} \int_{D^{(nack)}}^{D_u + D^{(nack)}} \frac{\lambda^{k+1} x^k e^{-\lambda x}}{\Gamma(k+1)} \mathrm{d}x \\ &= \sum_{k=0}^{\infty} \frac{\left(1-p_e\right)^k}{\lambda D_u \Gamma(k+1)} \Bigg[\gamma\Big(k+1, \lambda(D_u + D^{(nack)})\Big) - \gamma\Big(k+1, \lambda D^{(nack)}\Big) \Bigg], \end{aligned} \tag{4.30}$$

where $\Gamma(\cdot)$ and $\gamma(\cdot, \cdot)$ are gamma function and lower incomplete gamma function, respectively.

Remark: We used p_e to approximate $\hat{p}_e$ and $\tilde{p}_e(d_u, D_u)$, which underestimates and overestimates the theoretical analysis, respectively. This simplification tends to underestimate theoretical analysis when the number of neighbors is small (small λ) and overestimate otherwise.

b) p_1

It is defined as the probability that a receiver receives both the first transmission opportunity and the second one corresponding to a neighboring VE. According to the LoD modeled in Sec. 4.3.1, p_1 is meaningful only if a VE has missed at least one beacon. Therefore, p_1 is conditioned on a negative LoD. In other words, the event corresponding to p_1 happens if the receiver, VE1 in Fig. 4.5, is located within the feedback range of VE2. This probability is modeled as

$$\begin{aligned} p_1 &= \Pr[A_2, \overline{F}_1, \overline{F}_2, \overline{U}] \\ &= \Pr[A_2] \Pr[\overline{F}_1, \overline{F}_2 | A_2] \Pr[\overline{U} | A_2] \\ &= \Pr[A_2] \left[(1 - p'_e)^2 + \rho p'_e (1 - p'_e) \right] (1 - \Pr[U | A_2]), \end{aligned} \tag{4.31}$$

where A_2 denotes the event that the distance between the transmitter and the receiver is less than $D^{(nack)}$, i.e., $d \leq D^{(nack)}$. Similar to the models in (4.21) and (4.24), we have

$$\Pr[A_2] \approx \min \left[\frac{2D^{(nack)}}{\mathbb{E}[D_s]}, 1 \right], \tag{4.32}$$

$$p'_e = \frac{1}{D^{(nack)}} \int_0^{D^{(nack)}} 1 - e^{-\frac{y^\alpha N_0}{P_t K_0} SNR_T} \mathrm{d}y. \tag{4.33}$$

Derivation of $\Pr[U|A_2]$ is similar to $\Pr[U|A_1]$ in (4.28) and it is given by

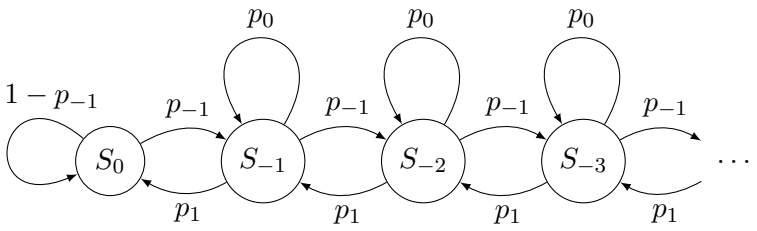

Figure 4.6: Markov chain using a VE's LoD as states.

$$\Pr[U|A_2] = 1 - \sum_{k=0}^{\infty} \int_0^{D^{(nack)}} \Bigg(\left[p'_e + (1-p'_e)B(x)\right]^k f'_{D_u}(x) \times \frac{(\lambda x)^k}{k!} e^{-\lambda x} \Bigg) \mathrm{d}x, \tag{4.34}$$

where $f'_{D_u}(x) = 1/D^{(nack)}$. Accordingly, p_1 is derived from (4.31) by substituting $\Pr[A_2]$ and $\Pr[U|A_2]$ obtained in (4.32) and (4.34), respectively .

c) p_0

Since p_{-1} and p_1 have been derived already, derivation of p_0 is straightforward as follows.

$$p_0 = \begin{cases} 1 - p_{-1} - p_1, & LoD \neq 0, \\ 1 - p_{-1}, & LoD = 0. \end{cases}$$

4.3.3 Metrics

Beacons Recovery Delay (BRD)

Assuming all of the VEs have received or recovered the previously sent beacons, i.e. LoD = 0 and according to (4.11) and the probabilities, p_1, p_0, and p_{-1}, derived in Sec. 4.3.2, the cumulative distribution function (CDF) of BRD is as follows,

$$F_{\mathrm{BRD}}(t) = \frac{\sum_{n=1}^{tN_c} P_N^0(n+1)}{\sum_{n=1}^{(N_t-1)N_c} P_N^0(n+1)}, \quad t = 1, 2, \ldots, N_t - 1, \tag{4.35}$$

where N_c and N_t are the total number of channels and the total number time slots in a beaconing period, respectively. VEs in the neighbor list will stop forwarding and recovering a tagged VE's beacon message generated in the last period once the VE sends out a new beacon in the current period. In other words, the expiration time for the beacons is one beaconing period. Therefore, $F_{\mathrm{BRD}}(t)$ is conditioned on the missing beacons which are recoverable within a period.

Successful Deliver Ratio, η

In Fig. 4.6, a discrete-time Markov chain has been built using a single VE's LoD as the states. The probability of each state, S_{-r}, is given by

$$S_{-r} = \left(1 - \frac{p_{-1}}{p_1}\right)\left(\frac{p_{-1}}{p_1}\right)^r, \quad r = 0, 1, 2, 3, \ldots. \tag{4.36}$$

Regardless of the states, once $\overline{F_1}|A_1$ happens, the message is successfully delivered, since a VE always transmits its own beacon message on the first transmission opportunity. Otherwise, the message may be recovered in time depending on the current state of LoD. We define the successful deliver ratio, η, from a VE's perspective. It is defined as the probability of successfully receiving or recovering a beacon sent by another VE in its neighbor list. Based on the derivations in Sec. 4.3.2, η is given as follows,

$$\begin{aligned}\eta =& \Pr[\overline{F_1}|A_1] + \Pr[F_1, \overline{F_2}, \overline{U}|A_1] \\ &\times \left[S_0 + \sum_{r=1}^{(N_t-1)N_c}\left(S_{-r}\sum_{n=r}^{(N_t-1)N_c} P_N^r(n)\right)\right] \\ &+ \left(1 - \Pr[\overline{F_1}|A_1] - \Pr[F_1, \overline{F_2}, \overline{U}|A_1]\right) \\ &\times \left[\sum_{r=0}^{(N_t-2)N_c}\left(S_{-r}\sum_{n=r+1}^{(N_t-1)N_c} P_N^{r+1}(n)\right)\right],\end{aligned} \tag{4.37}$$

Table 4.1: VEs' Parameters in SUMO

Parameter	Value	Description
Maxspeed	$[80, 200]$	The maximum speed that a VE will travel (km/h)
Length	$[2.2, 12]$	The length of a VE (m)
Accel	$[2, 5]$	The acceleration ability of VEs (m/s^2)
Decel	$[3, 8]$	The deceleration ability of VEs (m/s^2)
Mingap	$[2, 5]$	The offset to the leading VE when standing (m)
Sigma	$[0.2, 0.7]$	The VE's driver imperfection (between 0 and 1)
Car-following	*Krauss*	The model describing how a VE follows another one
Lane-changing	*LC2013*	The model describing how a driver changes a lane

where

$$\Pr[\overline{F_1}|A_1] = 1 - p_e,$$
$$\Pr[F_1, \overline{F_2}, \overline{U}|A_1] = \Pr[F_1, \overline{F_2}|A_1]\left(1 - \Pr[U|A_1]\right).$$

$\Pr[F_1, \overline{F_2}|A_1]$ and $\Pr[U|A_1]$ are obtained from (4.27) and (4.28), respectively.

4.4 Performance Evaluation

4.4.1 Topology Setup

To investigate whether the proposed solution is reliable and scalable for beaconing in V2X, we conducted extensive simulations in three different scenarios: (I) a linear network, (II) highway scenario, and (III) urban scenario. In the linear network, we assume that the topology of VEs follows a one-dimension Poisson point process (PPP) and the VEs are moving in a single-lane road. For the highway and urban scenario, we used SUMO to generate traffic traces. In the highway scenario, a 10 km bidirectional road is set where each direction contains four lanes with different speed limits, $[60, 80, 100, 120]$ km/h. In the urban scenario, there are two intersections where four bidirectional roads intersect. Each direction contains two lanes with

Table 4.2: Parameter Settings

Parameters	**Value**	**Description**
L	2 (km)	Road length
λ	$[0.05, 0.3]$ (VE/m)	VEs density
$D^{(rx)}$	$200, 250$ (m)	Beacon receiving range
$D^{(nack)}$	150 (m)	Feedback range
N_c	5	Number of channels
T_p	100 (ms)	Beaconing period
TTL	3	Time-to-live
K_0	$10^{-4.38}$ [85]	Path loss constant
α	3.68	Path loss exponent
P_t	250 (mW)	Transmission power
SNR_T	3.3 dB [86]	Decoding SNR threshold
W	180×6 KHz	Channel bandwidth
N_0	$W \times 10^{-17.4}$ (mW)	Noise power
ρ	0.5, 0.7, 0.9	Correlation factor

different speed limits, $[50, 60]$ km/h. The length of each road is set to 2 km and the network's area is totally 6×4, km^2. Traffic lights are set at each of the road segments at the intersections and the duration of green light is 25 s. Deployed VEs in both of the scenarios have different performance parameters such as length, acceleration, deceleration, and maximum speed from seven different types of VEs. In the trace generation, Krauss and LC2013 have been considered as car-following and lane-changing models, respectively. Driver imperfection has been considered in the traces as well. The attributes of VEs used in the SUMO are summarized in Table 4.1. The VEs' performance parameters and destination are chosen randomly when they enter the simulation system, and they leave the system when they reach the chosen destination.

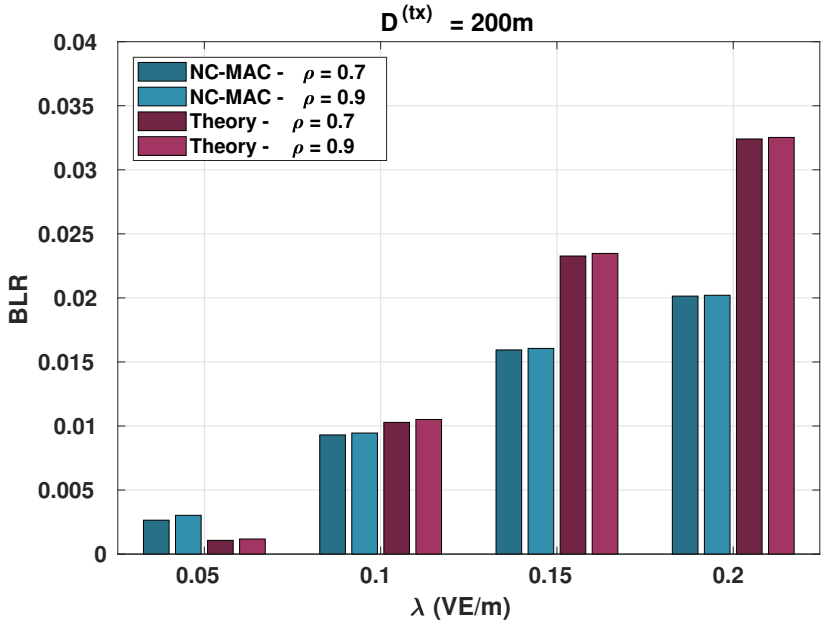

(a)

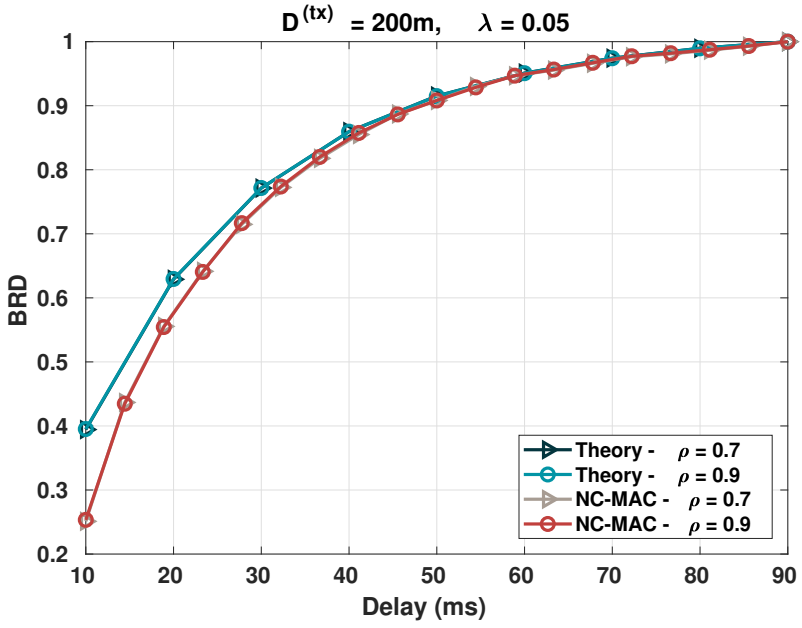

(b)

Figure 4.7: Comparison of the NC–MAC results and theoretical derivations. There is not any limitation on the VEs' forwarding queue size.

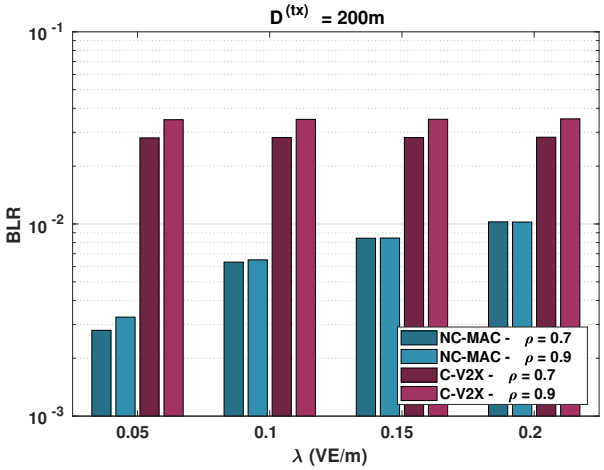

(a)

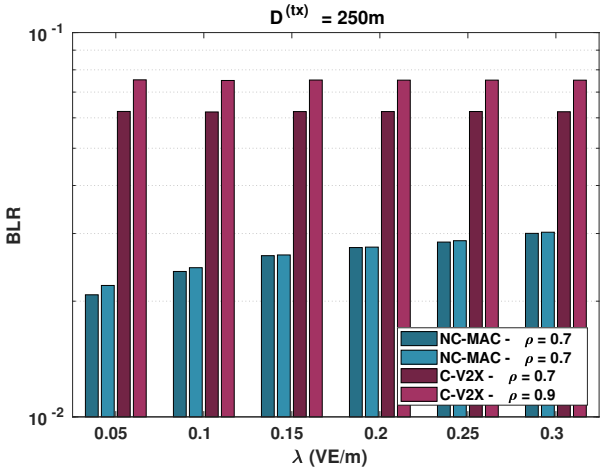

(b)

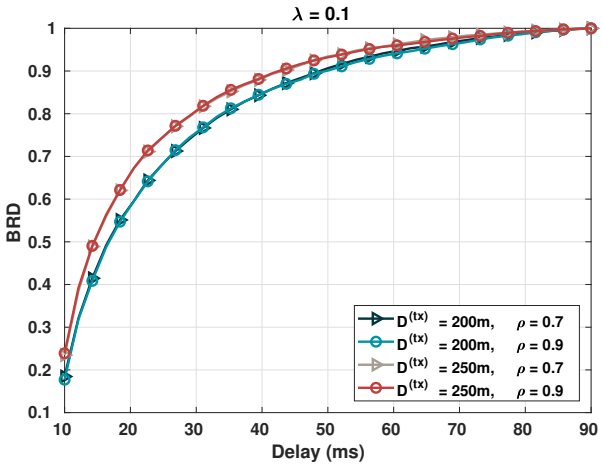

(c)

Figure 4.8: Comparison of the NC–MAC with the C–V2X in terms of BLR and BRD. The size of forwarding queue in the NC–MAC is set to $F_s = 11$ in this case.

4.4.2 Communication Setup

We apply the line of sight (LoS) device-to-device communication path loss model and Rayleigh fading. Parameters are summarized in Table 4.2. In the simulations, we assume that each VE has acquired a resource block before starting the beaconing process. Each VE will generate beacons periodically, and they expire after a period. The target receivers of a tagged VE are all of the VEs in the broadcasting range of the transmitter. For comparison, we also simulated the cases using LTE mode–4 (C–V2X) MAC. We assume that the VEs using the C–V2X have already made a reservation and thus, they can start the beaconing process based on fixed orthogonal semi-persistent scheduling patterns (every 100 ms) without any collisions. Note that this assumption exaggerates the C–V2X's performance due to the underestimation of the hidden terminal problem. The C–V2X does not utilize any feedback mechanism and it always transmits a beacon message twice during each allocated resource block.

4.4.3 Simulation Results

We compare BLR between the NC–MAC protocol and the C–V2X. The BLR was defined in (3.15). Moreover, the CDF of BRD according to (4.35) is compared with the results from simulations.

Figs. 4.7 (a) and (b) depict the BLR and BRD of the NC–MAC compared to the theoretical derivation in (4.35) and (4.36) where $D^{(rx)} = 200$ m, $\lambda = [0.05,\ 0.2]$ VE/m, and $\rho = 0.7, 0.9$. The correlation factor, ρ, measures how the temporal correlation affects two successive transmission opportunities in each resource block for a VE. The results are from a one-dimension linear network and there is no limitation on the number of linear combinations in a VE's forwarding queue. As it can be observed from Figs. 4.7 (a) and (b), the results from theoretical analysis for both BLR and BRD are in agreement with the NC–MAC simulation. It should be noted that the analysis underestimates the BLR when λ is small, and it overestimates it when λ is large. This is due to the probability simplification in the derivations.

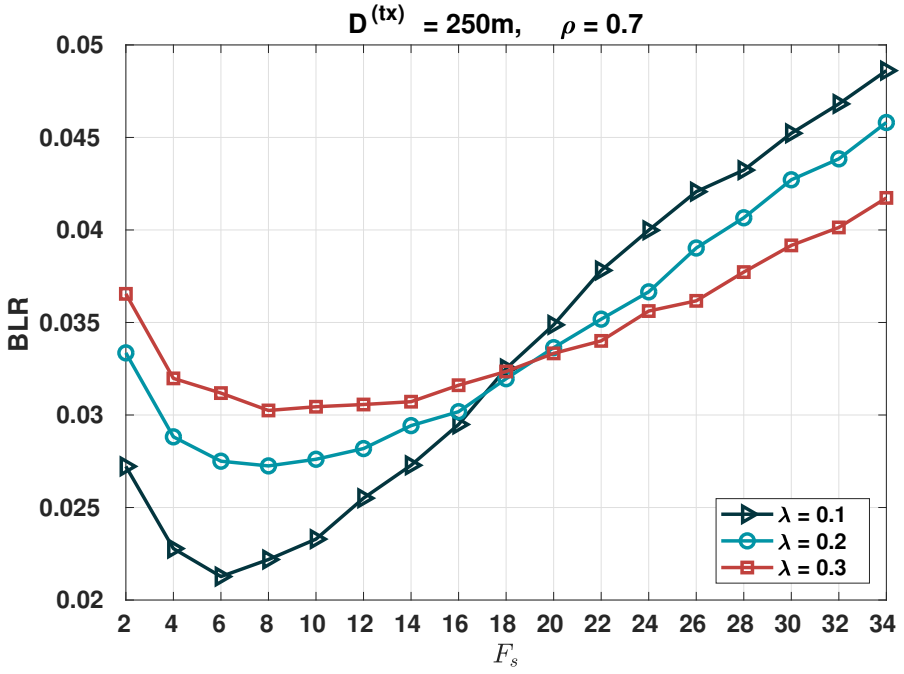

Figure 4.9: Comparison of the BLR corresponding to different VE densities with respect to the VE's forwarding queue size.

The performance of C–V2X and NC–MAC are compared in Figs. 4.8. As shown in Fig. 4.8 (a), the NC–MAC achieves a significant gain compared to the C–V2X when the beaconing range is fixed to $200, 250$ m. The BLR is reduced from 3% to around 0.3% and 1% for $\lambda = 0.05$ and $\lambda = 0.2$, respectively. The results show approximately about 75% of the missed beacons in the C–V2X can be recovered by the NC–MAC protocol. The proposed NC–MAC has a BLR of 1% in dense scenarios ($\lambda = 0.15$ and $\lambda = 0.2$), implying that NC–MAC is reliable and scalable compared to the C–V2X. In Fig. 4.8 (b), although the BLR degrades compared to Fig. 4.8 (a) where $D^{(rx)} = 200$ m, the performance gain of the NC–MAC protocol is still considerable and the NC–MAC can recover approximately 65% more beacons. The observable degradation in Fig. 4.8 (b) is because a larger number of neighbors increases the probability of receiving linear combinations containing unwanted beacons, which may be useless in the recovery process of missed beacons. These results are useful to identify the applicable scenarios for the proposed protocol. The channel correlation

factor, ρ, does not dramatically affect the results. All the schemes receive slightly better performances given a smaller ρ because of the time diversity gain.

In Fig. 4.8 (c), the CDF of the BRD for the proposed protocol, NC–MAC, in different scenarios is compared. The results in this figure is counted according to the beacons missed by at least a VE. The VE density, broadcasting ranges, and correlation factors are set to $\lambda = 0.1$ (VE/m), $D^{(rx)} = 200$, 250 m, and $\rho = [0.7, 0.9]$, respectively. The size of the VEs' forwarding queue is 11. Fig. 4.8 (c) shows that the CDF of the BRD for a larger broadcasting range is higher than the smaller one. In other words, by increasing the broadcasting range in the NC–MAC protocol, there would be a higher chance of beacons recovery with a smaller delay, which validates our expectation. Moreover, Fig. 4.8 (c) shows that among the recovered beacons in a beaconing period, a missed beacon can be recovered with probability of 90% within half of a period. Note that beacons expire after generation of a new beacon.

Fig. 4.9 shows the impact of the forwarding queue size on the BLR for different VE densities. As it was mentioned earlier, linear combination of the beacons play an important role in the NC–MAC performance. Fig. 4.9 implies that there is an optimum size for the forwarding queue. In other words, forwarding all of the requested beacons in the transmission opportunity may not lead to the lower BLR. The reason is that any VE can recover a missed beacon only during one beaconing period, and by combining more beacons in a linear combination, the VE needs more linear combinations to generate a full-rank matrix to be able to recover the missed beacons. Note that by increasing the queue size, the BLR will approach to the results in Fig. 4.7 where there is no limitation on the queue size. It is remarkable that there is a queue size where the BLR for different VE densities intersect. It may be a key factor for the scenarios where VE density changes and maintaining the BLR is of high importance.

Fig. 4.10 and Fig. 4.11 show the BLR and BRD results corresponding to the highway and urban scenarios, respectively, whose topology setup were explained earlier in this Section. The forwarding queue size is set to $F_s = 10$ in the simulation. These figures are in good agreement with the results in Fig. 4.8 (a). According to

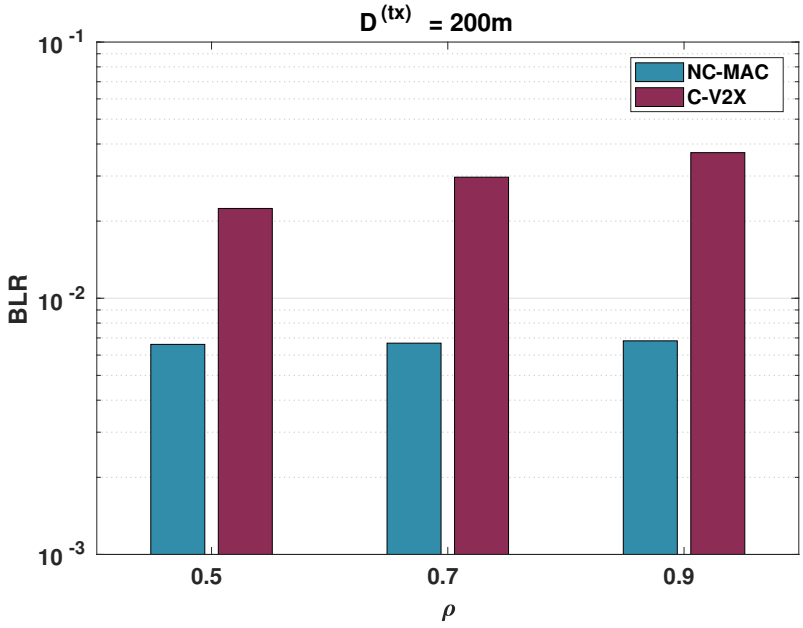

(a)

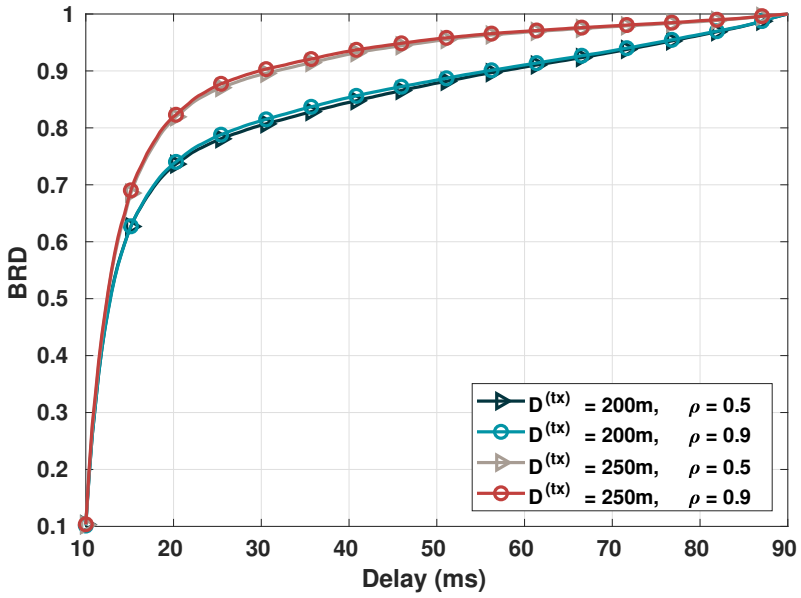

(b)

Figure 4.10: BLR and BRD of the NC–MAC and C–V2X in the highway scenario. The forwarding queue size is set to 10 in this case.

these results, in both highway and urban real scenarios, the proposed NC–MAC can recover around 70% of the missed beacons compared to the C–V2X. In terms of BRD, more than 80% of the missed beacons in one beaconing period can be recovered in

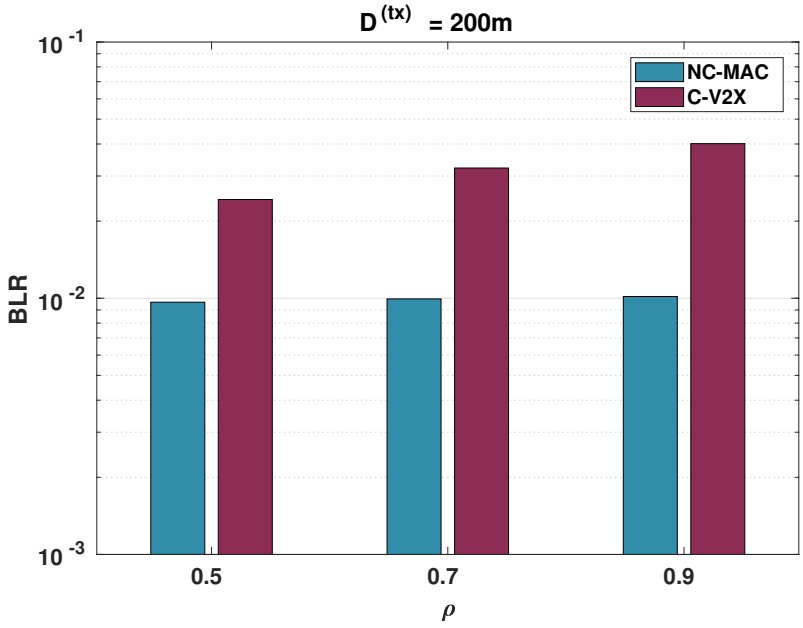

(a)

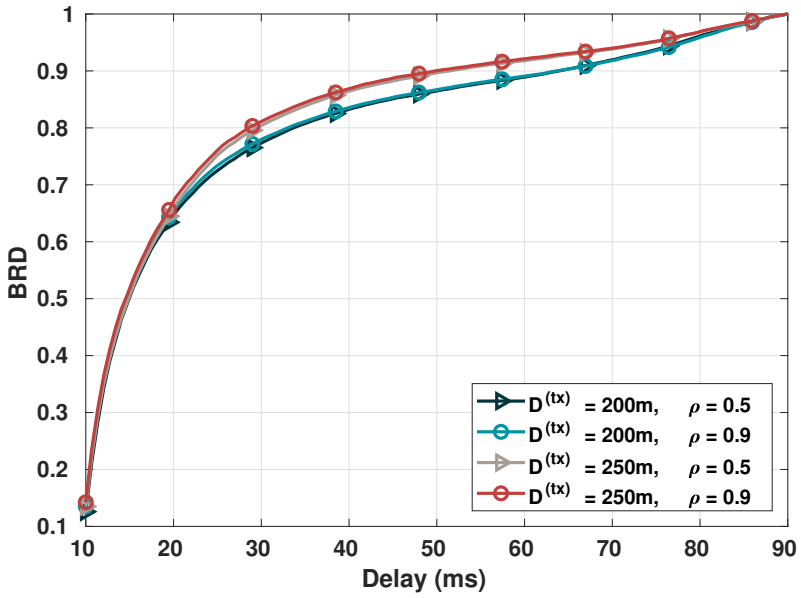

(b)

Figure 4.11: BLR and BRD of the NC–MAC and C–V2X in the urban scenario. The forwarding queue size is set to $F_s = 10$ in this case.

half of period in both of the scenarios. Compared to the highway scenario, the BLR and BRD are larger and smaller, respectively in the urban scenario despite the similar number of VEs in the networks. It is due to the higher VE density in the traffic con-

gestion of the intersections, while in the highway scenario, the VE density is roughly the same all over the road. According to this figures, a higher correlation between the transmission opportunities, ρ, increases the BLR slightly due to higher probability of two successive drop. Fig. 4.10 and Fig. 4.11 verify that the NC–MAC is more reliable and scalable, and can achieve significant performance even in real scenarios compared to the C–V2X.

4.5 Summary

In this chapter, a novel distributed protocol was proposed to improve the beacon transmission reliability in VANETs. The current solutions for V2X communications, DSRC and C–V2X, cannot support a reliable and scalable beacon broadcasting process. The former suffers from performance degradation in dense scenarios due to its contention-based medium access protocol, and in the latter beacon collision is inevitable and it does not exploit any HARQ feedback mechanism.

To address these issues, we combined a preamble-based feedback mechanism, beacon retransmission, and the network coding together to enhance the communication reliability. A complete protocol design, including forwarding operation and feedback, has been shown. Extensive simulations and numerical evaluations have been given to show the performance gain of the NC–MAC protocol over the conventional C–V2X. We evaluated the protocol in urban and highway traffic scenarios, generated by SUMO. Compared to the C–V2X, the NC–MAC protocol can achieve significant performance gains in the simulation scenarios.

Chapter 5

GNC–MAC: Grouping and Network Coding-assisted MAC for Reliable Group-casting

5.1 Introduction

In order to increase beacon broadcasting reliability, increasing the transmission power to maintain a larger beacon broadcasting range and a higher SNR may be an intuitive solution. However, the collisions and hidden-terminal problem may be intensified as well. To address this issue, keeping the number of target vehicles which directly receive the beacons small and applying multi-hop communications if necessary, can potentially improve reliability.

In addition, to address the security concern in VANETs, blockchain protocols, which rely on distributed consensus, have been proposed [87, 88, 89]. By reaching consensus, these protocols can inherently preserve privacy and ensure data immutability. In order to reach consensus, reliable group-casting mechanism in a locally formed group is a key. Therefore, group-casting within a neighbor group of vehicles can not only guarantee beacon transmission reliability, but also prepare a platform for a more

secure network. Although the group-cast and HARQ strategies have been introduced in Release-16 [90], they have not been specified yet.

In Chapter 4, the NC–MAC was designed to ensure beacon broadcasting reliability in a single-hop V2V communication. In order to extend this protocol to be able to deal with multi-hop communication, a simple grouping mechanism should be designed. The main contributions of this chapter are threefold. First, a novel group-casting MAC protocol, GNC–MAC, is proposed, which can enlarge group size by multi-hop relaying. In order to request a retransmission and report a NACK, a preamble mechanism in the frame structure is deployed and its functionality is the same as the preamble mechanism in NC–MAC. Second, similar to the NC–MAC, the NC mechanism is applied in order to generate independent linear combinations of messages. Therefore, more vehicles in a group within several hops can receive beacons. Moreover, it can help to recover missed beacons and increase the in-group communication reliability. Third, different controlling messages are designed for groups management.

5.2 GNC–MAC

5.2.1 Preliminary

We consider a V2X system where each VE needs to send beacons to its neighbors periodically. Assuming a fixed time period, and in each period, wireless resources are divided into time slots and sub-channels, respectively. Time synchronization is assumed using the global positioning system. In each time period, wireless resources are shared by the VEs in a group. A VE can reserve a resource block in the time and frequency domain when it joins a group. After acquiring a resource block, VEs may start broadcasting their beacons. The basic principles of transmissions are the same as the principles mentioned in Chapter 4, Section 5.2.

In the NC mechanism, each VE builds a coefficient matrix, according to the

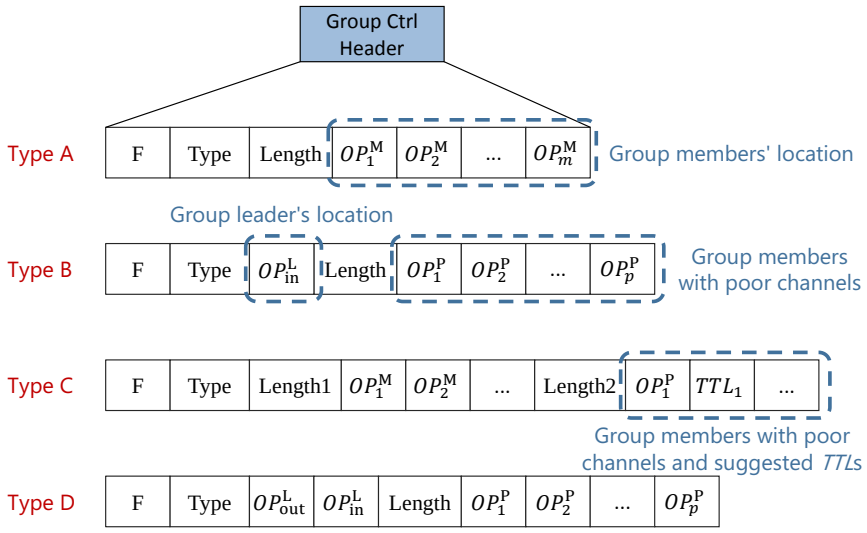

Figure 5.1: Different types of grouping control message.

messages' coefficients in the received independent linear combinations. The coefficient matrix has a size of $L \times M$ where L and M are the number of linear combinations and missed messages, respectively. This size changes due to recovering messages and receiving new linear combinations. If the coefficient matrix is a full-rank matrix, the missed messages can be recovered by solving the system of equations.

In the proposed GNC–MAC protocol, it is assumed that VEs can only perform the feedback and forwarding procedures within their own groups. Therefore, although the VEs on the edge may receive beacons from two groups, they do not relay messages belong to other groups.

5.2.2 Grouping Control Message

Management, joining, and leaving groups are all done through different grouping control messages. These controlling information are piggybacked in the PDU header as the *Group Ctrl* field and is shown in Fig. 5.1. There are four types of *Group Ctrl* with different functionalities. *S* and *Type* fields are common among all of the message types. Since these control messages are sent occasionally either by a group leader when the group needs to be managed, or by the VEs which need to enter or leave

the group. S field is defined to represent the status of the message which indicates whether the *Group Ctrl* is empty or not. The *Type* field specifies the message's types. The functionality of each type is as below.

- **Type A:** A group leader always broadcasts a *Type A* message to indicate the group members' reserved resources in the time and frequency domains.
- **Type B:** It is used to send a request to join a group. The chosen leader's reserved resource block and the VE's neighbours with poor channels are included in the message. The VEs with poor channel are reported to the leader to help the leader in the time-to-live (TTL) parameter setting.
- **Type C:** It is a regular *Type A* message which is sent by the group leader, followed by the corresponding TTL parameter suggestions which helps group members to set initial TTL values for different VEs with different channel qualities. The TTL field functionality is explained later in this Subsection.
- **Type D:** This message is used by a VE to leave its current group and join a new one. Different from the *Type B*, both old and new group leaders' reserved resource blocks are included in this message.

The OP field generally indicates a VE's reserved resource block in the time and frequency domain. In *Type A* and *Type C* messages, OP_i^{M} shows the i-th group member's reserved resource block. In *Type B* and *Type D* messages, OP_i^{P} describes the tagged VE's neighbours with poor channel. There is an OP^{L} field in *Type B* message which shows the chosen group leader's reserved resource block. In *Type C* message which is sent by the group leader, reserved resource blocks of the users with poor channel are reported with their corresponding TTL value as OP_i^{P} and TTL_i, respectively. *Type D* message which is sent when a user leaves a group includes old and new group leaders' reserved resource blocks as $OP_{\mathrm{out}}^{\mathrm{L}}$ and $OP_{\mathrm{in}}^{\mathrm{L}}$, respectively.

The field *length* in all types of messages indicates the header length.

***TTL* Parameter:** TTL is provided for each message, no matter whether it is an

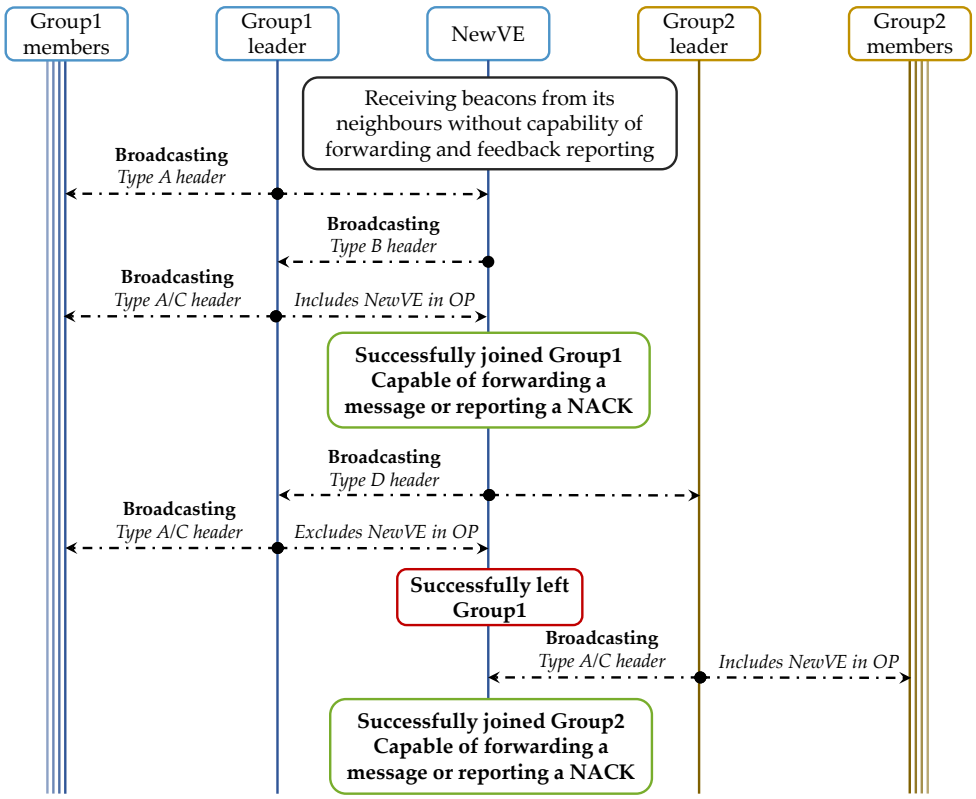

Figure 5.2: An example of the joining and leaving group procedure.

original transmission or included in a linear combination. The TTL is allocated to a message to represent its forwarding requirement. $TTL = 0$ is an indicator of a general transmission. If TTL of a message has a non-zero value ($TTL > 0$), the receiver may store the corresponding message in the forwarding queue upon receiving a NACK to include it in the future linear combinations. When a message is forwarded in a linear combination, the TTL is reduced by one based on the latest received value. The principles on TTL operations are summarized as follows.

- If a receiver successfully receives an original message with a $TTL = 0$ but also detected a NACK on the feedback channel corresponding to this transmission, the received message will be added to the forwarding queue.
- If a receiver successfully receives a message with a $TTL > 0$, the received message is considered as a forwarding message and added into the forwarding queue. When a forwarding message is added to the forwarding queue with

$TTL > 0$, its current TTL value is used. The TTL value of each forwarding message is kept updated to the latest value.

- An existing message in the forwarding queue will not be added again. However, its TTL value is updated to the latest value.
- When a forwarding message is newly added to the forwarding queue due to a detected NACK and TTL value of zero, the VE will set a new TTL value for it based on the group leader's TTL suggestions. When this forwarding message is sent out, the VE updates the TTL field in the PDU header as the value maintained in the forwarding queue minus one.
- Once the TTL value of a forwarding message reaches zero, the message is removed from the forwarding queue.

5.2.3 Joining and Leaving Procedure

When a new VE aims to join a new group, it first scans the channels to detect a *Type A* message from its neighbors, then it sends out a *Type B* message to the leader. In the case that the VE detects more than one leader, it chooses the leader with a better channel quality. If there is no available group to join, the new VE becomes a leader and includes a *Type A* message in its PDU. The group leader acknowledges the joining request by adding the new VE's *OP* in the *Group Ctrl*.

The leaving operation is performed based on either the group leader's decision or a VE's request. The group leader acknowledges the exit by removing the VE's *OP* from the message.

Fig. 5.3 illustrates an example of the joining and leaving group procedure. It is assumed that all of the VEs have successfully reserved a resource block for periodical beacon broadcasting through a collision-free MAC protocol in [81]. Therefore, collisions are avoidable and detectable. The detailed explanation is provided as follows.

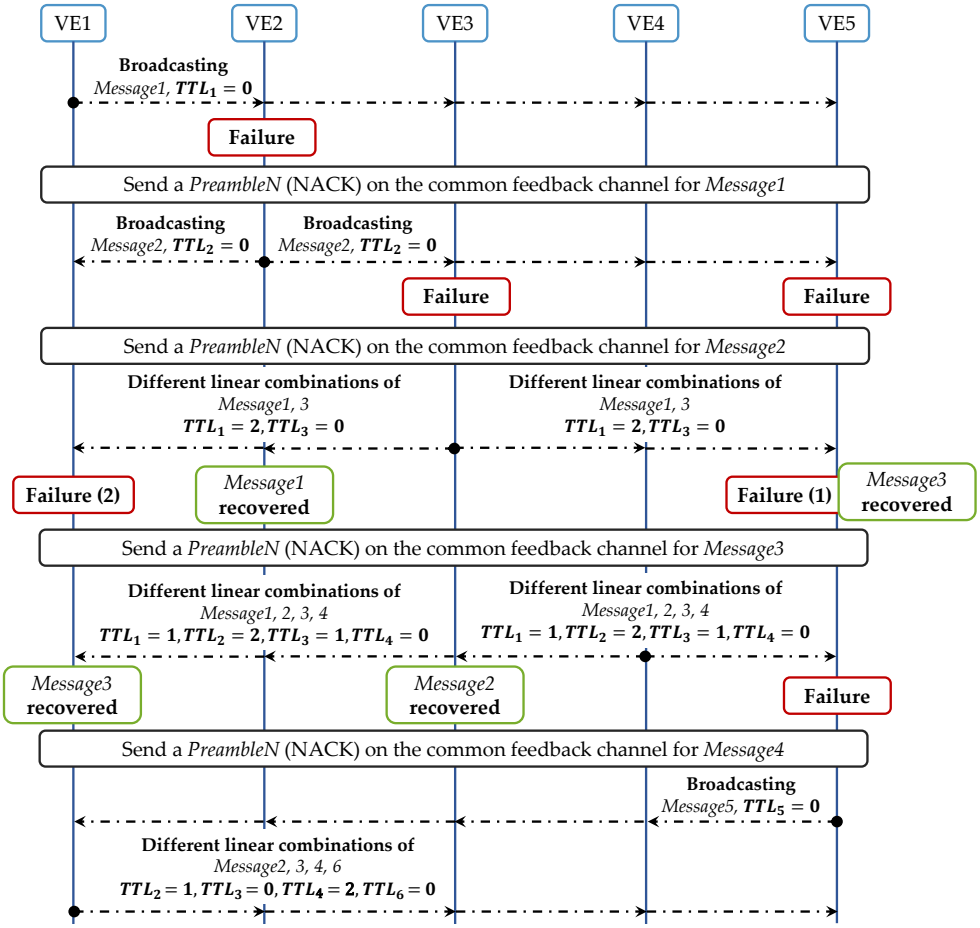

Figure 5.3: An example of the beacon broadcasting within a group.

- Upon arrival of a new VE and after acquiring a resource block, it scans all the resources on which other VEs broadcast their beacons periodically. Among the received beacon messages, the new VE identifies *Type A* or *Type C* messages from at least one group leader, and chooses one with the largest received signal strength as the leader. Otherwise, the new VE becomes a leader and broadcasts a *Type A Group Ctrl* in its PDU header.

- After the new VE determines the target group leader, it includes a *Type B* message in its beacon as a joining request.

- Upon reception of the new VE's beacon by the group leader, it decides to accept the request or not. If the joining process is successful, the group leader adds the new VE's reserved resource block in its message (*Type A* or *C*).

- The new VE officially joins the group after it finds its reserved resource block included in the member list of the message. Afterward, the new VE will receive the messages transmitted by the group members according to the member list, report NACK if failure happens in reception, and forward other users' messages.

- If a VE finds a group with a stronger signal from its leader, it can request to join the new group and leave the existing one. This procedure is performed through a *Type D* message in its PDU. The old and the new leaders may admit by removing it from the old member list and adding it to new one, respectively.

In the GNC–MAC, there is no strict order of joining and leaving a group. It is also possible that a VE is a member of multiple groups.

5.2.4 Diversity Transmissions and Relay Principles

Forwarding or relaying an already sent beacon starts while a NACK (*preambleN*) is received by a VE in the group. The NACK receiver broadcasts its own message and a linear combination of the requested beacons in the group. Fig. 5.3 illustrates an example of the message forwarding procedure and TTL settings in GNC–MAC. In this example, it is assumed that *VEs 1–5* have passed the channel accessing phase and successfully reserved their periodical beaconing resources. The detailed explanation is provided as below.

- *VE1* sends *Message1* on its reserved resource and sets $TTL = 0$ as the initial value for original messages. In Fig. 5.3, TTL_i represents the TTL value of the i-th message. *VE2* does not receive the expected message and sends a NACK on the dedicated feedback channel. By detection of the NACK by other *VEs*, *Message1* is stored in the *VEs'* forwarding queue.

- *VE2* only broadcasts its own message, *Message2*, since it failed to receive *Message1*. A NACK is broadcast on the feedback channel due to failure reception of *Message2* by *VE3* and *VE5*.

- *Message1* needs to be forwarded according to the NACK detection. Therefore, *VE3* generates two different linear combinations using *Message1* and its own message, *Message3*, and broadcasts them on the two transmission opportunities, respectively. Since *Message1* is being forwarded the first time, *VE3* needs to set a TTL value for it, $TTL_1 = 2$ in this example.

- *VE2* successfully receives both of the linear combinations with two linearly independent coefficient vectors. Thus, *Message1* and *Message3* can be recovered. However, *VE1* fails to receive both of the linear combinations and it cannot recover *Message3* at this point. A NACK is sent accordingly. On the other hand, though *VE5* did receive only one of the linear combinations, it can recover *Message3* with the help of previously received *Message1*.

- According to the received NACKs, *VE4* broadcasts two independent linear combinations of *Message1–3* and its own message, *Message4*. TTL of *Message1*, TTL_1, followed the setting made by *VE3* but reduced by one. *TTLs* of *Message2–3*, TTL_2 and TTL_3, are set by *VE4*. In this example, $TTL_2 = 2$ and $TTL_3 = 1$.

- *VE1* can successfully recover *Message3–4* by constructing a full rank matrix. Similarly, *VE3* can recover *Message2*.

- *VE5* only broadcasts its own message, *Message5*. Everyone successfully receives it and thus, there is no NACK reporting.

5.3 Performance Evaluation

To investigate whether the proposed GNC–MAC is reliable for group-casting in V2X systems, we conducted extensive simulations. The assumption behind the simulations is that the vehicles' topology follows a one dimensional PPP. LoS device-to-device communication path loss model and Rayleigh fading for non-LoS V2V communication

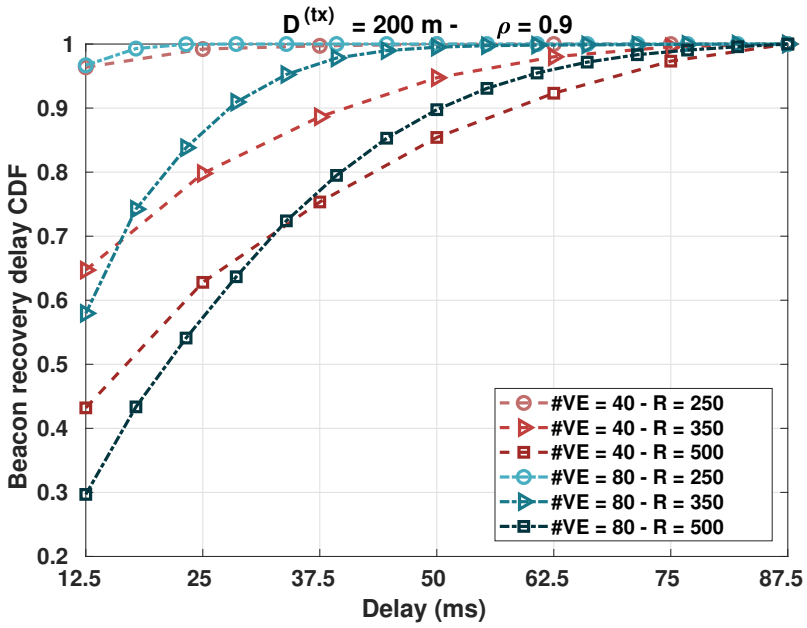

Figure 5.4: CDF of beacon recovery delay.

are considered for the channel model. Parameters used in the simulation is the same as the parameters in Table 4.2.

Each VE has acquired a resource block before starting its beacon group-casting process. The beacons are generated periodically and expired by generation of a new beacon after one period. The target receivers of a tagged VE are all of the VEs in the same group of the transmitter. In the simulation, all of the vehicles have two transmission opportunities. In the GNC–MAC protocol, a VE sends two linear combinations of the forwarding and original messages in the successive transmission opportunities, while in C–V2X, a beacon is sent twice to have a fair comparison.

Fig. 5.4 shows the CDF of beacon recovery for different number of vehicles and group diameters. The receiver range and the correlation factor are set to 200 m and 0.9, respectively. When the total number of the vehicles is fixed, the missing beacons in the group with the smaller diameter can be recovered with a higher probability and a smaller delay. That is thanks to a higher chance of retransmission and recovery in a group with a smaller diameter. This result confirms that increasing the total number of VEs in a group with a certain diameter will not change the beacon recovery delay

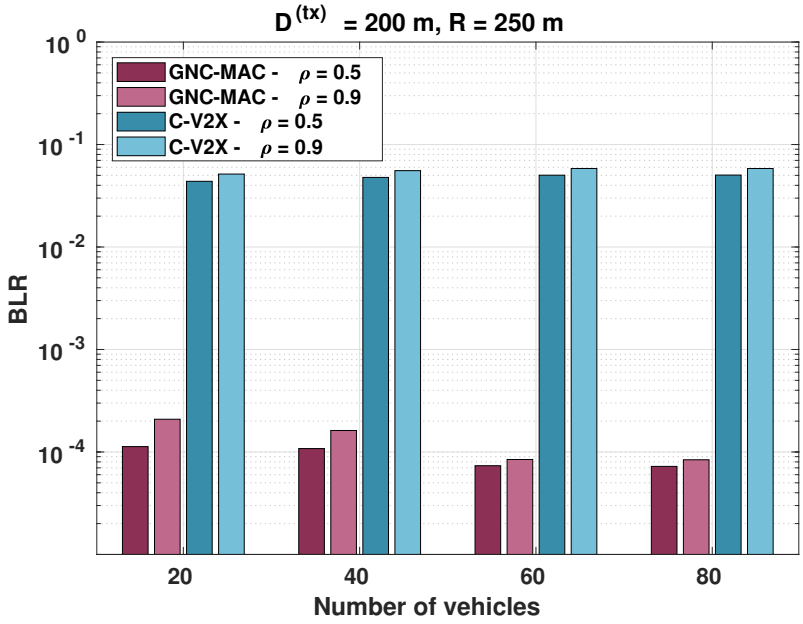

Figure 5.5: BLR of a group with a diameter of 250 m and a beacon receiving range of 200 m.

CDF significantly, and the GNC–MAC is scalable in dense scenarios.

The results corresponding to BLR are presented in Figs. 5.5–5.7. Throughout the simulation, even if vehicles are not within each other's transmission range, as long as they belong to the same group, the received and expected to be received beacons are counted in the BLR calculation. Obviously, the BLR within a group could be much higher than that counted for the VE's neighbours only if no appropriate error recovery scheme is deployed. The BLR is calculated based on the formula presented in (3.15).

Fig. 5.5 shows the BLR comparison of a group with diameter of 250 m and receiver range of 200 m. The BLR of the C–V2X is independent of number of vehicles due to the fact that the average error probability is fixed in this case as it does not have any feedback mechanism. The received packet is in error if the received SNR is below a certain threshold, SNR_T. Consequently, the average error probability for each transmission opportunity is fixed regardless of the number of vehicles. However, in the GNC–MAC, the improvement in BLR is quite significant. In different scenarios

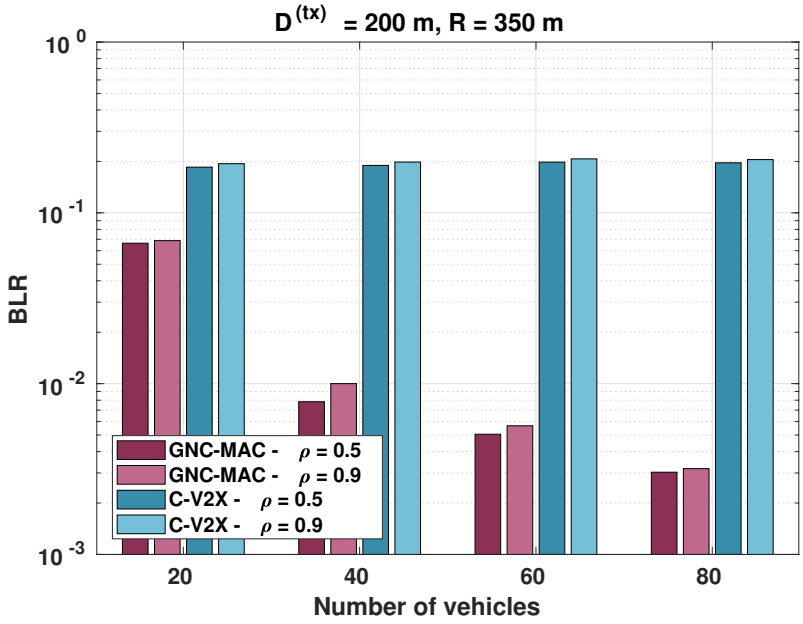

Figure 5.6: BLR of a group with a diameter of 350 m and a receiving range of 200 m.

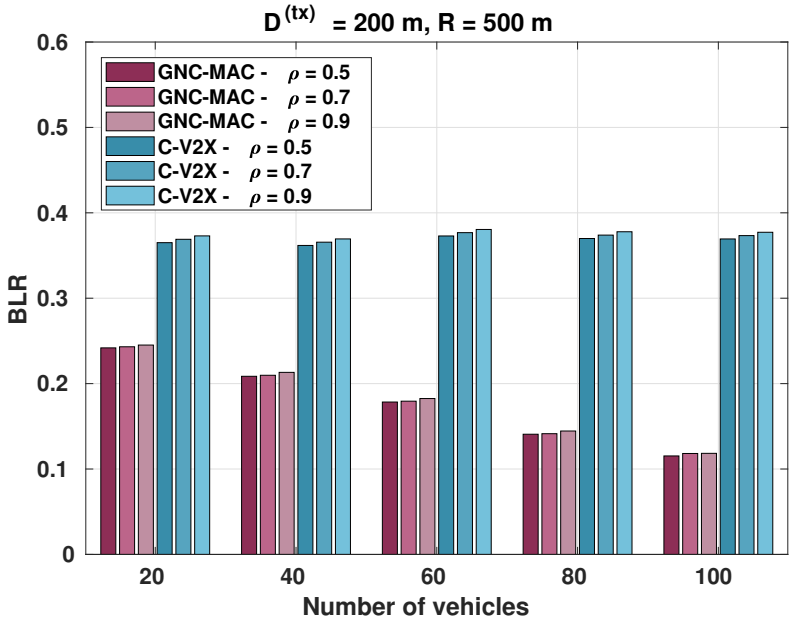

Figure 5.7: BLR of a group with a diameter of 500 m and a receiving range of 200 m.

with different number of vehicles, the BLR is reduced by more than two orders of magnitude, which is promising to ensure the performance of algorithms need grouping like consensus algorithm. Furthermore, by increasing the total number of vehicles,

it is anticipated to achieve a lower loss ratio thanks to more retransmission and recovery opportunities, as confirmed in the figure. As shown in the figure, increasing the correlation factor ρ from 0.5 to 0.9 increases the BLR slightly since higher ρ is equivalent to higher probability of drop or reception of two successive transmitted beacons.

Fig. 5.6 shows the BLR results corresponding to different numbers of vehicles for different scenarios (GNC–MAC and C–V2X). The group diameter and receiving range are set to 350 m and 200 m, respectively. It can be concluded from the figure that the GNC–MAC protocol can reduce the BLR around 50% on average. By increasing the total number of vehicles in a group, the BLR is decreased due to more retransmissions by the group members and higher chance of lost beacons recovery. In the highly dense scenario (100 vehicles in a group), the BLR reduction is about 60% compared to the C–V2X protocol. In Fig. 5.7, the protocols results comparison corresponding to the group diameter of 500 m are graphed, and similar results to Fig. 5.5 and Fig. 5.6 are achieved. The GNC–MAC can achieve a lower BLR and an average reduction of 50%. Comparing Figs. 5.5–5.7 verifies that by increasing the group-casting range, which increases the overall distance between the VEs on the group's edges, the BLR increases.

In the simulation, a delay-sensitive case has been considered in which we assumed that the beacons are expired after a beaconing period. In other words, generation of a new beacon by a VE will expire its previous beacon. Consequently, the linear combinations containing an expired beacon will be removed. As a result, each beacon may only be possible to reach other vehicles up to two-hop distance away from the sender. If the diameter of the group is larger than twice of the receiving range, $D^{(rx)}$, the vehicles located at the edges of the group cannot receive each other's beacons.

5.4 Summary

In this chapter, a novel distributed protocol was proposed to improve the group-casting reliability in VANETs. Due to performance degradation in single-hop communication in superdense scenarios caused by transmission of unwanted beacons in broadcasting mode, we focused on the targeted group-casting mode and keeping the number of target receivers small. In this case, a dynamic grouping mechanism helps to manage the target receivers and forwarding operations. First, we proposed a simple grouping strategy in which multi-hop relaying is applied to ensure beacons reception by the group members. Then, in order to enhance the in-group communication reliability, we combined a preamble-based feedback mechanism, beacon retransmission, and the network coding together. A complete protocol design, including forwarding and feedback operations as well as grouping control messages design, has been explained. Extensive simulations by considering different vehicular scenarios have been given to show the performance gain of the GNC–MAC protocol over the conventional C–V2X. Compared to the C–V2X, the GNC–MAC protocol can not only achieve significant performance gains in different simulation scenarios, but also recover the majority of the missed beacons within a period.

Chapter 6

Conclusions and Future Work

6.1 Conclusions

In this dissertation, we have studied resource management in dense wireless networks, and proposed different MAC protocols to improve efficiency and reliability of emerging technologies such as IoT and V2X systems. We employed NC method and preamble mechanism to enable HARQ feedback mechanism. The following outlines the contributions we have achieved

- In Chapter 2, a new grouping scheme for dense and large scale networks was introduced based on the IEEE 802.11ah. The *Max-Min* throughput fairness was exploited as the criterion of the network performance. Along with assignment constraints of the problem, the opportunistic hidden terminal avoidance constraint was applied to the problem. The problem was formulated as integer programming optimization problem. Since the problem is NP-hard, the ACO–MM was applied to the problem to accelerate finding the grouping strategy. Simulation results show that since the ACO–MM can avoid hidden terminals, it achieves a higher performance in terms of accumulative throughput, minimum throughput, and number of hidden terminals compared to the other methods.

- In Chapter 3, the beacon broadcasting problem was studied. The CSMA/CA-

based MAC protocols performance degrades when the density becomes high, and DARP, the novel distributed and adaptive reservation-based broadcasting MAC layer protocol was proposed to address broadcasting and delivery of beacons. In order to detect and mitigate the beacon collision probability, four different kinds of preambles were used in the proposed protocol under the assumption of periodic beaconing and a fixed MPDU. In DARP, as a decentralized and reservation-based protocol, the channel access chance of a vehicle is controlled by its neighbors and the occupied resources will not be released until collision occurs due to topology change or the vehicle leaves the system. Transmission power and the resource duration were optimized in the protocol to minimize the access collision probability. The 50 MHz DARP with variable data rate was simulated by NS-3 and SUMO traces for two different scenarios, linear network and map-based network, and compared to the 10 MHz IEEE 802.11p fixed data rate protocol. The results showed a substantial improvement in DARP in comparison to the existing standard performance. Although the access delay of the proposed protocol is at least two beaconing periods, it can secure stable and reliable communication in different scenarios. The simulation results demonstrate that the proposed DARP with power control is highly scalable and efficient in realistic vehicular network scenarios.

- In Chapter 4, we proposed a novel distributed protocol, NC–MAC, to improve the beacon transmission reliability in V2X systems. The current solutions for V2X communications, DSRC and C–V2X, cannot support a reliable and scalable beacon broadcasting process. The former suffers from performance degradation in dense scenarios due to its contention-based medium access protocol, and in the latter beacon collision is inevitable and it does not exploit any HARQ feedback mechanism. To address these issues, we combined a preamble-based feedback mechanism, beacon retransmission, and the network coding together to enhance the communication reliability. A complete protocol design, including

forwarding operation and feedback, has been shown. Extensive simulations and numerical evaluations have been given to show the performance gain of the NC–MAC protocol over the conventional C–V2X. We evaluated the protocol in urban and highway traffic scenarios, generated by SUMO. Compared to the C–V2X, the NC–MAC protocol can achieve significant performance gains in the simulation scenarios.

- In Chapter 5, we proposed a novel distributed protocol, GNC–MAC, to improve the group-casting reliability in V2X systems. Due to performance degradation in single-hop communication in superdense scenarios caused by transmission of unwanted beacons in broadcasting mode, we focused on the targeted group-casting mode and keeping the number of target receivers small. In this case, a dynamic grouping mechanism help to manage the target receivers and forwarding operations. We proposed a simple yet effective grouping strategy in which multi-hop relaying is applied to ensure beacons reception by the group members. Then, in order to enhance the in-group communication reliability, we combined a preamble-based feedback mechanism, beacon retransmission, and the network coding together. A complete protocol design, including forwarding and feedback operations as well as grouping control messages design, has been explained. Extensive simulations by considering different vehicular scenarios have been given to show the performance gain of the GNC–MAC protocol over the conventional C–V2X. Compared to the C–V2X, the GNC–MAC protocol can not only achieve significant performance gains in different simulation scenarios, but also recover the majority of the missed beacons within a period.

6.2 Future Work

For the future work that plans beyond this dissertation, there are still many open issues of importance. We list some of the future works as follows.

- In Chapter 2, the total number of groups was fixed in proposed grouping strategy. It is obvious that increasing the total number of groups can reduce the groups size. Consequently, less users contend for the communication channel. Based on the this open issue, the study can be done on the total number of available groups by deploying the ACO–MM meta-heuristic algorithm for the case that the channel state information (CSI) is available. Moreover, for the case that the CSI is not available, a Markov model can be adopted for the channel state, and a Q-learning grouping algorithm can be developed to learn the optimal policy when the underlying transition probabilities are unknown. According to the this open issue, we may have a user-assignment problem whose uncertainty comes from the channel dynamic change due to the users mobility. Modeling the channel change with a Markov chain needs further research. Similar to the ACO–MM scheme, in reinforcement learning, different possible choices of users assignment are explored to maximize an objective function in long term. Similar to the *Max-Min* fairness, a new objective function can be defined in order to find am optimal policy. Since considering the users mobility is closer to the real problem in the IEEE 802.11ah standard, the online grouping strategy may be helpful and can improve the performance significantly. By applying the reinforcement learning method to the problem, the optimal solution of the grouping problem in an online fashion is anticipated to be achieved.

- In Chapter 3, a simple version of SINR corresponding to two dominant sources of interference and constant length resources were investigated. A more general case of the SINR and also, the resources with variable length may be taken into account as the extension of this protocol. Furthermore, priority level can be assigned to the broadcasting packets in order to make difference between safety and non-safety messages broadcasting. Moreover, in the DARP, when a user enters the network and try to access the channel, at the beginning, it needs to scan the channel for one period, select an empty slot, and start broadcasting

its beacon. This procedure introduces a delay which equals at least twice the broadcasting period. However, this access delay can be reduced by designing a new controlling frame and including the occupied blocks and user's neighbor list.

- In Chapter 4, the NC–MAC, an enhancement solution for C–V2X systems, was proposed. We assumed that the resource blocks' duration and transmission power are fixed. However, how to enable and optimize distributed power control in a dynamic environment, and how to adjust and optimize the beacon period in a distributed manner need further study. Also, in the proposed NC–MAC, each vehicle is allowed to transmit a linear combination of the forwarding beacons in one of the transmission opportunities. The total number of forwarding beacons in the linear combination, i.e., the F_s parameter, is a key parameter that can be optimized given the channel quality, vehicle density, transmission power level, and the delay and reliability requirements. Furthermore, the NACK feedback range is another important parameter whose impact on the effectiveness and efficiency of the protocol may be crucial. Optimizing and adjusting the NACK range needs more investigation. In the NC–MAC, it was assumed that each beacon is expired after a broadcasting period, which makes several linear combinations useless.

- In Chapter 5, the proposed GNC–MAC is effective to relay the message within a small range, due to the delay constraint, i.e., vehicles in a group will not retransmit any expired beacons. The expiration time of each beacon can be adjusted according to the vehicle density, reliability requirement, and emergency/non-emergency situations. The TTL parameter in the protocol plays an important role in beacons delivery. The optimal TTL value in different environments needs further study. Moreover, the proposed GNC–MAC is simple, yet effective. For more complicated scenarios and dynamic V2X systems, the control messages can be redesigned and modified. In addition to the proposed grouping protocol,

in-group routing protocols are worth further research as well.

Chapter 7

Publications

• **H. Mosavat-Jahromi**, Yue Li, Yuanzhi Ni, and Lin Cai, "DARP: Distributed and Adaptive Reservation MAC Protocol for Beaconing in Vehicular Networks," in IEEE Transactions on Mobile Computing, doi: 10.1109/TMC.2020.2992045.

• Yuanzhi Ni, Lin Cai, Jianping He, Alexey Vinel, Yue Li, **H. Mosavat-Jahromi**, and Jianping Pan, "Toward Reliable and Scalable Internet of Vehicles: Performance Analysis and Resource Management," in Proceedings of the IEEE, vol. 108, no. 2, pp. 324–340, Feb. 2020.

• W. Cui, C. Liu, **H. Mosavat-Jahromi**, and L. Cai, "SigMix: Decoding Superimposed Signals for IoT," in IEEE Internet of Things Journal, vol. 7, no. 4, pp. 3026–3040, April 2020.

• **H. Mosavat-Jahromi**, Yue Li, Lin Cai, and Jianping Pan, "Prediction and Modeling of Spectrum Occupancy for Dynamic Spectrum Access Systems," *Accepted for publication in IEEE Transaction on Cognitive Communication and Networking.*

• **H. Mosavat-Jahromi**, B. Maham and T. A. Tsiftsis, "Maximizing Spec-

tral Efficiency for Energy Harvesting-Aware WBAN," in IEEE Journal of Biomedical and Health Informatics, vol. 21, no. 3, pp. 732–742, May 2017.

• **H. Mosavat-Jahromi**, Yue Li, Lin Cai, and Lei Lu, "NC–MAC: A Distributed MAC Protocol for V2X Networks to Improve Broadcast Reliability," *Submitted to IEEE Transaction on Vehicular Technology.*

• Xiangyu Ren, **H. Mosavat-Jahromi**, Lin Cai, and David Kidston, "Spatio-temporal Spectrum Load Prediction using Convolutional Neural Network and ResNet," *Submitted to IEEE Transaction on Cognitive Communication and Networking.*

• **H. Mosavat-Jahromi**, Yue Li, and Lin Cai, "A Throughput Fairness-based Grouping Strategy for Dense IEEE 802.11ah Networks," in *IEEE 30th Annual International Symposium on Personal, Indoor and Mobile Radio Communications (PIMRC)*, Istanbul, Turkey, 2019, pp. 1–6

• **H. Mosavat-Jahromi**, Yue Li, Lin Cai, and Lei Lu, "NC–MAC: Network Coding-based Distributed MAC Protocol for Reliable Beacon Broadcasting in V2X," *Accepted for presentation in the 2020 IEEE Globecom conference.*

• Lei Liu, **H. Mosavat-Jahromi**, Lin Cai and David Kidston, "A Spectrum Load Prediction Method Combining Hierarchical Agglomerative Clustering and LSTM", Accepted for presentation in the 2021 IEEE Consumer Communications and Networking Conference (CCNC).

• Xiangyu Ren, **H. Mosavat-Jahromi**, Lin Cai, and David Kidston, "Spatio-temporal Spectrum Load Prediction using Convolutional Neural Network and Bayesian Estimation," *Accepted for presentation in the 2020 IEEE Globecom*

conference.

• Yue Li, **H. Mosavat-Jahromi**, Lin Cai, and Lei Lu, "GNC–MAC: Grouping and Network Coding-assisted MAC for Reliable Group-casting in V2X," *Accepted for presentation in the 2020 IEEE 92nd VTC Workshops conference.*

• A. Sadeghi, **H. Mosavat-Jahromi**, F. Lahouti and M. Zorzi, "Multi-hop Wireless Transmission with Half Duplex and Imperfect Full Duplex Relays", in *IEEE International Symposium on Telecommunications, IST'14*, pp. 1026–1029, September 2014.

Bibliography

[1] N. Lu, N. Cheng, N. Zhang, X. Shen, and J. W. Mark, "Connected vehicles: Solutions and challenges," *IEEE Internet of Things Journal*, vol. 1, no. 4, pp. 289–299, 2014.

[2] "Cisco annual internet report (2018–2023) white paper," tech. rep., Cisco, February 2020.

[3] Al-Fuqaha et al, "Internet of Things: A survey on enabling technologies, protocols, and applications," *IEEE Communications Surveys and Tutorials*, vol. 17, no. 4, pp. 2347–2376, 2015.

[4] J. Zhang, F. Y. Wang, K. Wang, W. H. Lin, X. Xu, and C. Chen, "Data-driven intelligent transportation systems: A survey," *IEEE Transactions on Intelligent Transportation Systems*, vol. 12, pp. 1624–1639, December 2011.

[5] Y. C. Lai, P. Lin, W. Liao, and C. M. Chen, "A region-based clustering mechanism for channel access in vehicular ad hoc networks," *IEEE Journal on Selected Areas in Communications*, vol. 29, pp. 83–93, January 2011.

[6] K. Golestan, A. Jundi, L. Nassar, F. Sattar, F. Karray, M. Kamel, and S. Boumaiza, *Vehicular ad hoc Networks (VANETs): Capabilities, Challenges in Information Gathering and Data Fusion*, pp. 34–41. Berlin, Heidelberg: Springer Berlin Heidelberg, 2012.

[7] G. Karagiannis, O. Altintas, E. Ekici, G. Heijenk, B. Jarupan, K. Lin, and T. Weil, "Vehicular networking: A survey and tutorial on requirements, architectures, challenges, standards and solutions," *IEEE Communications Surveys Tutorials*, vol. 13, pp. 584–616, July 2011.

[8] Y. Ni, J. He, L. Cai, and Y. Bo, "Data uploading in hybrid V2V/V2I vehicular networks: Modeling and cooperative strategy," *IEEE Transactions on Vehicular Technology*, vol. 67, pp. 4602–4614, May 2018.

[9] J. He, L. Cai, P. Cheng, and J. Pan, "Delay minimization for data dissemination in large-scale VANETs with buses and taxis," *IEEE Transactions on Mobile Computing*, vol. 15, pp. 1939–1950, August 2016.

[10] Network Simulator 3

[11] P. A. Lopez, M. Behrisch, L. Bieker-Walz, J. Erdmann, Y.-P. Flötteröd, R. Hilbrich, L. Lücken, J. Rummel, P. Wagner, and E. Wießner, "Microscopic traffic simulation using sumo,"

[12] E. Khorov, A. Lyakhov, A. Krotov, and A. Guschin, "A survey on IEEE 802.11ah: An enabling networking technology for smart cities," *Comput. Commun.*, vol. 58, pp. 53–69, 2015.

[13] *IEEE 802.11ah Task Group, 11/0905r5 functional requirements and evaluation methodology*, Jan. 2012.

[14] L. Tian, E. Khorov, S. Latré, and J. Famaey, "Real-time station grouping under dynamic traffic for IEEE 802.11ah," *Sensors*, vol. 17, pp. 1559–1583, Jul. 2017.

[15] L. Tian, J. Famaey, and S. Latré, "Evaluation of the IEEE 802.11ah restricted access window mechanism for dense IoT networks," in *IEEE WoWMoM*, pp. 1–9, Jun. 2016.

[16] L. Zheng et al, "Performance analysis of group-synchronized DCF for dense IEEE 802.11 networks," *IEEE Trans. Wireless Commun.*, vol. 13, pp. 6180–6192, Nov. 2014.

[17] S.-G. Yoon, J.-O. Seo, and S. Bahk, "Regrouping algorithm to alleviate the hidden node problem in 802.11ah networks," *Comput. Netw.*, vol. 105, pp. 22–32, Aug. 2016.

[18] W. Damayanti, S. Kim, and J.-H. Yun, "Collision chain mitigation and hidden device-aware grouping in large-scale IEEE 802.11ah networks," *Comput. Netw.*, vol. 108, pp. 296–306, Oct. 2016.

[19] C. W. Park, D. Hwang, and T. J. Lee, "Enhancement of IEEE 802.11ah MAC for M2M communications," *IEEE Commun. Lett.*, vol. 18, pp. 1151–1154, Jul. 2014.

[20] T. C. Chang et al, "Load-balanced sensor grouping for IEEE 802.11ah networks," in *IEEE GLOBECOM*, pp. 1–6, Dec. 2015.

[21] M. Ghasemiahmadi, Y. Li, and L. Cai, "RSS-based grouping strategy for avoiding hidden terminals with GS-DCF MAC protocol," in *IEEE WCNC*, pp. 1–6, Mar. 2017.

[22] "IEEE Standard for Information technology–Part 11: Wireless LAN Medium Access Control (MAC) and Physical Layer (PHY) Specifications Amendment 2: Sub 1 GHz License Exempt Operation," *IEEE std 802.11ah-2016 (Amendment to IEEE std 802.11-2016, as amended by IEEE std 802.11ai-2016)*, pp. 1–594, May 2017.

[23] D. Tse and P. Viswanath, *Fundamentals of wireless communication*. Cambridge university press, 2005.

[24] G. Bianchi, "Performance analysis of the IEEE 802.11 distributed coordination function," *IEEE J. Sel. Areas Commun.*, vol. 18, pp. 535–547, Mar. 2000.

[25] R. Stephan, "Cardinality constrained combinatorial optimization: Complexity and polyhedra," *Discrete Optimization*, vol. 7, no. 3, pp. 99–113, 2010.

[26] A. Miller, *Subset selection in regression. Monographs on Statistics and Applied Probability.* CRC Press, 2002.

[27] J. Gao and D. Li, "A polynomial case of the cardinality-constrained quadratic optimization problem," *J. Glob. Optim.*, vol. 56, pp. 1441–1455, Aug. 2013.

[28] W. William J., "Algorithmic complexity: three NP-hard problems in computational statistics," *J. Stat. Comput. Simul.*, vol. 15, no. 1, pp. 17–25, 1982.

[29] A. Carbonaro and V. Maniezzo, "The ant colony optimization paradigm for combinatorial optimization," in *Advances in Evolutionary Computing: Theory and Applications*, Berlin, Heidelberg: Springer, 2003.

[30] M. Dorigo, M. Birattari, and T. Stutzle, "Ant colony optimization," *IEEE Comput. Intell. Mag.*, vol. 1, pp. 28–39, Nov. 2006.

[31] D. Sajjadi, M. Tanha, and J. Pan, "Meta-heuristic solution for dynamic association control in virtualized multi-rate WLANs," in *IEEE LCN*, pp. 253–261, Nov. 2016.

[32] M. Dorigo and G. Di Caro, "The ant colony optimization meta-heuristic," in *New Ideas in Optimization*, pp. 11–32, Maidenhead, UK, England: McGraw-Hill Ltd., UK, 1999.

[33] D. Arthur and S. Vassilvitskii, "K-means++: The advantages of careful seeding," tech. rep., 2006.

[34] K. Ota, M. Dong, S. Chang, and H. Zhu, "MMCD: Cooperative downloading for highway VANETs," *IEEE Transactions on Emerging Topics in Computing*, vol. 3, pp. 34–43, March 2015.

[35] M. Xing, J. He, and L. Cai, "Utility maximization for multimedia data dissemination in large-scale VANETs," *IEEE Transactions on Mobile Computing*, vol. 16, pp. 1188–1198, April 2017.

[36] S. A. Mohammad, A. Rasheed, and A. Qayyum, *VANET Architectures and Protocol Stacks: A Survey*, pp. 95–105. Berlin, Heidelberg: Springer Berlin Heidelberg, 2011.

[37] S. Al-Sultan, M. M. Al-Doori, A. H. Al-Bayatti, and H. Zedan, "A comprehensive survey on vehicular ad hoc network," *Journal of Network and Computer Applications*, vol. 37, pp. 380–392, January 2014.

[38] *IEEE Std 802.11p-2010*, pp. 1–51, July 2010.

[39] X. Shen, X. Cheng, R. Zhang, B. Jiao, and Y. Yang, "Distributed congestion control approaches for the IEEE 802.11p vehicular networks," *IEEE Intelligent Transportation Systems Magazine*, vol. 5, pp. 50–61, October 2013.

[40] H. Zhou, W. Xu, J. Chen, and W. Wang, "Evolutionary V2X technologies toward the Internet of vehicles: Challenges and opportunities," *Proceedings of the IEEE*, vol. 108, no. 2, pp. 308–323, 2020.

[41] G. Naik, B. Choudhury, and J. Park, "IEEE 802.11bd & 5G NR V2X: Evolution of radio access technologies for V2X communications," *IEEE Access*, vol. 7, pp. 70169–70184, 2019.

[42] D. Smely, S. Rührup, R. K. Schmidt, J. Kenney, and K. Sjöberg, "Decentralized congestion control techniques for VANETs," in *Vehicular ad hoc Networks*, pp. 165–191, Springer, 2015.

[43] H. A. Omar, N. Lu, and W. Zhuang, "Wireless access technologies for vehicular network safety applications," *IEEE Network*, vol. 30, pp. 22–26, July 2016.

[44] G. Karagiannis, O. Altintas, E. Ekici, G. Heijenk, B. Jarupan, K. Lin, and T. Weil, "Vehicular networking: A survey and tutorial on requirements, architectures, challenges, standards and solutions," *IEEE Communications Surveys Tutorials*, vol. 13, pp. 584–616, July 2011.

[45] L. Zheng and L. Cai, "AFDA: Asynchronous flipped diversity ALOHA for emerging wireless networks with long and heterogeneous delay," *IEEE Transactions on Emerging Topics in Computing*, vol. 3, pp. 64–73, March 2015.

[46] J. Sahoo, E. H. K. Wu, P. K. Sahu, and M. Gerla, "Congestion-controlled-coordinator-based MAC for safety-critical message transmission in VANETs," *IEEE Transactions on Intelligent Transportation Systems*, vol. 14, pp. 1423–1437, September 2013.

[47] F. Lyu, H. Zhu, H. Zhou, W. Xu, N. Zhang, M. Li, and X. Shen, "SS-MAC: A novel time slot-sharing MAC for safety messages broadcasting in VANETs," *IEEE Transactions on Vehicular Technology*, vol. 67, pp. 3586–3597, April 2018.

[48] G. Bansal, J. B. Kenney, and C. E. Rohrs, "LIMERIC: A linear adaptive message rate algorithm for DSRC congestion control," *IEEE Transactions on Vehicular Technology*, vol. 62, pp. 4182–4197, November 2013.

[49] F. J. Ros, P. M. Ruiz, and I. Stojmenovic, "Acknowledgment-based broadcast protocol for reliable and efficient data dissemination in vehicular ad hoc networks," *IEEE Transactions on Mobile Computing*, vol. 11, pp. 33–46, January 2012.

[50] W. Benrhaiem, A. S. Hafid, and P. K. Sahu, "Multi-hop reliability for broadcast-based VANET in city environments," in *IEEE International Conference on Communications (ICC)*, pp. 1–6, May 2016.

[51] H. A. Omar, W. Zhuang, A. Abdrabou, and L. Li, "Performance evaluation of VeMAC supporting safety applications in vehicular networks," *IEEE Transactions on Emerging Topics in Computing*, vol. 1, pp. 69–83, June 2013.

[52] H. A. Omar, W. Zhuang, and L. Li, "VeMAC: A TDMA-based MAC protocol for reliable broadcast in VANETs," *IEEE Transactions on Mobile Computing*, vol. 12, pp. 1724–1736, September 2013.

[53] F. Borgonovo, A. Capone, M. Cesana, and L. Fratta, "ADHOC MAC: New MAC architecture for ad hoc networks providing efficient and reliable point-to-point and broadcast services," *Wireless Networks*, vol. 10, pp. 359–366, July 2004.

[54] Z. Xu, M. Wang, Y. Wu, and X. Lin, "Adaptive multichannel MAC protocol based on SD-TDMA mechanism for the vehicular ad hoc network," *IET Communications*, vol. 12, pp. 1509–1516, July 2018.

[55] F. Lyu, H. Zhu, H. Zhou, L. Qian, W. Xu, M. Li, and X. Shen, "MoMAC: Mobility-aware and collision-avoidance MAC for safety applications in VANETs," *IEEE Transactions on Vehicular Technology*, vol. 67, pp. 10590–10602, November 2018.

[56] Y. Cao, H. Zhang, X. Zhou, and D. Yuan, "A scalable and cooperative MAC protocol for control channel access in VANETs," *IEEE Access*, vol. 5, pp. 9682–9690, May 2017.

[57] L. A. Villas, A. Boukerche, G. Maia, R. W. Pazzi, and A. A. Loureiro, "DRIVE: An efficient and robust data dissemination protocol for highway and urban vehicular ad hoc networks," *Computer Networks*, vol. 75, pp. 381–394, December 2014.

[58] S. Bharati and W. Zhuang, "CRB: Cooperative relay broadcasting for safety applications in vehicular networks," *IEEE Transactions on Vehicular Technology*, vol. 65, pp. 9542–9553, December 2016.

[59] C. Xu, L. Song, and Z. Han, *Resource Management for Device-to-Device Underlay Communication*. New York, USA: Springer, 2014.

[60] 3rd Generation Partnership Project, "Evolved universal terrestrial radio access (E-UTRA), Physical channels and modulation (Release 10)," *3GPP TS 36.211*, v10.4.0, December 2011.

[61] E. Dahlman, S. Parkvall, and J. Skold, *4G, LTE-Advanced Pro and The Road to 5G*. Orlando, FL, USA: Academic Press, Inc., 3rd ed., 2016.

[62] L. Comtet, *Advanced Combinatorics: The Art of Finite and Infinite Expansions*. Amsterdam, The Netherlands: Springer, 2012.

[63] Y. D. Chen, Y. P. Shih, and K. P. Shih, "An emergency message dissemination protocol using n-way search with power control for VANETs," in *IEEE International Conference on Communications (ICC)*, pp. 3653–3658, June 2015.

[64] J. Mittag, F. Schmidt-Eisenlohr, M. Killat, J. Härri, and H. Hartenstein, "Analysis and design of effective and low-overhead transmission power control for VANETs," in *Proceedings of the 5th ACM VANET Workshop*, pp. 39–48, 2008.

[65] S. H. Bouk, G. Kim, S. H. Ahmed, and D. Kim, "Hybrid adaptive beaconing in vehicular ad hoc networks: A survey," *International Journal of Distributed Sensor Networks*, vol. 11, January 2015.

[66] W. Liu, X. Wang, W. Zhang, L. Yang, and C. Peng, "Coordinative simulation with SUMO and NS3 for vehicular ad hoc networks," in *22nd Asia-Pacific Conference on Communications (APCC)*, pp. 337–341, August 2016.

[67] Y. Li and L. Cai, "Cooperative device-to-device communication for uplink transmission in cellular system," *IEEE Transactions on Wireless Communications*, vol. 17, pp. 3903–3917, June 2018.

[68] J. B. Kenney, "Dedicated short-range communications (DSRC) standards in the united states," *Proceedings of the IEEE*, vol. 99, pp. 1162–1182, July 2011.

[69] 3GPP TS 36.212, "Physical Layer Procedures (Release 14)," V15.2.1, July 2018.

[70] 3GPP, "Proximity-Based Services (ProSe); Stage 2; Release 12," TS 23.303, 3rd Generation Partnership Project (3GPP), 2014.

[71] 3GPP TS 36.331, "Radio Resource Control (Release 14)," V15.2.2, July 2018.

[72] 3GPP TS 36.300, "Overall Description (Release 14)," V15.2.0, July 2018.

[73] J. K. Sundararajan, D. Shah, M. Medard, S. Jakubczak, M. Mitzenmacher, and J. Barros, "Network coding meets TCP: Theory and implementation," *Proceedings of the IEEE*, vol. 99, pp. 490–512, March 2011.

[74] R. Ahlswede, N. Cai, S. R. Li, and R. W. Yeung, "Network information flow," *IEEE Transactions on Information Theory*, vol. 46, pp. 1204–1216, July 2000.

[75] S. R. Li, R. W. Yeung, and N. Cai, "Linear network coding," *IEEE Transactions on Information Theory*, vol. 49, pp. 371–381, February 2003.

[76] Y. Li, K. Sun, and L. Cai, "Cooperative device-to-device communication with network coding for machine type communication devices," *IEEE Transactions on Wireless Communications*, vol. 17, pp. 296–309, January 2018.

[77] T. Zhou, B. Xu, T. Xu, H. Hu, and L. Xiong, "User-specific link adaptation scheme for device-to-device network coding multicast," *IET Communications*, vol. 9, pp. 367–374, February 2015.

[78] Q. Wang, P. Fan, and K. B. Letaief, "On the joint V2I and V2V scheduling for cooperative VANETs with network coding," *IEEE Transactions on Vehicular Technology*, vol. 61, pp. 62–73, January 2012.

[79] J. Bhatia and B. Shah, "Review on various security threats & solutions and network coding based security approach for VANET," *IEEE Transactions on Vehicular Technology*, vol. 6, pp. 361–370, March 2013.

[80] C. Wu, S. Ohzahata, Y. Ji, and T. Kato, "Multi-hop broadcasting in VANETs integrating intra-flow and inter-flow network coding," in *2014 IEEE Vehicular Technology Conference (VTC Fall)*, pp. 1–6, September 2014.

[81] H. Mosavat-Jahromi, Y. Li, Y. Ni, and L. Cai, "Distributed and adaptive reservation MAC protocol for beaconing in vehicular networks," *IEEE Transactions on Mobile Computing*, doi: 10.1109/TMC.2020.2992045 2020.

[82] W. Feller, *An Introduction to Probability Theory and its Applications Vol. I.* Wiley, 1968.

[83] A. Papoulis and S. U. Pillai, *Probability, random variables, and stochastic processes.* New York, NY, USA: McGraw-Hill, 4 ed., 2002.

[84] V. V. Chetlur and H. S. Dhillon, "Success probability and area spectral efficiency of a VANET modeled as a Cox process," *IEEE Wireless Communications Letters*, vol. 7, no. 5, pp. 856–859, 2018.

[85] C. Xu, L. Song, and Z. Han, *Resource management for device-to-device underlay communication.* New York, NY, USA: Springer, 2014.

[86] ITU, "Link-level simulation results for IMT.EVAL," Tech. Rep. TTA PG707.

[87] H. Li, L. Pei, D. Liao, G. Sun, and D. Xu, "Blockchain meets VANET: An architecture for identity and location privacy protection in VANET," *Peer-to-Peer Networking and Applications*, vol. 12, no. 5, pp. 1178–1193, 2019.

[88] Z. Zheng, J. Pan, and L. Cai, "Lightweight Blockchain consensus protocols for vehicular social networks," *IEEE Transactions on Vehicular Technology*, pp. 1–14, 2020.

[89] L. Xie, Y. Ding, H. Yang, and X. Wang, "Blockchain-based secure and trustworthy Internet of things in SDN-enabled 5G-VANETs," *IEEE Access*, vol. 7, pp. 56656–56666, 2019.

[90] 3GPP TR 38.885, "Study on NR Vehicle-to-Everything (V2X) (Release 16)," V16.0.0, March 2019.